PH.D. DISSERTATION

Optimization of Positioning Capabilities in Wireless Sensor Networks

From power efficiency to medium access

Ana Moragrega Estrany

Centre Tecnològic de Telecomunicacions de Catalunya (CTTC)
e-mail: ana.moragrega@cttc.es

Thesis Advisor: Dr. Christian Ibars Casas
Intel Corporation
2200 Mission College Blvd.
Santa Clara, CA 95054 USA

Thesis Advisor: Dr. Pau Closas
Centre Tecnològic de Telecomunicacions de Catalunya (CTTC)
Parc Mediterrani de la Tecnologia
Av. Carl Friedrich Gauss 7 B4
08860 Castelldefels, Barcelona (Spain)
e-mail: pau.closas@cttc.es

Thesis Tutor: Prof. Jordi Mateu Mateu
Universitat Politècnica de Catalunya (UPC)
Departament Teoria del Senyal i Comunicacions
Edifici C4-208 (PMT-EETAC)
Esteve Terradas, 7, 08860 Castelldefels, Spain
e-mail: jmateu@tsc.upc.edu

Barcelona, 2016

A la meva família i amics

Abstract

In Wireless Sensor Networks (WSN), the ability of sensor nodes to know its position is an enabler for a wide variety of applications for monitoring, control, and automation. Often, sensor data is meaningful only if its position can be determined. Many WSN are deployed indoors or in areas where Global Navigation Satellite System (GNSS) signal coverage is not available, and thus GNSS positioning cannot be guaranteed. In these scenarios, WSN may be relied upon to achieve a satisfactory degree of positioning accuracy.

Typically, batteries power sensor nodes in WSN. These batteries are costly to replace. Therefore, power consumption is an important aspect, being performance and lifetime of WSN strongly relying on the ability to reduce it. It is crucial to design effective strategies to maximize battery lifetime. Optimization of power consumption can be made at different layers. For example, at the physical layer, power control and resource optimization may play an important role, as well as at higher layers through network topology and Medium Access Control (MAC) protocols.

The objective of this Thesis is to study the optimization of resources in WSN that are employed for positioning purposes, with the ultimate goal being the minimization of power consumption. We focus on anchor-based positioning, where a subset of the WSN nodes know their location (anchors) and send ranging signals to nodes with unknown position (targets) to assist them in estimating it through distance-related measurements. Two well known of such measurements are received signal strength (RSS) and time of arrival (TOA), in which this Thesis focuses. In order to minimize power consumption while providing a certain quality of positioning service, in this dissertation we research on the problems of power control and node selection. Aiming at a distributed implementation of the proposed techniques, we resort to the tools of non-cooperative game theory.

First, transmit power allocation is addressed for RSS based ranging. Using game theory formulation, we develop a potential game leading to an iterated best response algorithm with sure convergence. As a performance metric, we introduce the geometric dilution of precision (GDOP), which is shown to help achieving a suitable geometry of the selected anchor nodes. The proposed scheme and relative distributed algorithms provide good equilibrium performance in both static and dynamic scenarios. Moreover, we present a distributed, low complexity implementation and analyze it in terms of computational complexity. Results show that performance close to that of exhaustive search is possible.

We then address the transmit power allocation problem for TOA based ranging, also resorting to a game theoretic formulation. In this setup, and also considering

GDOP as performance metric, a supermodular game formulation is proposed, along with a distributed algorithm with guaranteed convergence to a unique solution, based on iterated best response. We analyze the proposed algorithm in terms of the price of anarchy (PoA), that is, compared to a centralized optimum solution, and shown to have a moderate performance loss.

Finally, this dissertation addresses the effect of different MAC protocols and topologies in the positioning performance. In this direction, we study the performance of mesh and cluster-tree topologies defined in WSN standards. Different topologies place different constraints in network connectivity, having a substantial impact on the performance of positioning algorithms. While mesh topology allows high connectivity with large energy consumption, cluster-tree topologies are more energy efficient but suffer from reduced connectivity and poor positioning performance. In order to improve the performance of cluster-tree topologies, we propose a cluster formation algorithm. It significantly improves connectivity with anchor nodes, achieving vastly improved positioning performance.

Resum

En les xarxes de sensors sense fils (Wireless Sensor Networks, WSN), l'habilitat dels nodes sensors per conèixer la seva posició facilita una gran varietat d'aplicacions per la monitorització, el control i l' automatització. Freqüentment, les dades que proporciona un sensor tenen sentit només si la posició pot ésser determinada. Moltes xarxes de sensors són desplegades en interiors o en àrees on la senyal de sistemes globals de navegació per satèl.lit (Global Navigation Satellite System, GNSS) no té prou cobertura, i per tant, el posicionament basat en GNSS no pot ésser garantitzat. En aquests escenaris, les xarxes de sensors poden proporcionar una bona precisió en posicionament.

Normalment, en xarxes de sensors els nodes són alimentats amb bateries. Aquestes bateries són difícils de reemplaçar. Per tant, el consum de potència és un aspecte important a tenir en compte i és crucial dissenyar estratègies efectives per maximitzar el temps de vida de la bateria. L'optimització del consum de potència pot ser fet a diferents capes del protocol. Per exemple, en la capa física, el control de potència i l'optimització dels recursos juguen un rol important, igualment que la topologia de xarxa i els protocols MAC (Medium Access Control) en les capes més altes.

L'objectiu d'aquesta tesi és estudiar l'optimització de recursos en xarxes de sensors que s'utilitzen per fer posicionament, amb el propòsit de minimitzar el consum de potència. Ens focalitzem en el posicionament basat en àncora, en el qual un conjunt de nodes sensors coneixen la seva localització (nodes àncora) i envien missatges als nodes que no saben la seva posició (nodes desconeguts) per ajudar-los a estimar les seves coordenades amb mesures de distància. Dues classes de mesures són la potència de la senyal rebuda (received signal strength, RSS) i el temps d'arribada (time of arrival, TOA) en les quals aquesta tesi està focalitzada. Per minimitzar el consum de potència mentre que es proporciona suficient qualitat en el servei de posicionament, en aquesta tesi estudiem els problemes de control de potència i selecció de nodes. Tenint en compte una implementació distribuïda de les tècniques proposades, utilitzem eïnes de teoria de jocs no cooperatius.

Primer, l'assignació de potència transmesa és abordada pel càlcul de la distància amb RSS. Utilitzant la teoria de jocs, desenvolupem un joc potencial que convergeix amb un algoritme iteratiu basat en millor resposta (best response). Com a mètrica d'error, introduïm la dilució de la precisió geomètrica (geometric dilution of precision, GDOP) que mostra quant d'apropiada és la geometria dels nodes àncora seleccionats. L'esquema proposat i els algoritmes distribuïts proporcionen una bona resolució de l'equilibri en l'escenari estàtic i dinàmic. Altrament, presentem una im-

plementació distribuïda i analitzem la seva complexitat computacional. Els resultats obtinguts són similars als obtinguts amb un algoritme de cerca exhaustiva.

El problema d'assignació de la potència transmesa en el càlcul de la distància basat en TOA, també és tractat amb teoria de jocs. En aquest cas, considerant el GDOP com a mètrica d'error, proposem un joc supermodular juntament amb un algoritme distribuït basat en millor resposta amb convergència garantida cap a una única solució. Analitzem la solució proposada amb el preu de l'anarquia (price of anarchy, PoA), és a dir, es compara la nostra solució amb una solució òptima centralitzada mostrant que les pèrdues són moderades.

Finalment, aquesta tesi tracta l'efecte que causen diferents protocols MAC i topologies en el posicionament. En aquesta direcció, estudiem les topologies de malla (mesh) i arbre formant clusters (cluster-tree) que estan definides als estàndards de xarxes de sensors. La diferència entre les topologies crea diferents restriccions en la connectivitat de la xarxa, afectant els resultats amb els algoritmes de posicionament. Així, la topologia de malla permet una elevada connectivitat entre els nodes amb gran consum d'energia, mentre que les topologies d'arbre són més energèticament eficients però amb baixa connectivitat entre els nodes i baix rendiment pel posicionament. Per millorar la qualitat del posicionament en les topologies d'arbre, proposem un algoritme de formació de clústers. Aquest algoritme millora la connectivitat amb els nodes àncora, aconseguint millorar el posicionament.

Resumen

En las redes de sensores inalámbricas (Wireless Sensor Networks, WSN), la habilidad de los nodos sensores para conocer su posición facilita una gran variedad de aplicaciones para la monitorización, el control y la automatización. Frecuentemente, los datos que proporciona un sensor tienen sentido solamente si la posición puede ser estimada. Muchas redes de sensores son desplegadas en interiores o en áreas donde la señal de sistemas globales de navegación por satélite (Global Navigation Satellite System, GNSS) no tiene suficiente cobertura, y por lo tanto, el posicionamiento basado en GNSS no puede ser garantizado. En estos escenarios, las redes de sensores pueden proporcionar buena precisión en posicionamiento.

Normalmente, en las redes de sensores los nodos son alimentados con baterías. Estas baterías son difíciles de reemplazar. Por lo tanto, el consumo de potencia es un aspecto importante a tener en cuenta y es crucial diseñar estrategias efectivas para maximizar el tiempo de vida de la batería. La optimización del consumo de potencia puede ser llevado a cabo en diferentes capas del protocolo. Por ejemplo, en la capa física, el control de potencia y la optimización de los recursos juegan un rol importante, igualmente que la topología de red y los protocolos MAC en las capas más altas.

El objetivo de esta tesis es estudiar la optimización de recursos en las redes de sensores inalámbricas que se usan para posicionamiento, con el próposito de minimizar el consumo de potencia. Nos focalizamos en el posicionamiento basado en áncora, en el cual un conjunto de nodos sensores conocen su localización (nodos áncora) y envían mensajes a los nodos que no saben su posición (nodos deconocidos) para ayudarlos a estimar sus coordenadas con medidas de distancia. Dos clases de medidas son la potencia de la señal recibida (received signal strength, RSS) y el tiempo de llegada (time of arrival, TOA) en las cuales esta tesis está focalizada.

Para minimizar el consumo de potencia mientras que se proporciona suficiente calidad en el servicio de posicionamiento, en esta tesis estudiamos los problemas de control de potencia y selección de nodos. Teniendo en cuenta una implementación distribuida de las técnicas propuestas, usamos herramientas de teoría de juegos no cooperativos.

Primero, la asignación de potencia transmitida es abordada para el cálculo de la distancia con RSS. Usando la teoría de juegos, desarrollamos un juego potencial que converge con un algoritmo iterativo basado en mejor respuesta (best response). Como métrica de error, introducimos la dilución de la precisión geométrica (geometric dilution of precision, GDOP) que muestra cuanto de apropiada es la geometría de los nodos áncora seleccionados. El esquema propuesto y los algoritmos distribuidos

proporcionan una buena resolución del equilibrio en el escenario estático y dinámico. Por otro lado, presentamos una implementación distribuida y analizamos su complejidad computacional. Los resultados obtenidos son similares a los obtenidos con un algoritmo de búsqueda exhaustiva.

El problema de la asignación de potencia transmitida en el cálculo de la distancia basada en TOA, también se trata con teoría de juegos. En este caso, considerando GDOP como métrica de error, proponemos un juego supermodular y un algoritmo distribuido basado en la mejor respuesta con convergencia garantizada hacia una solución única. Analizamos la solución propuesta con el precio de la anarquía (price of anarchy, PoA), es decir, se compara nuestra solución con una solución óptima centralizada mostrando que las pérdidas son moderadas.

Finalmente, esta tesis trata el efecto que causan diferentes protocolos MAC y topologías en el posicionamiento. En esta dirección, estudiamos las topologías de malla (mesh) y árbol formando clústers (cluster-tree) que están definidas en los estándares de las redes de sensores. La diferencia entre las topologías crea diferentes restricciones en la conectividad de la red, afectando los resultados con los algoritmos de posicionamiento. La topología de malla permite una elevada conectividad entre los nodos con gran consumo de energía, mientras que las topologías de árbol son más energéticamente eficientes pero con baja conectividad entre los nodos y bajo rendimiento para el posicionamiento. Para mejorar la calidad del posicionamiento en las topologías de árbol, proponemos un algoritmo de formación de clústers. Este algoritmo mejora la conectividad con los nodos ancla, consiguiendo mejorar el posicionamiento.

Preface

El doctorat ha estat un camí llarg i voldria donar les gràcies a les persones que m'han acompanyat i ajudat. Voldria agrair als meus directors i tutor de tesi la confiança que m'han demostrat en tot moment. Christian, ha estat un plaer treballar amb tu tant a nivell de feina com a nivell personal. Els teus consells han estat sempre molt enriquidors. Pau, et vull agrair la paciència que has tingut i tens en escoltar-me i comentar temes. Ha estat i serà un plaer treballar amb tu tant a nivell de recerca com personal. Com en qualsevol cursa, durant el doctorat hi ha moments de presses, dubtes, moments bons, divertits i gratificants, gràcies Christian i Pau per la vostra dimensió humana, els vostres consells i acompanyar-me en aquest camí.

Vull agrair al CTTC les facilitats que m'ha ofert per fer el doctorat mentre treballava com enginyera, he estat rodejada d'un bon entorn de treball tant de recerca com d'accés a equipament. Durant aquest temps he pogut coicidir amb moltes persones tant en els projectes on he treballat com per altres temes. Com que la llista és llarga, vull agrair haver-me trobat amb bons professionals i persones que m'han enriquit tant a nivell de feina com humà. Concretament, voldria agrair el suport que em doneu els meus companys i caps de grup o departament en el que estic actualment, i també als revisors d'aquesta tesi pels esforços de revisió.

També vull enrecordar-me de les persones amb qui vaig començar a treballar en recerca, abans del CTTC, al Departament d'Electrònica de la Facultat de Físiques de la Universitat de Barcelona.

Els agraiments més personals els començo amb un record especial per la meva mare que va marxar quan vaig començar la tesi. Gracias por todo, tantas cosas, no sabría por donde empezar...Una buena madre a quién seguimos recordando. Gracias a los dos, gracias a mis padres por vuestro apoyo, afecto, transmitirme vuestros valores, curiosidad por aprender y disfrutar de las cosas sencillas de la vida. Vull seguir els agraiments amb la família més propera (la llista és llarga), pel vostre afecte, recolçament i consells durant aquests anys. Sabeu estar al meu costat faci sol o plogui, amb qui creixo i seguim aprenent, m'heu ajudat molt. També agrair el recolçament als amics que sóu com de la família des de fa molts anys o des de fa poc (de la colla del barri, de la colla de la universitat, o d'altres), gràcies pels moments de desconexió durant aquests anys, divertits o de converses, i per fer camí amb mi. I un record al meu gos per estar sempre de bon humor, tu també ets de la família. Amb cadascú de vosaltres em venen al cap molts moments inoblidables des de sempre fins ara i en seguirem compartint. Vull aprofitar aquesta ocasió per mostrar-vos el meu afecte.

Ana Moragrega Estrany, Barcelona, Setembre de 2015

Contents

List of Figures

Notation

$\mathbb{R}$, $\mathbb{C}$	The set of real and complex numbers, respectively.
$\mathbb{R}^{N\times M}$, $\mathbb{C}^{N\times M}$	The set of $N \times M$ matrices with real- and complex-valued entries, respectively.
$\hat{x}$	Estimation and true value of parameter x.
$\lvert x\rvert$	Absolute value (modulus) of scalar x.
$\lVert\mathbf{x}\rVert$	ℓ^2-norm of vector $\mathbf{x}$, defined as $\lVert\mathbf{x}\rVert = \left(\mathbf{x}^H\mathbf{x}\right)^{\frac{1}{2}}$.
$\dim\{\mathbf{x}\}$	Dimension of vector $\mathbf{x}$.
$\mathrm{Tr}\{\mathbf{X}\}$	Trace of matrix $\mathbf{X}$. $\mathrm{Tr}\{\mathbf{X}\} = \sum_{n=1}^{N}[\mathbf{X}]_{nn}$.
$\det(\mathbf{X})$	Determinant of matrix $\mathbf{X}$.
$\mathrm{diag}(\mathbf{x})$	A diagonal matrix whose diagonal entries are given by $\mathbf{x}$.
$\mathbf{I}$	Identity matrix. A subscript can be used to indicate the dimension.
$\mathbf{X}^*$	Complex conjugate of matrix $\mathbf{X}$ (also applied to scalars).
$\mathbf{X}^T$	Transpose of matrix $\mathbf{X}$.
$\mathbf{X}^H$	Complex conjugate and transpose (Hermitian) of matrix $\mathbf{X}$.
$\mathbf{X}^\dagger$	Moore-Penrose pseudoinverse of matrix $\mathbf{X}$. If $\mathbf{X}$ is $M \times N$, $\mathbf{X}^\dagger = \mathbf{X}^H\left(\mathbf{X}\mathbf{X}^H\right)^{-1}$ if $M \leq N$, $\mathbf{X}^\dagger = \mathbf{X}^{-1}$ if $M = N$, and $\mathbf{X}^\dagger = \left(\mathbf{X}^H\mathbf{X}\right)^{-1}\mathbf{X}^H$ if $M \geq N$.
$\mathcal{N}(\mu, \Sigma)$	Gaussian distribution with mean μ and covariance matrix Σ.
$Log-\mathcal{N}(\mu, \Sigma)$	log-normal Gaussian distribution with mean μ and covariance matrix Σ.
$\ln(\cdot)$	Natural logarithm (base e).
Tr	Trace of a matrix.

Acronyms

ADC	Analogue to Digital Converter.
AWGN	Additive White Gaussian Noise.
BR	Best Response.
CAP	Contention Access Period.
CCA	Clear Channel Assessment.
CDF	Cumulative Distribution Function.
CFP	Contention Free Period.
CRB	Cramér Rao Bound.
CRC	Cyclic Redundancy Check.
CSMA-CA	Carrier Sense Multiple Access with Collision Avoidance.
DSSS	Direct Sequence Spread Spectrum.
DSP	Digital Signal Processor.
ECC	Electronic Communications Community.
ED	Energy Detection.
EKF	Extended Kalman Filter.
EPG	Exact Potential Game.
FDMA	Frequency Division Multiple Access.
FFD	Full Function Device.
FPGA	Field Programmable Gate Array.
GA	Gradient Ascent.
GDOP	Geometric Dilution Of Precision.
GNSS	Global Navigation Satellite Systems.
IoT	Internet of Things.
IR-UWB	Impulse Radio Ultra-Wideband.
LLS	Linear Least Squares.

LNA	Low Noise Amplifier.
LOS	Line Of Sight.
LPL	Low Power Listening.
LQI	Link Quality Indication.
LR-WPAN	Low Rate Wireless Personal Area Network.
LS	Least Squares.
LWLS	Linear Weighted Least Squares.
MAC	Medium Access Control.
MEMS	Micro-Elechtromechanical Systems.
MIMO	Multiple Input Multiple Output.
MPDU	MAC Protocol Data Unit.
ML	Maximum Likelihood.
NE	Nash Equilibrium.
NLS	Non-linear Least squares.
NLOS	Non-Line Of Sight.
NWK	Network.
OPG	Ordinal Potential Game.
PA	Power Amplifier.
PAN	Personal Area Network.
PCB	Printed Circuit Board.
pdf	Probability Density Function.
PHY	Physical.
PoA	Price of Anarchy.
PPDU	Physical Protocol Data Unit.
PPM	Pulse Position Modulation.
PSSS	Parallel Sequence Spread Spectrum.
PSDU	Physical layer Service Data Unit.
PU	Processing Unit.

QoS	Quality of Service.
RAM	Random Access Memory.
RFID	Radio Frequency IDentification.
RF	Radio Frequency.
RFD	Reduced Function Device.
RTOA	Round Trip Time Of Arrival.
RMSE	Root Mean Square Error.
RSS	Received Signal Strength.
RSSI	Radio Signal Strength Indicator.
(SDS) TW-TOA	(Symmetric Double Side) Two-Way Time Of Arrival.
SINR	Signal to Interference plus Noise Ratio.
SNR	Signal to Noise Ratio.
SoC	System on Chip.
SSI	Synchronous Serial Interface.
TDBB	Transceiver Digital Base-Band.
TDMA	Time Division Multiple Access.
TDOA	Time Differential Of Arrival.
TOA	Time Of Arrival.
UWB	Ultra Wide Band.
VHDL	Very high speed integrated circuit Hardware Description Language.
WLAN	Wireless Local Area Network.
WLS	Weighted Least Squares.
WPAN	Wireless Personal Area Network.
WSN	Wireless Sensor Networks.

1 Introduction

WIRELESS sensor networks (WSN) have emerged as a promising technology for a wide variety of low range applications. They consist of small, low-complexity sensor nodes interconnected through wireless links [1]. WSN provide an efficient mean to collect, analyze and transmit data. Thus, WSN allow applications for monitoring, control, automation and actuate in different fields, such as agriculture, industrial environments, home or smart cities.

The ability of sensor nodes to know its position is an enabler for many location-based applications. The reason is that, typically, a sensor position should be known for its data to be meaningful in applications such as monitoring. Other motivations for sensor positioning and localization are geographic routing algorithms. Also in applications like logistics, the position of nodes is in fact the data that needs to be sensed. For example, boxes could be tagged with sensors that could monitor storage conditions and help to control the air conditioning, but also nodes can report their location when the equipment needs to be found.

New applications such as mapping, navigation, location, location based services, monitoring or emergency services with indoor location technologies are arising for smartphones which provides navigation services inside malls, megastores, offices, airports and so on with different technologies (WSN, WIFI, Bluetooth). For indoor applications or outdoor scenarios like city streets, positioning using Global Navi-

gation Satellite Systems (GNSS) cannot be guaranteed due to lack of coverage. In these scenarios, WSN are promising candidates to achieve a high degree of positioning accuracy.

Usually, each sensor node of the WSN has an embedded processor, a hardware accelerator, which implements the physical layer of the protocol stack, a short-range radio communication, a sensor or group of sensors and finally, a power supply source. Power is normally suplied by batteries with a limited life time. The main issue with the performance and viability of such systems is the ability to reduce power consumption. For all these reasons, it is crucial to design very low power nodes and employ energy-efficient protocols and algorithms to maximize the lifetime of the battery.

WSN have limitations in terms of power consumption that are not required in traditional positioning techniques with GNSS. The GNSS module is well-known to be power hungry, therefore power consumption can be an issue in GNSS based techniques for WSN. Thus, other techniques can be used that take advantage of the nature of the WSN. Some approaches such as range-based algorithms rely on distance between nodes that is usually measured with Received Signal Strength (RSS) and Time of Arrival (TOA). Anchor based algorithms rely on some sensors knowing its own location (by means of GNSS, or because they were installed at points with known coordinates) and helping localize other sensors. The coordinates of sensors with unknown location information can be estimated using a positioning algorithm, that uses the available a priori knowledge of positions of anchor nodes in the network. Cooperative localization takes advantage of the peer-to-peer communications to gain additional information of the measurements to anchor nodes but also to unknown sensors. Moreover target nodes that are able to determine their position become anchor nodes, thus providing new references for remaining nodes. With respect to processing strategies, while in centralized algorithms measurements are collected at a central location where they are processed to estimate the position, in distributed strategies the coordinates are estimated locally.

1.1 Motivation and Objectives of the Thesis

The main issue with the performance and viability of WSN is the ability to reduce power consumption. It is important to take into account this constraint in different levels of study or protocol layers. Thus it is crucial to optimize resources, employ energy-efficient standards (IEEE 802.15.4 and 802.15.4a standards and Zigbee specification) and design efficient processing algorithms to maximize the lifetime of the battery. This thesis proposes algorithms and techniques to improve and optimize the

power and energy efficiency in positioning with sensor networks. The requirement of reducing power consumption together with the requirement of accuracy as well as how they are related are studied. This study is done at different layers of the protocol stack.

Due to the nature of WSN, positioning algorithms should be efficient and scalable, therefore they should require little computation and, particularly, little communication. Under these constraints, anchor and range based positioning techniques are good candidates. With these methods, target node coordinates can be estimated using the available a priori knowledge of positions of anchor nodes in the network. Also they allow distributed algorithms to estimate the position. For all these reasons, in this thesis these type of algorithms for positioning are considered.

In WSN, the study to save energy and power has been addressed from a crosslayer point of view. In this work, there are different levels or protocol stack layers of optimization to save power consumption in positioning. In Physical layer, the objective is to optimize resource allocation such as transmit power maintaining a certain level of accuracy. Distributed algorithms are designed based on Game Theory. In network and Medium Access Control (MAC) level, the objective is to study how topology and MAC parameters affects to the anchor and range-based positioning and how this type of positioning can be performed with some MAC protocols. We also address with topology formation (clustering algorithm) for distributed positioning. In general, these optimizations used to satisfy the condition of energy efficiency can affect the accuracy of the position estimation. Thus, from a general point of view, we focus on the study of the trade-off between energy consumption and accuracy of the position estimation. Specific objectives of this proposal are described in the following paragraphs.

In Physical layer, we study the optimization of resource's utilization and the related trade-off between position accuracy and energy consumption. Chapter 4 and Chapter 5 address this issue. They focus on transmit power in anchor and range based positioning. In this type of positioning anchor sensor nodes make a big effort transmitting ranging signals needed for positioning. However there are target nodes that are positioned with enough accuracy and do not need more ranging information from more anchor nodes. Therefore a tradeoff exists between transmit power and positioning performance: if an anchor node transmits with lower power, it will reach a smaller number of sensors, and those left outside coverage will obtain a worse position estimate. Here arises one objective of this PhD dissertation that is the minimizing the transmitted power of anchor nodes in order to maximize their battery life. Moreover, anchor nodes that are not needed can go to low power mode. Therefore, these anchor nodes save transmit power, but also they save the energy needed to access to the medium with a corresponding protocol and optimize needed communications. For

this objective, we propose distributed game theoretical approaches taking advantage of the nature of WSN. Game Theory is an interesting collection of models and analytic tools used to study interactive and distributed decision processes [2] that can be applied to our objective. The ranging techniques considered are RSS and TOA based ones. The considered error model in the distance estimation with RSS depends on the actual distance between transmitter and receiver. Due to this dependence a potential game is used in Chapter 4. In Chapter 5, a supermodular game is proposed that is suitable for TOA based positioning.

At the MAC and network layers, we study the effect of different topologies and MAC protocols in the performance of positioning algorithms. In this direction and due to the advantages of the standards in terms of energy consumption, the formation of complex networks and routing facilities, Chapter 6 focuses on studying the performance of anchor and range based positioning on mesh and cluster-tree topologies that are defined in 802.15.4/Zigbee and 802.15.4a standards. The success of this type of positioning depends on the connectivity. Mesh topology allows high connectivity but is energy consuming. Cluster-tree topology is more energy efficient but the connectivity between nodes is limited to parent-children relationships. A cluster-tree formation algorithm is proposed that allows good positioning performance increasing the connectivity between anchor and target nodes.

To sum up, the objectives of this thesis are:

- A review of positioning algorithms for WSN, with advantages and disadvantages. Range and anchor based positioning is selected because of its scalability, accuracy and low complexity. Moreover, an analysis of non-cooperative Game Theory is presented.
- The minimizing of the transmit power of the anchor nodes while a certain level of accuracy is maintained. Node selection, the anchor nodes that are not needed can go to low power mode saving energy.
- An study of the performance of anchor and range based positioning on mesh and cluster-tree topologies that are defined in 802.15.4/Zigbee and 802.15.4a standards. To improve range based positioning on cluster-tree topology and to perform an algorithm for cluster-tree formation that allows good positioning.

1.2 Outline

This PhD dissertation focuses on the design and analysis of techniques for power and energy saving in positioning with WSN. It is organized as follows:

Chapter 2 and Chapter 3 provide the reader with some background on the concepts which are a prerequisite to subsequent chapters. There are three main topics to be used throughout the dissertation. First, in Chapter 2, a general overview of sensor networks is provided. Main strategies to save power and energy are explained at each layer of the protocol stack. A short review of IEEE 802.15.4 standard is presented. Second, ranging and positioning with WSN is revisited. Ranging with RSS and TOA techniques as well as a classification of algorithms for positioning are explained. Third, in Chapter 3, non-cooperative Game Theory is revisited with focus on Potential and Supermodular games.

Chapter 4 and Chapter 5 are devoted to the optimization of power and energy consumption in positioning with WSN from a Physical layer point of view. We resort to Game Theory for the optimal resource allocation of transmit power and anchor selection. More specifically, in Chapter 4, we consider a scenario where some target sensor nodes obtain position estimation with ranging signals from anchor sensor nodes. RSS technique is assumed. Our goal is to optimize the power and energy consumption of the anchor sensor nodes maintaining enough accuracy in positioning of target nodes. It is a distributed optimization problem in which anchor nodes and their power are selected based on error metric. We provide a game theoretical solution with a non-cooperative potential game. The error metric is a global metric with all the information of the network. It is based on GDOP for RSS case that depends on geometry of the anchor nodes and the distance between target and anchor nodes. Furthermore, we consider two distributed error metrics, first, an average metric with local information, second, a local metric based on worst case GDOP. Next, a possible solution to implement the distributed algorithm is explained as well as its computational complexity analysis. The performance of the distributed algorithm with the global and local metrics is assessed in two scenarios: a static scenario in which target nodes estimate its position with Least Squares (LS) algorithm, and moving one in which an extended Kalman filter is used for tracking.

Chapter 5 is a natural extension of Chapter 4. In Chapter 5 we also consider a scenario where some target sensor nodes obtain position estimation with ranging signals from anchor sensor nodes. While in Chapter 4 was considered RSS ranging technique, in Chapter 5, TOA based technique is performed for positioning. Again, the aim is to identify the minimum transmit power and optimal group of anchor nodes for positioning with enough accuracy in TOA ranging positioning. In this case the error metric GDOP is related to Cramér Rao Bound (CRB) on the variance of a position estimator. The error metric depends inversely on the transmit power of the anchor nodes. We propose a supermodular game that determines the trade-off between transmit power and error. We prove the game is supermodular and the uniqueness of Nash equilibrium (NE). Moreover, we extend our analysis to

multiple target nodes. Next, we present a possible implementation of the distributed algorithm and its computational complexity. Finally, we assess the performance of the algorithm in scenarios with multiple target nodes.

Chapter 6 addresses the problem of optimizing the energy of sensor nodes in positioning with WSN from a MAC and higher layer point of view. We study the anchor and range based positioning performance in different topologies of standards. Cluster-tree topology tends to limit connectivity between nodes to save energy. As a result, the performance of anchor and range based positioning is poor. The goal of the chapter is to propose techniques to increment the connectivity between nodes. Moreover, we propose a network formation algorithm that increases the probability of positioning based on range. Graph theory is used. The network formation algorithm is also explained in a mobile WSN. The techniques and algorithm are assessed with simulations.

Finally, Chapter 7 concludes the dissertation with a summary of the contributions, conclusions and guides for future research. At the end of the document, the list of publications performed during the PhD are presented. Moreover, at the end of each chapter the publications related to the particular topics are provided.

2

Wireless Sensor Networks and Positioning

IN this chapter, we provide an overview of concepts which will be used throughout this dissertation. First, in Section 2.1, we provide an overview of WSN, energy saving strategies and IEEE 802.15.4 standard. Then, in Section 2.2, techniques and processing algorithms for ranging and positioning in WSN are discussed. Finally, in Section 2.3, we present GDOP metric.

2.1 Overview of Wireless Sensor Networks

In last decade the increase of Wireless Sensor Networks (WSN) has come due to the rapid advances in embedded microprocessors, wireless technologies, micro-electromechanical systems (MEMS) and sensors. Thus, around 2000 appeared first commercial motes that included the well known IEEE 802.15.4 compliant transceiver CC2420 [3] from Texas Instruments for low-rate wireless personal area networks. An example was TelosB from Crossbow (2004) that included CC2420 transceiver with a data rate of 250 kbs and a transmission range of 50m in indoors and 125m in outdoors with an integrated onboard antenna. Usually, each sensor node of the WSN

consists of an embedded processor, a radio subsystem for wireless data communication, a sensor or group of sensors and finally, a power supply source. The main digital blocks of a sensor node are the embedded processor such as a microcontroller and the communication subsystem like a radio chip. These main blocks are shown in Figure 2.1.

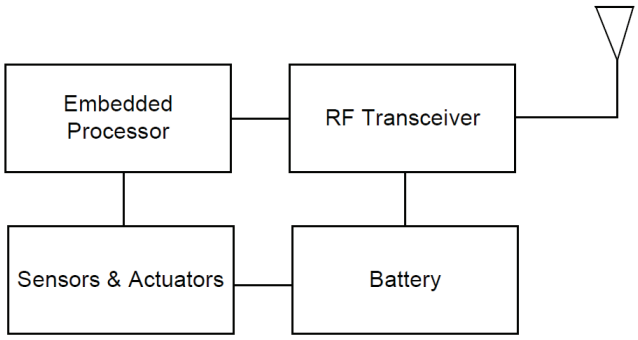

Figure 2.1: Main blocks of a commercial sensor mote.

Different motes have been developed for WSN. Low complexity commercial nodes are Mica (2002), Mica2 (2003), MicaZ (2004), TelosB (2005) from Crossbow, Tmote (2004) from Moteiv, Z1 (2010) from Zolertia, WiSense (2014) etc. [4]. Most of them are low powered, low complex motes equipped with CC2420 radio chips and low power MSP430xx microcontrollers from Texas Instruments. CC2420 is an IEEE 802.15.4 compliant Radio Frequency (RF) transceiver that performs the functionalities of Physical and MAC layer of this communication standard. MSP430xx low powered microcontroller is the control and processing unit of the mote. The user programs the required application in the microcontroller through different interfaces. There are two main operating systems, that are open source, namely TinyOS and Contiki. For more complex functionalities there are other motes that include powerful microcontrollers with more memory and power consumption. Furthermore, other motes include CC2538 that is a powerful System-On-Chip for 2.4-GHz IEEE 802.15.4-2006 and ZigBee applications. The device combines a powerful ARM Cortex-M3-based MCU system with up to 32KB on-chip RAM and up to 512KB on-chip flash with a robust IEEE 802.15.4 radio. In [5], an implementation of an IEEE 802.15.4 compliant sensor node is presented. It is an example of design and development of a mote. In [6], a comparative analysis of sensor motes is presented based on their main features: qualitative parameters such as battery capacity, computational logic like microprocessor and memory, software support, radio modules, onboard sensors and power source. The selection of a mote depends on the application and project requirements.

The power supply normally consists of batteries with a limited lifetime, although energy harvesting blocks can extend battery life. Therefore the main issue of the performance and viability of such systems is the ability to reduce their power consumption. For all these reasons, it is crucial to design low power nodes and employ energy-efficient protocols and related algorithms to maximize the lifetime of the battery.

2.1.1 Energy Saving Strategies in WSN

Energy costs in WSN can be classified under data transmission/reception, data processing, and data acquisition or sensing. Data acquisition and transmission/reception consume significantly more energy than data processing as it is shown in [7]. The energy wasted in transmission and reception depends on the used protocol. Therefore, energy efficient aspects must be addressed as a topic that affects different layers of the protocol stack [1]. In this section we provide a brief explanation of the functionalities given by each layer. Moreover, energy costs and its efficient solutions are discussed.

Physical Layer and Hardware

Hardware is composed of the analog and digital blocks. The Physical layer deals with transmitting bits reliably over a point-to-point wireless link. From this layer point of view, the techniques to save energy take into account the optimization of resources, for example the power. Moreover, other possible causes of power and energy consumption are the used modulation, coding, diversity, MIMO, equalization, multi-carrier modulation, spread spectrum and hardware design. With respect to the power supply, energy harvesting techniques extend the lifetime of batteries taking energy from the environment or other energy sources that can be converted to electrical energy. Therefore, energy harvesting techniques affect the tradeoff between performance parameters and lifetime of sensor nodes [8].

With respect to the optimization of resources, transmission power control minimizes power consumption while avoiding collisions. From a physical layer perspective, performance is generally estimated as a function of Signal to Interference plus Noise Ratio (SINR). Thus, in general, in power control problems, the quality of service (QoS) requirements are formulated as constraints of the SINR of each user.

Another method to optimize resources is duty cycling. Normally, the communication subsystem (radio chip) of a sensor node has an energy consumption much higher than the computation subsystem (microcontroller). Therefore, from the sensor node structure level, the most effective energy-conserving operation is putting

the radio transceiver in a low power mode when communication is not required. In this way nodes alternate between active and low power periods depending on network activity. For example, for the MSP430 microcontroller the current consumption is around 200μA in active mode and for the radio CC2420, the current consumption is 19.7 mA in reception and 17.4 mA in transmission (maximum transmitted power). Usually, the sensor motes can work in different states depending on the states of the transceiver and the microcontroller. For example, the MSP430 microcontroller [9] has the active mode and five low power modes (LPM0-4) that consume less power when less parts and clocks are active (32μA for LMP0 and 0.1μA for LMP4). The main states of the radio chip, usually are the following: transmission and reception (communication module on), idle (radio is not receiving or transmitting) and sleep (communication module off). For example, for the CC2420 radio typically the current consumption for idle state is 426μA.

The radio module of a sensor node consists of the main blocks shown in Figure 2.2 [10].

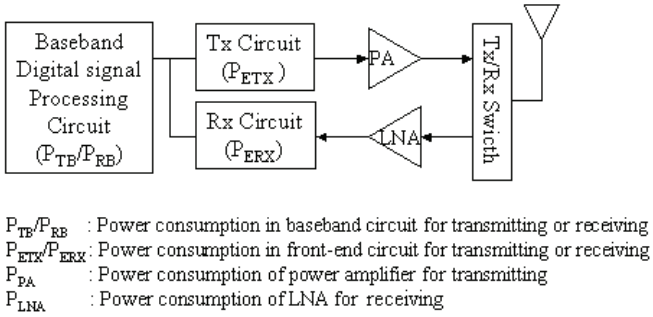

Figure 2.2: Communication module scheme.

Based on this structure and the power consumption of each component, the power consumption for transmit mode P_{TX}, receive mode P_{RX}, idle mode P_{ID} and sleep mode P_{SL} take the form [11]:

$$\begin{aligned} P_{TX} &= P_{ETX} + P_{TB} + P_{PA} \\ P_{RX} &= P_{ERX} + P_{RB} + P_{LNA} \\ P_{ID} &\approx 0 \\ P_{SL} &\approx 0 \end{aligned} \tag{2.1}$$

where the consumed power in idle mode (P_{ID}) is negligible. Also P_{ETX} and P_{TB} can be modeled as a constant P_{TX0} because these components do not depend on the transmission range; similarly, P_{ERX}, P_{RB} and P_{LNA} can be modeled as a constant P_{RX0}.

$$P_{TX} = P_{TX0} + P_{PA}$$

$$P_{RX} = P_{RX0} \tag{2.2}$$

The effect on the total power depends on the relative importance of P_{PA} power consumption and electronics power consumption P_{TX0}. Short range systems such as WSN are typically not P_{PA} dominated. Therefore the best way of saving energy is turning the radio to idle mode which is the low power mode of the radio chips.

Some researchers have worked on energy consumption models applied to cooperative WSN [12] [13], multihop WSN [14] or cross-layer analysis for WSN energy efficiency [15]. In [12] they considered that the power consumption of the communication module depends on the power consumption of RF circuits and the power amplifier (PA). In [12], [14] and [15] they argued that PA power consumption grows linearly with the transmit power and that the PA drain efficiency is constant. However in [10], it was shown that drain efficiency of most types of PA vary when output power increases. Moreover, in [10] the power consumption model considered the front-end circuits and the power amplifier, but also the baseband circuits. In [11], we presented a power consumption model for WSN transceivers, including the communication hardware components and the modes of operation. The power consumption for transmitting is modeled by the output power and the drain efficiency of the power amplifier, considering drain efficiency is a linear function of output power. Power consumption model parameters are extracted for a commercial sensor node. This model is applied on a WSN based on cooperative clusters to obtain the outage performance of the cooperative model and the optimal node number per cluster.

MAC Layer

The Medium Access Control (MAC) layer controls how different users share the given spectrum and ensures reliable packet transmissions. Thus the error control is studied with different coding schemes for error correction and there are different MAC protocols that take into account the Physical layer resources. From a MAC point of view, useful energy consumption can be due to the following main causes:

- Data transmission or reception, processing query requests and data forwarding to neighboring nodes.
- Listening to an idle channel in order to receive possible frames (idle listening).
- Collision.
- When a node receives packets that are intended for other nodes, it is named overhearing.
- Control-packet overhead, that can be avoided minimizing of control packets for data transmission.

- Over-emitting, which occurs when a frame is transmitted and the destination node is not ready [16].

The design of efficient protocols that take into account the previous facts and the active/low power scheduling is the best way to prevent these energy waste.

As sensor nodes perform a cooperative task, they need to coordinate their active/low power periods with a scheduling algorithm allowing neighboring nodes to be active at the same time. The protocols with active/low power scheduling can be classified into the following categories: i) scheduled protocols, ii) protocols with common active periods, iii) asynchronous duty-cycling protocols and iv) hybrid protocols.

i) *Scheduled protocols* [17] follow a reservation based approach. Such medium access control protocols are TDMA (Time Division Multiple Access) combined with FDMA (Frequency Division Multiple Access) where different time slots and frequency channels can be used by different nodes. TDMA is attractive because minimizes collisions, overhearing, and idle listening. Flexibility and scalability are the main challenges of these protocols.

ii) In *protocols with common active periods*, nodes maintain a certain level of synchronization to keep active/low power periods common to all nodes. In this type of protocols, nodes access the medium using contention-based approaches. An example is CSMA (Carrier Sense Multiple Access) scheme in which a node first senses the channel before transmitting. In the case that the node finds the channel busy, it postpones its transmission to avoid interfering. After a random time, if the node finds the channel clear, it starts transmitting. The contention-based approach achieves its highest performance in applications in which traffic is periodic such as monitoring. But the use of common active/low power periods of a fixed size reduces flexibility. The difficulty is determining suitable length of active periods taking into account idle listening and collisions. An example that minimizes this drawback is TMAC (Timeout MAC) that proposes the variation of the duration of active periods depending on the traffic and thus adapting the duty-cycle.

iii) In *asynchronous duty-cycling protocols* [18] nodes do not maintain common active periods. Thus each node can wake up independently of the others, but the protocols guarantee that neighbors always have overlapping active periods within a specified number of cycles. Preamble-sampling protocols fall in this category [17] in which a node transmits long discovery frames and the receiver listening time is very short. The transmitted frame length (with long enough preamble) is higher than the duration between two periodic listening intervals. An example is LPL (Low Power Listening). This technique reduces synchronization overhead and saves energy, but long preambles can cause collisions in applications with high traffic. Also the duty cycle of the receivers is limited by the transmitted frame length. For example, BMAC

minimizes this limitation with versatile low power listening in which each node can configure dynamically several MAC layer parameters, such as the duration between two periodic listening periods.

iv) There are *hybrid protocols* [17] that combine the characteristics of the described protocols to achieve high performance under variable traffic situations. The principal example of this type of protocols is the IEEE 802.15.4 standard. It proposes a flexible MAC with two modes of operation: beacon-enabled mode that is based on a scheduled protocol, and non-beacon mode based on Carrier Sense Multiple Access with Collision Avoidance (CSMA-CA) protocol. Beacon-enabled mode allows an active period in which there is a Contention Access Period (CAP) and a Collision Free Period (CFP) with guaranteed time slot transmission. During the CAP period nodes access to the medium with CSMA-CA protocol, while CFP operates under the reservation based approach. IEEE 802.15.4e was originally intended to amend 802.15.4-2006 to better support the industrial markets. The Time Synchronized Channel Hopping MAC enables high reliability while maintaining very low duty cycles and maximizing power efficiency.

Higher Layers

Network layer establishes and maintains end-to-end connections in the network. In this layer data aggregation is a method in which intermediate nodes may aggregate redundant data from sensors into a single frame to reduce transmissions and total data size, while network coding can reduce traffic by mixing of data at intermediate network nodes. Moreover efficient routing [17] and clustering algorithms (topology formation) [19] can save energy consumption.

Upper layers are defined by other specifications like Zigbee. ZigBee is the only open, global wireless standard to provide the foundation for the Internet of Things (IoT) by enabling simple and smart objects to work together. The IEEE 802.15.4/Zigbee 2004 protocol stack is shown in Figure 2.3. IEEE 802.15.4 defines Physical and MAC layers, while Zigbee 2004 defines the network (NWK) and application layers. Application layer of last Zigbee specification is intended for low-power, low-cost, low-complexity networking for the IoT with applications such as building automation, health care or services as indoor location.

Processing Algorithms

The processing algorithms process and analyze the data transmitted and received over the network for the selected application. They could use or modify parameters from other layers. As example, power control algorithms control transmit power from Physical layer. Therefore, the processing and control algorithms are designed for an objective or application. They may use the nodes in an energy efficient way,

taking into account the energy consumption causes and solutions of the other layers. Moreover, it is desirable that they minimize communications, data processing and acquisitions to save energy while maintaining the functionality required by the application.

Due to the interdisciplinary nature of sensor network design, the layers are not isolated from each other. Therefore, the parameters optimized in Physical layer to save energy can affect the MAC layer configuration and also the performance of the processing. Thus, for example the optimization of resources in Physical layer such as power may affect the functionality of the processing algorithm. If the processing is designed for positioning, a tradeoff also exists between the optimization of resources and positioning performance.

2.1.2 Overview of IEEE 802.15.4 Standard

IEEE 802.15.4 specifies the Physical and MAC layers for low-rate wireless personal area networks (LR-WPANs). IEEE 802.15.4a also specify Physical and MAC layers but being an amendment to IEEE 802.15.4 specifying two additional physical layers as it is commented after. In 802.15.4 [20], two types of devices, reduced function device (RFD) and full function device (FFD) are defined, where only an FFD may be the coordinator of a personal area network (PAN) or cluster. The IEEE 802.15.4/Zigbee 2004 protocol and IEEE 802.15.4a stacks are shown in Figure 2.3.

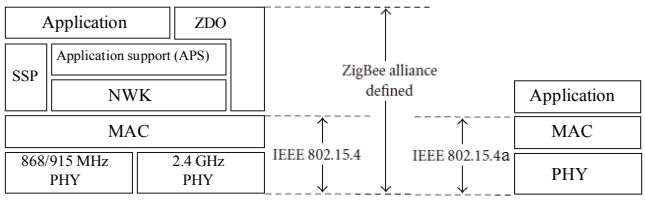

Figure 2.3: IEEE 802.15.4/Zigbee 2004 protocol stack and IEEE 802.15.4a stack.

The Physical layer provides the data transmission service, as well as the interface to the Physical layer management entity, which offers access to every layer management function and maintains a database of information on related personal area networks. Thus, the Physical layer manages the physical RF transceiver and performs channel selection, medium status measurement and signal management functions. It operates on one of three possible unlicensed frequency bands:

- 868.0-868.6 MHz: Europe, allows one communication channel

- 902-928 MHz: North America, up to thirty channels
- 2400-2483.5 MHz: worldwide use, up to sixteen channels

The 868/915 MHz bands support a rate of 100 and 250 kbit/s, respectively. Also the standard defines four Physical layers depending on the modulation method used. Three of them are based on direct sequence spread spectrum (DSSS) techniques: in the 868/915 MHz bands, using either binary or offset quadrature phase shift keying (the second of which is optional); in the 2450 MHz band, using the latter. An alternative, optional 868/915 MHz layer is defined using a combination of binary keying and amplitude shift keying (thus based on parallel, not sequential spread spectrum, PSSS).

The MAC layer defined by the 802.15.4 standard [20] specifies two modes of operation: beacon-enabled and non-beacon. In the non-beacon mode, Carrier Sense Multiple Access with Collision Avoidance (CSMA-CA) is used, which requires long listening periods which decrease the energy efficiency of the protocol. The beacon-enabled mode improves energy efficiency by defining a so-called superframe that contains the synchronization beacon, followed by a contention access period (CAP), and an optional contention free period (CFP). During the CAP, the channel is accessed using slotted CSMA-CA.

The 802.15.4/Zigbee standard supports star and peer-to-peer topologies. Within peer-to-peer topologies, we distinguish between mesh and cluster tree networks. In a mesh network, any sensor may communicate with any other sensor within its range. In a cluster-tree network, sensors are then grouped in clusters where a coordinator is the cluster head and several other devices are leaf or child nodes.

Data frame structure of the protocol consists of a Physical packet and a MAC data frame. The MAC data frame is passed to the Physical layer as the Physical layer Service Data Unit (PSDU), which becomes the Physical payload [20]. Figure 2.4 shows the frame format of the IEEE 802.15.4.

IEEE 802.15.4e specifies a MAC amendment to IEEE 802.15.4. It provides a better support for industrial markets and includes changes like deterministic and synchronous multi-channel extension mode and time slotted channel hopping mode.

Furthermore, IEEE 802.15.4f is an standard for local and metropolitan area networks with Active Radio Frequency Identification (RFID) System Physical Layer (PHY). It provides two PHYs, Minimum Shift Keying (MSK) and Low Rate Pulse Repetition Frequency LRP UWB, that can be used in a wide range of applications requiring various combinations of low cost, low energy consumption, multiyear battery life, reliable communications, precision location, and reader options.

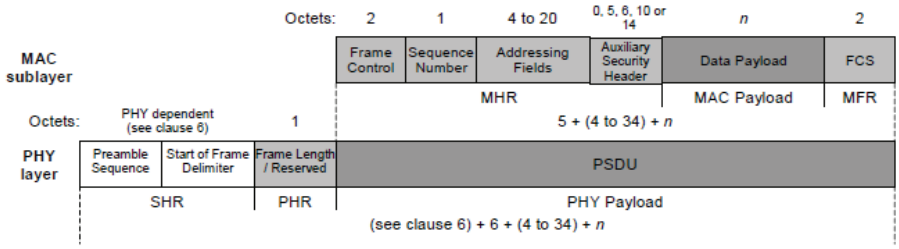

Figure 2.4: Schematic view of the data frame and the Physical packet from IEEE 802.15.4 standard.

2.2 Positioning in Wireless Sensor Networks

During last decade, a number of positioning algorithms and ranging techniques have been proposed for WSN [21] and indoor positioning [22]. In this Section we introduce the main ranging techniques, the IEEE 802.15.4a standard, a classification of positioning algorithms and the cooperative, anchor, range based positioning that allows distributed algorithms.

2.2.1 Received Signal Strength Based Ranging

Ranging with Received Signal Strength (RSS) based techniques presents some challenges. RSS measurements are readily available by all common wireless transceivers, but they may yield large ranging errors.

RSS estimates the range directly with the attenuation of emitted signal strength that decreases with the distance. With theoretical and empirical models such as path loss model, the difference between the transmitted signal strength and the received signal strength is translated into a range estimate. RSS based ranging technique is enabled by IEEE 802.15.4 and IEEE 802.15.4a compliant nodes. The necessary hardware is simple, thus most commercial wireless devices such as WSN nodes include the possibility of measuring RSS. The drawback of this method is due to the possible severe multipath fading and shadowing present in the indoor environments which results in variability to propagation loss and errors in range estimation. Channel hopping was studied for WSN and it is applied in the IEEE 802.15.4e standard. It is known that multipath fading can be improved by switching the communication carrier frequency. The averaging of the RSS values reduces its standard deviation when samples are collected over different frequency channels in a short time period, rather than on a single channel but over a longer time interval [23].

In the literature different approaches have been studied to model the path loss. RSS based ranging measures are commonly modeled using the one-slope log-normal path loss model [24]. However, in [25], we studied a two-slope RSS channel model and compared its validity to classical one-slope path loss model with real data. Furthermore, other distributions were studied as in [23]. We consider the common one-slope log-normal path loss model [24], defined as,

$$L_{j,i} = L_o + 10\eta \log_{10}\left(\frac{\rho_{j,i}}{\rho_o}\right) \ . \tag{2.3}$$

Where the geometrical distance between the target node j and the i-th anchor is defined as

$$\rho_{j,i}(\mathbf{x}) = \| \ \mathbf{x}^{(j)} - \mathbf{x}_a^{(i)} \ \|, \ i = 1, \ldots, N \ , \tag{2.4}$$

with $\| \cdot \|$ being the Euclidean norm in $\mathbb{R}$. The two-dimensional coordinates of the j-th target node and i-th anchor node may be

$$\mathbf{x}^{(j)} = [x^{(j)}, y^{(j)}]^T \qquad j = 1, \ldots, M \tag{2.5}$$

$$\mathbf{x}_a^{(i)} = [x_a^{(i)}, y_a^{(i)}]^T \qquad i = 1, \ldots, N \ . \tag{2.6}$$

Moreover, ρ_o is a reference distance, L_o is the attenuation at such reference distance in dB, $L_{j,i}$ the path loss for the distance $\rho_{j,i}$ in dB, and η the path loss exponent (typ. 3 in our scenarios). Notice that $L_{j,i} = P_{Tx,i} - P_{Rx,j}$, where $P_{Tx,i}$ and $P_{Rx,j}$ are the transmitted and received powers in dBm for the pair $\{j, i\}$, respectively. In a real environment, the path loss may have a random contribution, which is modeled in dBm by $\upsilon_{j,i} \sim \mathcal{N}(0, \sigma_{j,i}^2)$. Then

$$P_{Rx,j} = P_{Tx,i} - L_o - 10\eta \log_{10}\left(\frac{\hat{\rho}_{j,i}}{\rho_o}\right) + \upsilon_{j,i} \ , \tag{2.7}$$

where $\hat{\rho}_{j,i}$ is the estimated distance, $\sigma_{j,i}$ is due to the fading effects in static and dynamic environments (node movement or environment changes, e.g. people movement). It is known that multipath fading can be overcome by switching the communication carrier frequency. Channel hopping was studied for WSN and it is applied in the IEEE 802.15.4e standard. The averaging of the RSS values reduces its standard deviation when samples are collected over different frequency channels in a short time period, rather than on a single channel but over a longer time interval [23].

Rearranging terms in (2.7) we obtain a distance estimate

$$\hat{\rho}_{j,i} = \rho_o \cdot 10^{\frac{L_o - L_{j,i} + \upsilon_{j,i}}{10 \cdot \eta}} \ . \tag{2.8}$$

From (2.3), $\rho_{j,i} = \rho_o \cdot 10^{\frac{L_o - L_{j,i}}{10 \cdot \eta}}$ that we use to obtain the observation equation for RSS-based ranging

$$\hat{\rho}_{j,i} = \rho_{j,i} \cdot 10^{\frac{\upsilon_{j,i}}{10 \cdot \eta}} \ . \tag{2.9}$$

It becomes clear that it depends on a log-normal random variable $\omega \sim Log - \mathcal{N}(\mu_\omega, \sigma_\omega^2)$ as

$$\hat{\rho}_{j,i} = \rho_{j,i} \cdot \omega \ , \tag{2.10}$$

where $\mu_\omega = 0$ and $\sigma_\omega^2 = (e^{\sigma_\xi^2} - 1)e^{2\mu_\xi + \sigma_\xi^2} = (e^{\sigma_\xi^2} - 1)e^{\sigma_\xi^2}$. Recall that the logarithm of a log-normal random variable is normally distributed. Thus, if ω is distributed log-normally, then ξ is a normal random variable as $\xi = \ln(\omega) \sim \mathcal{N}(\mu_\xi, \sigma_\xi^2)$. Therefore,

$$\xi = \ln \omega \sim \mathcal{N}\left(0, \left(\frac{\ln 10 \cdot \sigma_{j,i}}{10 \cdot \eta}\right)^2\right) \ , \tag{2.11}$$

where $\mu_\xi = 0$ and $\sigma_\xi = \frac{\ln 10 \cdot \sigma_{j,i}}{10\eta}$. Therefore, the variance of the distance estimation $\hat{\rho}_{j,i}$ may be

$$\sigma_{\hat{\rho}_{j,i}}^2 = \rho_{j,i}^2 \cdot (e^{\sigma_\xi^2} - 1)e^{\sigma_\xi^2} \ . \tag{2.12}$$

In fact, the CRB for a distance estimate from RSS measurements provide the following inequality [26]:

$$\sqrt{\sigma_{\hat{\rho}_{j,i}}^2} \geq \frac{\ln 10 \cdot \sigma_{j,i}}{10\eta} \rho_{j,i} \ . \tag{2.13}$$

From the previous equations, it can be noticed that the variance of the distance estimation $\hat{\rho}_{j,i}$ between target j and anchor node i is proportional to the distance between both nodes. Therefore, larger distances cause higher error in distance estimation. Moreover, the variance also depends on the channel parameters.

2.2.2 Time of Arrival Based Ranging

In Time Of Arrival (TOA) based ranging the distance is estimated by multiplying the radio signal velocity and the travel time. The main techniques are TOA, Roundtrip Time of Arrival (RTOA) and Time Difference of Arrival (TDOA). With the TOA technique one-way propagation time is measured between transmitter and receiver. But all transmitters and receivers have to be precisely synchronized. This drawback can be improved with RTOA estimation, which measures the time-of-flight of the signal traveling from the transmitter to the measuring unit and back. With TDOA technique, the difference in time at which the signal arrives at multiple measuring nodes is measured to determine the relative position of the mobile transmitter.

The errors in distance estimation with TOA based techniques have different origins. The signal traveling between sensor nodes is affected by the environment and obstacles, e.g., objects, people and walls, causing multipath propagation. When the direct path is blocked, the distance measured between sensor nodes will be affected

by Non-Line Of Sight (NLOS) error. There are works in the literature that address positioning taking into account NLOS, but in general, it is an ongoing challenging topic because statistics of NLOS errors may be unknown in real scenarios. The distance estimate by sensor nodes can be expressed as

$$\hat{\rho}_{j,i} = \rho_{j,i}(\mathbf{x}) + b_{j,i} + \nu_{j,i}, \tag{2.14}$$

where $b_{j,i}$ and $\nu_{j,i}$ are the NLOS error and measurement error, respectively. In the literature different distributions have been proposed to model the NLOS error e.g., an exponential distribution or a uniform distribution [27]. Distance estimation is also affected by the clock of the systems. The distance between two sensors is computed with the velocity and the travel time of a signal from one node to another one. Thus, the time of flight depends on parameters like channel behaviors or turn-around time in one of the nodes for two-way ranging. The TOA is measured with respect to the local clocks of the nodes. Therefore, any delay or clock imperfection can affect the accuracy of range estimate. The behavior of the local clock of a sensor node is modeled in the literature in terms of offset and clock skew [28].

Normally, ranging with TOA based techniques with UWB is a much more robust ranging technique against multipath than RSS based since the large bandwidth of an UWB signal provides high time resolution [21]. The effect of fading can be diminished by using a spread-spectrum method (e.g., direct-sequence or time hopping) that averages the received power over a wide range of frequencies. A simple protocol determines the range between two UWB transceivers via two-way exchange of a frame and tracking its RTOA. The ranging performance depends on how accurate TOA can be estimated by the processing algorithms. When there is no common timing reference, clock offset between the transceivers appears affecting the range measurement. The IEEE 802.15.4a [29] standard defines a mandatory ranging protocol called Two-Way Time Of Arrival (TW-TOA) and an optional Symmetric Double Sided (SDS) TW-TOA protocol that reduces the effect of imperfect timing reference [29]. Both protocols are shown in Figure 2.5, and are explained in the sequel.

Distance estimation with the TW-TOA protocol is performed using D1 and A1 messages as

$$\hat{\rho}_{j,i} = \frac{c \cdot \text{TOA}}{2} = \frac{c \cdot (\text{Tr'} - \text{Tta})}{2} \,. \tag{2.15}$$

While distance estimation with the SDS TW-TOA protocol is performed using D1, A1 and D2 messages as

$$\hat{\rho}_{j,i} = \frac{c \cdot \text{TW-TOA}}{4} = \frac{c \cdot (\text{Tr'} - \text{Tta} + \text{Tr} - \text{Tta'})}{4} \,, \tag{2.16}$$

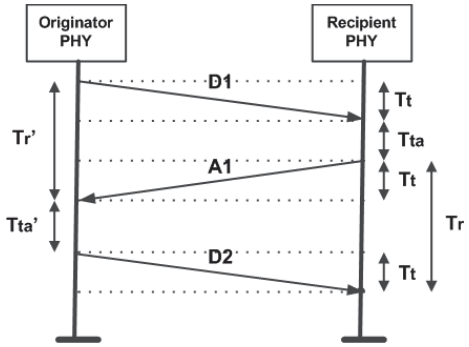

Figure 2.5: Illustration of the ranging protocols supported by the IEEE 802.15.4a standard.

with c being the speed-of-light and the factor 4 in the denominator stemming from the fact that two round trip times (with independent TOA error) are used to obtain a distance estimate with the SDS TW-TOA ranging protocol [1].

We consider the LOS common model with TOA based ranging that considers noisy range measurements as

$$\hat{\rho}_{j,i} = \rho_{j,i}(\mathbf{x}) + \nu_{j,i}, \tag{2.17}$$

where $\nu_{j,i} \sim \mathcal{N}(0, \sigma^2_{\rho_{j,i}})$ and where the standard deviation of the observations depends on the standard deviation of TOA measurements σ_{TOA_i} as [26]

$$\sigma_{\rho_{j,i}} = \frac{c \cdot \sigma_{TOA_i}}{4} \ , \tag{2.18}$$

when using SDS TW-TOA ranging protocol.

The algorithms to estimate TOA are based on time and frequency domain [26], [30]. For time domain, several authors addressed an approach that consists on a two step TOA estimation process with an initial coarse estimation of the TOA followed by a higher resolution stage [30].

For a single-path additive white Gaussian noise (AWGN) channel (clock jitter is not considered), the squared CRB for TOA [26] is given by

$$\sigma_{TOA} \geq \sqrt{\frac{1}{8\pi^2 B \ SNR}} = \sqrt{\frac{N_0}{8\pi^2 B \ L_i p_i}} \ , \tag{2.19}$$

where $L_i = (4\pi\rho_i/\lambda)^2$ is the path loss, p_i the transmitted power of the i-th sensor node, N_0 the noise spectral density and B is the effective (or root mean square)

[1] In this case we assume no deviation from the nominal frequency in the sensor clocks, which would further increase the error.

signal bandwith defined by

$$B^2 = \frac{\int_{-\infty}^{\infty} f^2 |S(f)|^2 df)}{\int_{-\infty}^{\infty} |S(f)|^2 df} \ , \tag{2.20}$$

where $S(f)$ is the Fourier transform of the transmitted signal. Achievable accuracy under ideal conditions is very high, for example, with a receive UWB pulse of 1.5 GHz bandwidth and SNR=0 dB, an accuracy of less than 3 cm can be obtained [26]. However, clock synchronization between the nodes affects TOA estimation accuracy, thus techniques to reduce them should be used like SDS TW-TOA protocol. Therefore, we calculate the CRB with SDS TW-TOA protocol, from (2.18), the squared CRB of σ_{ρ_i} is given by

$$\sigma_{\rho_i} = \frac{c \cdot \sigma_{TOA}}{4} \geq \sqrt{\frac{c^2}{16\pi^2 B \ SNR}} = \sqrt{\frac{c^2 N_0}{16\pi^2 B \ L_i p_i}} \ . \tag{2.21}$$

Note that CRB of TOA (2.19) and CRB of the distance with SDS TW-TOA (2.21) depend on the SNR and the effective signal bandwidth. Since the CRB depends on bandwith inversely, TOA based ranging with high bandwith technologies, such as UWB, achieves higher accuracy. The accuracy can be improved by increasing the SNR which value is influenced by metrics: transmit power p_i, modulation, rate, etc. Thus, when increasing the distance between both nodes, the received power decreases due to the path loss model, the SNR decreases and hence the CRB of the TOA gets worse.

If we compare CRB of TOA (2.19) and RSS (2.13), we find that for TOA the accuracy can be improved with suitable signal shape and bandwidth, while ranging with RSS measurements does not depend on the shape of the transmitted signal, but it rapidly increases with distance [22]. The CRB for RSS and TOA positioning are compared for a peer-to-peer WSN in [31]. A network with target and anchor nodes is considered in which sensor location estimation is performed with RSS and TOA measurements between themselves and neighboring nodes. As more devices are added to the network, better location estimation accuracy can be achieved. For TOA measurements, the CRB depends on the device coordinates. It indicates that the size of the network can be scaled without changing the CRB as long as the geometry is kept the same. However, in the case of RSS measurements, the variance bound scales with the size of the network even if the geometry is kept the same. Authors say that these scaling characteristics indicate that TOA measurements would be preferred for sparse networks, but for sufficiently high density, RSS can perform as well as TOA.

In [32], [33] and [34] the design and implementation of an Ultra-Wideband testbed for 6.0-8.5 GHz ranging and low data rate communication (ULAND®) is

presented. Results of [33] confirm the high accuracy for ranging with TW-TOA and UWB.

2.2.3 Overview of IEEE 802.15.4a Standard

Impulse Radio (IR) techniques have been widely used over the last three decades [35]. The Electronic Communications Community (ECC) has released the Ultra Wide Band (UWB) European emission spectral mask, limiting the radiated power in the band between 6.0 GHz and 8.5 GHz. The large bandwidth of UWB signal provides high time resolution, therefore UWB signals are suitable for ranging purposes. The main source of ranging errors in UWB ranging systems is multi-path in NLOS propagation. Multiple copies of a transmitted signal with various attenuation levels and time-delay arrive at the receiver. When the direct LOS between ranging nodes is obstructed, the first peak may not be the strongest one [36].

Considering UWB systems there are two different possibilities: high data rate for short-range distances; or, low data rate for high-range distances for ranging and location. A standard for the latter is IEEE 802.15.4a [29] that is an amendment to IEEE 802.15.4 specifying two additional physical layers [29]:

- Ultra-wide band (UWB) PHY at frequencies of 3 GHz to 5 GHz, 6 GHz to 10 GHz, and less than 1 GHz
- Chirp spread spectrum (CSS) PHY at 2450 MHz (low data rate for high-range distances case)

The UWB PHY supports an over-the-air mandatory data rate of 851 kb/s with optional data rates of 110kb/s, 6.81 Mb/s, and 27.24 Mb/s. The CSS PHY supports an over-the-air data rate of 1000 kb/s and optionally 250kb/s.

The 802.15.4a standard supports both star and mesh topologies, while the cluster-tree topology falls outside the scope of the standard, since upper layers are not addressed.

RSS based ranging technique is enabled by IEEE 802.15.4 and IEEE 802.15.4a compliant nodes while IEEE 802.15.4a defines primitives for TOA based ranging. The IEEE 802.15.4a standard defines the mandatory ranging protocol TW-TOA and the optional Symmetric Double Sided TW-TOA protocol explained in Section 2.2.2.

2.2.4 Comparison of IEEE 802.15.4 and IEEE 802.15.4a for Positioning

The main advantage of UWB with TOA is that it allows high accuracy, however the complexity of some receivers is higher than RSS with 2.4 GHz IEEE 802.15.4/Zigbee technology that does not need additional hardware, but has lower accuracy. In Table 2.2.4 a comparison between 2.4GHz 802.15.4/Zigbee and UWB technologies is presented [37].

	2.4GHz 802.15.4/Zigbee	**UWB**
Data rate	Low, 250kbps	Medium, 1 Mbit/s mandatory, and up to 27Mpbs for 802.15.4a
Transmission distance	Short, <30m	Short, <30m
Location accuracy	Low, several meters	High, <50cm
Power consumption	Low, 20mW-40mW	Low, 30mW
Multipath performance	Poor	Good
Interference resilience	Low	High with high complexity receivers, low with simplest receivers
Interference to other systems	High	Low
Complexity and cost	Low	Low - medium - high are possible

Table 2.1: Comparison of 2.4GHz 802.15.4/Zigbee and UWB technologies.

There are other technologies like Wireless Local Area Network (WLAN), Bluetooth, RFID or inertial sensors that can be used jointly with sensor networks in order to achieve more accurate results. In [38] a survey of wireless indoor positioning techniques is presented. Moreover, in other works the accuracy of joint RSS and TOA techniques is studied. In [26], the authors explain that in short-range UWB communications, the use of RSS measurements (within close proximity) jointly with TOA or TDOA leads to enhancements in positioning with respect to the case where only TOA or TDOA measurements are used.

2.2.5 Classification of Positioning Algorithms in Wireless Sensor Networks

Positioning algorithms for WSN are designed to take into account the characteristics of such kind of networks like limited battery life time and short range. But these algorithms also take advantage of the peer-to-peer, ad hoc and cooperative nature of WSN. Positioning algorithms for WSN can be classified based on many criteria, for instance: range-based versus range-free, anchor based versus anchor free, centralized versus distributed, cooperative versus non-cooperative and non-Bayesian versus Bayesian.

Range-Based and Range-Free Algorithms

Range-free algorithms are not based on range, but they rely on connectivity between the nodes. The most attractive feature of range-free algorithms is their simplicity. However, they typically provide a higher estimation error than range-based approaches. Well known examples of algorithms based on connectivity measurements are centroid [39] and DV-hop [40]. Centroid algorithm estimates the position of a target averaging the coordinates of the anchor nodes within range [39]. Improved versions with distance based weights have been studied. DV-hop algorithm [40] is more complex than centroid, but more accurate estimations are achieved. First, each anchor node broadcasts a message that contains coordinates and hop count value. Each target node can construct a table with the number of hops required to reach every anchor node. Then, they choose the shortest possible path (having the minimum hop-count value). Second, hop-count value is converted into physical distance. The average hop-length is estimated averaging the distances between anchors and the number of hops needed. Each anchor node will broadcast this average distance per hop calculated. Thus, the distance between a target node and anchor node can be estimated as the average hop-length multiplied by the minimum hop-count. Third, lateration method is used to estimate the target position.

Pattern matching algorithms, also called fingerprint algorithms, are among the most viable solutions for range-free localization methods, however they need a training phase. First, there is a calibration phase of range values where several measurements are taken in order to describe the propagation pattern of the signal. Second, the position can be estimated by comparing the multipath signal received by a sensor node with the prior known pattern stored in a database through matching algorithms. In [41], IEEE 802.15.4 motes are used for indoor pattern matching based localization with an average position error of 2.7m.

Range-based algorithms [42] rely on distance between nodes that is usually measured with RSS and TOA based techniques (Sections 2.2.1 and 2.2.2), although other measures are possible as well [22]. Hybrid algorithms combine two or more positioning algorithms or ranging techniques. For example, a hybrid TOA/RSS wireless positioning technique is proposed for gaining favorable position accuracy in indoor UWB systems [43].

Anchor Based and Anchor Free Algorithms

Anchor based algorithms rely on some sensors, called anchor nodes, aware of their own location (by means of GNSS, or because they were installed at points with known coordinates) and helping localize other sensors. Sensors with unknown location information are called non-reference or target nodes and their coordinates can be estimated using a positioning algorithm, that uses the available a priori

knowledge of positions of anchor nodes in the network [44]. In contrast, anchor-free [45] algorithms use local distance information to estimate node coordinates. Therefore they need an additional algorithm to transform relative coordinates into absolute coordinates.

Centralized and Distributed Algorithms

While in centralized algorithms measurements are collected at a central location where they are processed to estimate the position, in distributed algorithms the coordinates are estimated locally. To perform positioning with distributed algorithms, sensors can share information with neighbors. As generally the processing power of sensor nodes is low and its memory is small, distributed positioning should be done with algorithms that respect the limitations of processing power of the sensor nodes. Although centralized algorithms can provide more processing power and more accurate location estimates, the most important limitation is the necessary information exchange. Therefore, due to the ad hoc nature of WSN, distributed algorithms may be more attractive than centralized ones. When the average number of hops to the central processor exceeds the necessary number of iterations of the algorithm, distributed algorithms will likely save communication energy costs [21].

Examples of algorithms that were designed for be centrally performed are Multidimensional scaling [46] and Semidefinite programming [47]. Distributed posterior versions of some of these algorithms have been proposed to overcome limitations of central processing, with results similar to central ones [46].

Examples of distributed algorithms are lateration or Min-max method of N-hop multilateration algorithm [48]. The position can be estimated solving the trilateration problem once range measurements are available, either resorting to TOA or RSS techniques for example. It can be seen as a geometrical problem, where each geometrical distance $\rho_{j,i}$ between the target node j and the i-th anchor define a sphere centered at the corresponding $\mathbf{x}_{a_{(i)}}$ and with radii equal to the measured range (Figure 2.6). The geometrical distance may be defined by

$$\rho_{j,i}(\mathbf{x}) = \parallel \mathbf{x}^{(j)} - \mathbf{x}_a^{(i)} \parallel,\ i = 1, \ldots, N\ , \tag{2.22}$$

The optimal positioning solution is given by the point in space where all spheres intersect. Since the accuracy of range estimates is affected by noise (among other phenomena such as multipath components), the spheres are not likely to intersect at one single point (X in Figure 2.6) and instead an uncertainty area (comprised between Y, Y', Y" and Y"' in Figure 2.6) is obtained which contains the actual node position.

The N-hop multilateration algorithm presents an alternative positioning technique, simpler than trilateration, that constructs a bounding box for each anchor

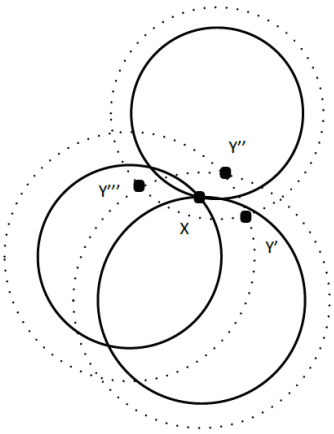

Figure 2.6: The position can be estimate solving the trilateration problem once range measurements are available. The optimal positioning solution is given by the point X in space where all spheres intersect. Since the accuracy of range estimates is affected by noise instead an uncertainty area comprised between Y' and Y", Y"' is obtained which contains the actual node position.

using its position and distance estimate. The position of the node is set to the center of the intersection box (Min-max method) instead of the intersection of circles (trilateration) [48].

In [48] lateration is compared to Minmax method. Lateration obtains more accurate positions than Min-max, but it is sensitive to accuracy of distance estimates. Min-max is more robust than lateration, but is more sensitive to the placement of anchor nodes.

Cooperative and Non-Cooperative Algorithms

On one hand, we consider as non-cooperative algorithms the ones that only allow target nodes to make distance measurements with anchor nodes. On the other hand, in cooperative localization, measurements from target nodes to target nodes are also allowed. In Figure 2.7, a cooperative scenario for localization is presented. Black nodes known its position and other nodes do not know it. The additional information gained from measurements between target nodes enhances positioning accuracy and also allows positioning of target nodes that can not determine its own position based on distance estimates with respect to the anchor nodes [21]. Moreover target nodes that are able to determine their position become anchor nodes, thus providing new references for remaining target nodes. As example, in N-hop multilateration algorithm [49] a collaborative multilateration technique allows

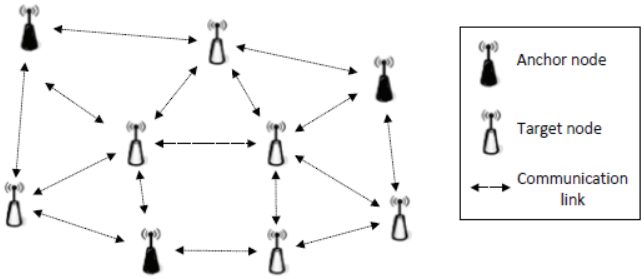

Figure 2.7: Cooperative scenario for localization.

mechanisms that enables nodes found several hops away from location aware beacon nodes collaborate with each other to estimate their locations.

In [50], a cooperative algorithm is compared with non-cooperative one. Results show that cooperation between nodes improve localization. The 90% of the non-cooperative nodes do not achieve an error below 1m, while the 40% of the nodes do not achieve an error below 1m for the cooperative algorithm.

Non-Bayesian and Bayesian Estimators

Non-Bayesian algorithms use measurements to estimate the positions by applying, typically, multilateration, Least Squares (LS), Maximum Likelihood (ML) based algorithms or other techniques. In favor of computational simplicity, Non-Bayesian algorithms rarely provide an estimate of the remaining uncertainty at each sensor location. Moreover most of them assume a Gaussian model for uncertainties, which may be questionable in the real world.

Bayesian estimators take into account uncertainty of the measurements. They estimate the posterior probability density function (pdf) of positions given the measured distance and the prior pdf. Besides methods operating sequentially (e.g. Kalman filters [51] or particle filters), there is another family of methods based on graphical models. Graphical models such like Bayesian Networks, Markov Random Fields or factor graphs with message passing algorithms (e.g., [50] and [52]) are powerful methods to perform Bayesian inference. They assume that posterior pdf is factorized into marginal probabilities that can be estimated with message passing algorithm applied to the graphical model. In [50], a cooperative distributed and Bayesian algorithm based on a factor graph has been presented for cooperative localization and applied to UWB wireless networks. Results show that the cooperative and Bayesian algorithm based on a factor graph outperforms the cooperative Non-Bayesian LS algorithm. For the Non-Bayesian algorithm, 40% of the nodes do

not achieve an error below 1m while for the Bayesian algorithm, the percentage is reduced to 1% of the nodes.

In a real scenario there is the presence of non-linear relationships and highly non-Gaussian uncertainties. Random variables (i.e. ranging measurements) that follow Gaussian densities can be characterized with the mean and covariance simplifying the message passing algorithm of the factor graph. However, non-Gaussian assumptions can cause high computational and communication cost for sensor networks. Nevertheless, particle-based approximation via nonparametric representation Bayesian algorithms with factor graphs are acceptable for sensor networks [52].

2.2.6 Non-Bayesian Estimators

The intention of this section is to review the typical statistical estimators such as Least Squares (LS) and Maximum Likelihood estimator (ML) (both nonlinear and linear) for the positioning problem. They are used throughout the Thesis.

Least Squares

The lateration problem consists in the minimization of the error:

$$\hat{\mathbf{x}}^{(j)} = \arg\min_{\mathbf{x}} \left\{ \sum_{i \in \mathcal{N}_j}^{n} \left(\hat{\rho}_{j,i} - \parallel \mathbf{x}^{(j)} - \mathbf{x}_a^{(i)} \parallel \right)^2 \right\} \tag{2.23}$$

to estimate the coordinates of the j-th node. Equation 2.23 involves measurements that are modeled with non-linear equations. Moreover, this model assumes that $\sigma^2_{\rho_{j,i}} = \sigma^2_{\rho_j}$ for all $i = 1, ..., N$, meaning that for a target node j that does ranging measurements from N anchor nodes, the variance of these measurements is equal for all the anchor nodes. Thus, the positioning problem is formulated as a non-linear and non-convex problem, which is difficult to solve. One technique to solve the nonconvex problem is approximating it by a convex problem. One method consists in linearizing the measurements based on the position of the target nodes and then to employ the linear least squares (LLS) algorithm. To find a signal model that is linear in unknown parameters $\mathbf{x}^{(j)}$, there are different techniques that yield different linear estimators [53]. Compared with non linear LS (NLS), LLS has low computational complexity, however in general the linear estimators derived in the positioning literature are suboptimal [54]; hence, there are different techniques to improve the estimate [53]. A method to linearize equation (5.2) comes from using Taylor series around the approximate user position $\hat{\mathbf{x}}^{(j)}$ and neglecting the higher order terms. For TOA based ranging with model (5.2), as in [55] the linear model for one target node j

may be

$$\mathbf{\Delta}\rho \;=\; \mathbf{H}\Delta\mathbf{x} + \nu \tag{2.24}$$

where

$$\mathbf{\Delta}\rho = \left[\hat{\rho}_1 - \rho_1(\mathbf{x}^0), \ldots, \hat{\rho}_{|\mathcal{N}|} - \rho_{|\mathcal{N}|}(\mathbf{x}^0)\right]^T \;, \tag{2.25}$$

$\Delta\mathbf{x} = \mathbf{x} - \hat{\mathbf{x}}$ and the so-called, $|\mathcal{N}| \times 2$, visibility matrix is given by

$$\mathbf{H} \;=\; \left.\begin{pmatrix} \frac{x_a^{(1)} - x}{\varrho_1(\mathbf{x})} & \frac{y_a^{(1)} - y}{\varrho_1(\mathbf{x})} \\ \frac{x_a^{(2)} - x}{\varrho_2(\mathbf{x})} & \frac{y_a^{(2)} - y}{\varrho_2(\mathbf{x})} \\ \vdots & \vdots \\ \frac{x_a^{(|\mathcal{N}|)} - x}{\varrho_{|\mathcal{N}|}(\mathbf{x})} & \frac{y_a^{(|\mathcal{N}|)} - y}{\varrho_{|\mathcal{N}|}(\mathbf{x})} \end{pmatrix}\right|_{\mathbf{x}=\mathbf{x}^0} \tag{2.26}$$

where $|\mathcal{N}|$ indicates the cardinality of set $\mathcal{N}$, i.e., the number of ranging measurements at the target node and ν is the error vector as $\nu = [\nu_1, ..., \nu_{|\mathcal{N}|}]$. From (2.24), the LLS problem can be solved by minimizing the square of the residual $(\mathbf{H}\Delta\mathbf{x} - \mathbf{\Delta}\rho)^2$. The solution can be obtained differentiating this square of the residual with respect to $\Delta\mathbf{x}$, setting the derivative to zero and solving it for $\Delta\mathbf{x}$ to seek a minimum value. The optimization admits a closed-form solution [51] based on the Moore-Penrose pseudoinverse for $i \geq 3$ in 2-dimensions in which $\mathbf{H}$ is full rank:

$$\widehat{\Delta\mathbf{x}} = (\mathbf{H}^T\mathbf{H})^{-1}\mathbf{H}^T\mathbf{b} \;. \tag{2.27}$$

Notice that the solution in (2.27) requires initialization of the unknown coordinates, which we have defined as $\mathbf{x}^0$.

The lateration problem of (2.23) for RSS measurements can also be solved with NLS or LLS. An example of LLS based on Taylor series expansion is explained in [56]. From (2.3) we define $p_r = L - L_0$ and the system of nonlinear equations for location estimation can be rewritten as

$$p_{r_i} = g_i(\mathbf{x}) + \upsilon_i, 1 \leq i \leq N \;, \tag{2.28}$$

where $g_i(\mathbf{x}) = 10\eta \log_{10} \rho_i$. (2.28) can be formulated into the vector form

$$\mathbf{p}_r = \mathbf{g}(\mathbf{x}) + \mathbf{v}, \tag{2.29}$$

where $\mathbf{p}_r = [\mathbf{p}_{r_i}, ..., \mathbf{p}_{r_N}]^T$, $\mathbf{g}(\mathbf{x}) = [g_1, ..., g_N)]^T$ and $\mathbf{v} = [\nu_1, ..., \nu_N)]^T$. The NLS solution of the system can be formed as the $\mathbf{x}$ that minimizes the function

$$\hat{\mathbf{x}} = \arg\min_{\mathbf{x}}\{(\mathbf{p}_r - \mathbf{g}(\mathbf{x}))^2\} \;. \tag{2.30}$$

To apply LLS, $\mathbf{g}(\mathbf{x})$ is linearized by using a first order approximation of the Taylor series around the approximate user position $\hat{\mathbf{x}}$

$$\mathbf{g}(\mathbf{x}) = \mathbf{g}(\mathbf{x}^0) + \mathbf{J}^{(0)} \cdot (\mathbf{x} - \mathbf{x}^0) \ , \tag{2.31}$$

where $\mathbf{J}^{(0)}$ is the Jacobian matrix of $\mathbf{g}(\mathbf{x})$ at $\mathbf{x}^0$ and

$$\mathbf{g}(\mathbf{x}) \ = \ \left(\begin{array}{cc} \frac{-10\eta}{\ln 10} \cdot \frac{x_a^{(1)} - x}{\rho_1(\mathbf{x})} & \frac{-10\eta}{\ln 10} \cdot \frac{y_a^{(1)} - y}{\rho_1(\mathbf{x})} \\ \frac{-10\eta}{\ln 10} \cdot \frac{x_a^{(2)} - x}{\rho_2(\mathbf{x})} & \frac{-10\eta}{\ln 10} \cdot \frac{y_a^{(2)} - y}{\rho_2(\mathbf{x})} \\ \vdots & \vdots \\ \frac{-10\eta}{\ln 10} \cdot \frac{x_a^{(|\mathcal{N}|)} - x}{\rho_{|\mathcal{N}|}(\mathbf{x})} & \frac{-10\eta}{\ln 10} \cdot \frac{y_a^{(|\mathcal{N}|)} - y}{\rho_{|\mathcal{N}|}(\mathbf{x})} \end{array} \right) \Bigg|_{\mathbf{x}=\mathbf{x}^0} \tag{2.32}$$

The LS solution of the linearized problem may be obtained as [51]

$$\hat{\mathbf{x}} = \mathbf{x}^0 + ((\mathbf{J}^{(0)})^T \mathbf{J}^{(0)})^{-1} (\mathbf{J}^{(0)})^T (\mathbf{p}_r - \mathbf{g}(\mathbf{x}^\mathbf{0})) \ . \tag{2.33}$$

The approach of (2.33) approximate the NLS solution and this approximation is not accurately when the initial estimate is far away from the optimum. Iterative algorithms such as the Gauss-Newton algorithm can be applied to improve the linearized estimation [51]

$$\hat{\mathbf{x}}^{k+1} = \mathbf{x}^k + ((\mathbf{J}^{(k)})^T \mathbf{J}^{(k)})^{-1} (\mathbf{J}^{(k)})^T (\mathbf{p}_r - \mathbf{g}(\mathbf{x}^\mathbf{k})) \ , \tag{2.34}$$

where k is the iteration number for the estimation.

The Weighted Least Square (WLS) algorithm considers that $\sigma^2_{\rho_{j,i}}$ are different for each measurement. Thus, measurements where the error is large play a smaller role in the estimation of the position because they are less accurate. The WLS minimize the weighted error [51]

$$\hat{\mathbf{x}} \ = \ \arg\min_{\mathbf{x}} \left\{ \sum_{i \in \mathcal{N}_j}^{n} (\mathbf{H}\Delta\mathbf{x} - \mathbf{\Delta}\rho)^T \, \mathbf{W} \, (\mathbf{H}\Delta\mathbf{x} - \mathbf{\Delta}\rho) \right\} \tag{2.35}$$

$$= \ \arg\min_{\mathbf{x}} \left\{ \sum_{i \in \mathcal{N}_j}^{n} w_i \left(\hat{\rho}_i - \parallel \mathbf{x} - \mathbf{x}_a^{(i)} \parallel \right)^2 \right\} \ , \tag{2.36}$$

where $\mathbf{W}$ is a diagonal matrix which elements are the weights w_i that are inversely proportional to the corresponding variances $w_i = \frac{1}{\sigma^2_{\rho_i}}$. One example for the solution of linear WLS (LWLS) applied to (2.35) may be

$$\widehat{\Delta\mathbf{x}}_j = (\mathbf{H}^T\mathbf{W}\mathbf{H})^{-1}\mathbf{H}^T\mathbf{W}\mathbf{b} \ . \tag{2.37}$$

Maximum Likelihood

The main difference between LS and ML estimator is that ML depends on statistical information of the measurements. In fact, ML is a more general framework. ML and LS solution coincide if AWGN assumption holds. The joint density function of the measurements is the likelihood function ($\mathcal{L}$)

$$\mathcal{L} = \prod_{i=1}^{N} \hat{\rho}_{j,i}(\rho_{j,i}, \sigma^2_{\hat{\rho}_{j,i}}) \ . \tag{2.38}$$

The position estimate is obtained as the values that maximizes the $\mathcal{L}$ function, or the values that minimizes the negative log-$\mathcal{L}$ function that is

$$\hat{\mathbf{x}}^{(j)} = \arg \min_{\hat{\mathbf{x}}} \sum_{i=1}^{N} -\log \hat{\rho}_{j,i}(\rho_{j,i}, \sigma^2_{\hat{\rho}_{j,i}}) \ . \tag{2.39}$$

As an example, the ML for range-based measurements using the TOA estimates with the model of (5.2) that considers Gaussian distribution for the measurements, may be expressed as

$$\hat{\mathbf{x}}^{(j)} = \arg \min_{\hat{\mathbf{x}}} \sum_{i=1}^{N} \frac{1}{\sigma^2_{\rho_{j,i}}} \left(\hat{\rho}_{j,i} - \parallel \mathbf{x}^{(j)} - \mathbf{x}_a^{(i)} \parallel\right)^2 \ . \tag{2.40}$$

For RSS measurements, the ML for range-based measurements using the RSS measurements with the log normal model of (5.2), may be [57]

$$\hat{\mathbf{x}}^{(j)} = \arg \min_{\hat{\mathbf{x}}} \sum_{i=1}^{N} \left(P_{Rx,j} - P_{Tx,i} + L_0 + 10p \log \rho_{j,i}\right)^2 \ . \tag{2.41}$$

As it can be seen in (2.40) and (2.41), the ML forces a difficult global optimization problem due to nonlinearity issues.

Comparing ML and LS estimators, ML is more efficient than LS under some regularity conditions, i.e., ML attains the CRB [51]. Thus, for positioning, ML estimator tends to provide reliable position estimates for high SINR, large number of observations, or large number of reference nodes. In front of the simplicity of LS based algorithms, for the ML computation, it is necessary to know the distribution of measurements.

A comparison between LS and ML is shown in [57]. Results show that the performance of WLS estimators perform better than LS. Moreover results show that the ML has a superior performance to LS based algorithms.

2.2.7 Cooperative, Anchor, Range and Distributed Algorithms for Positioning

Requirements of WSN, for example low power consumption and low power computation capacity, impose limitations for the positioning algorithms. Thus, positioning algorithms that provide energy efficiency, require little computation and little communication are suitable for WSN. Under these constraints, cooperative, anchor and range based positioning techniques are good candidates since they provide scalability, flexibility, limited computational power and memory, and are suitable for distributed implementation.

Anchor and range based positioning requires two types of sensor nodes: target and reference nodes (the latter also referred to as anchor or beacon nodes). Both can cooperate to estimate the coordinates of target sensor nodes using the available a priori knowledge of positions of anchor sensor nodes. Typically, the main phases of these positioning algorithms are ranging, coordinate estimation, and refinement [48]:

i) Ranging phase: During the ranging phase, the distance between target and anchor nodes is estimated. As we commented earlier, IEEE 802.15.4a provides mechanisms for precision ranging using TOA by means of an Ultra Wide-Band (UWB) PHY layer and location primitives, while RSS based range estimation methods are also possible with IEEE 802.15.4. Ranging can be done with single-hop (the distance calculation is performed with nodes within range) or multi-hop algorithms.

ii) Position estimation phase: Once range measurements are available, either resorting to TOA or RSS techniques for example, the target node computes its position based on an algorithm to solve the trilateration problem. The most simple solution for trilateration problem is obtained with LS based algorithms. The trilateration method has its limitation in that at least four beacons are needed to determine the position of a node. In a sensor network, in which nodes are randomly deployed, this may not be possible. As we explained before, cooperative methods are proposed to relieve this limitation.

iii) Refinement phase: The objective of the refinement phase is to enhance the position estimate obtained in the previous phase. Some algorithms try to find the optimum of a global cost function, e.g., Least Squares (LS), Weighted Least Squares (WLS) or Maximum Likelihood (ML). In another approach for cooperative localization, after each sensor has estimated its location, it then transmits the assertion to its neighbors, which must then recalculate their location and transmit again, until convergence occurs.

2.3 Geometric Dilution of Precision (GDOP)

In any radio positioning system in which a receiver measures its range to a set of transmitters to determine its position, the number of transmitters and their spatial disposition affects the final position estimation of the receiver. A typical measure of the *goodness* of a certain geometry for positioning purposes is the Geometric Dilution of Precision (GDOP) [58]. The GDOP is a dimensionless value that quantifies the degradation on positioning due to geometry.

2.3.1 GDOP for Time of Arrival Ranging

The origin of the GDOP measure comes from the trilateration procedure, from which a receiver computes its position based on range measurements to a set of transmitters. Trilateration involves solving a geometrical problem, whose solution is given by the intersection of spheres centered at the transmitters and radii equal to the measured ranges. The problem is nonlinear and typically solved by a LS algorithm after linearization. Such linearization is the Jacobian of the distance function that relates changes in the position domain to changes in range values, resulting in the so-called *visibility matrix*. The GDOP is constructed from the covariance of the inverse visibility matrix, and thus it relates the covariance of range-errors to that of position solution (in fact, it is highly related to the CRB on the variance of a position estimator) given by:

$$\sigma^2_{\hat{\mathbf{x}}} = \sigma^2_{\hat{\rho}} (\mathbf{H}^T \mathbf{H})^{-1} \ , \tag{2.42}$$

where

$$\text{GDOP} = \sqrt{\text{Tr}\{(\mathbf{H}^T \mathbf{H})^{-1}\}} \ . \tag{2.43}$$

LWLS solution of the form in (2.37) has an associated covariance matrix which can be calculated as [51]

$$\mathbf{C}_{\hat{\mathbf{x}}} = (\mathbf{H}^T \boldsymbol{\Sigma}^{-1} \mathbf{H})^{-1} \ , \tag{2.44}$$

with

$$\boldsymbol{\Sigma} = \text{diag}\left(\sigma^2_{\rho_1}, \ldots, \sigma^2_{\rho_{|\mathcal{N}|}}\right) \tag{2.45}$$

being a diagonal matrix whose entries are the corresponding variances of each range measurement as in (2.18). Moreover, from (2.37), note that $\mathbf{W} = \boldsymbol{\Sigma}^{-1}$ [51]. Accounting for the quality of each range measurement, the weighted GDOP is defined as

$$\text{GDOP} \triangleq \sqrt{\text{Tr}\{(\mathbf{H}^T \boldsymbol{\Sigma}^{-1} \mathbf{H})^{-1}\}} \ , \tag{2.46}$$

where its relation to the estimation covariance (2.44) is apparent.

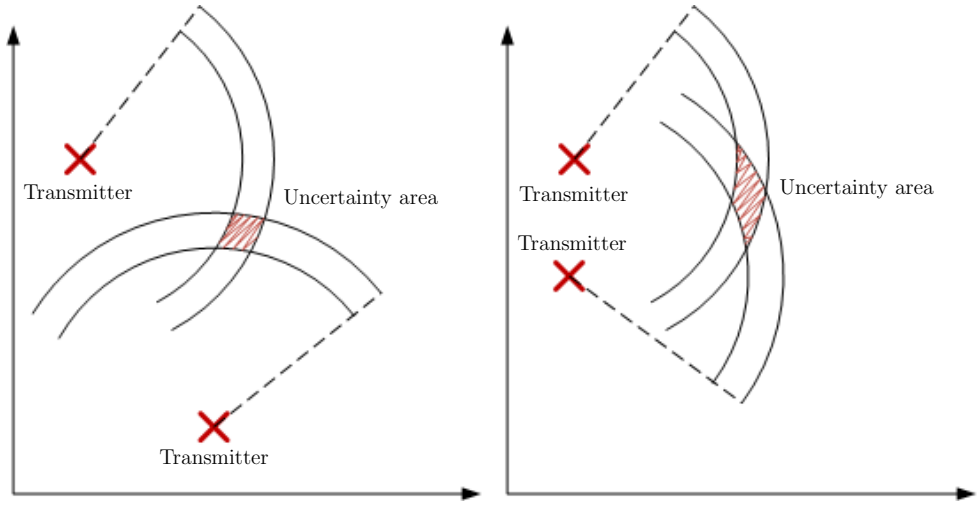

(a) (b)

Figure 2.8: Conceptual representation of *good* and *bad* two-dimensional geometries, 2.8(a) and 2.8(b) respectively.

It is important to notice that the GDOP value is a multiplicative factor on the measurement errors. Therefore, larger values of GDOP imply worse positioning accuracy than a geometry that provides a low GDOP. As a guide, the minimum GDOP value in two-dimensional scenarios was shown to be $2/\sqrt{N}$, with N being the number of visible transmitters [59].

A conceptual representation of the concept behind GDOP is depicted in Figure 2.8, where two transmitters are used to solve for a two-dimensional position in the plane using range measurements. In the presence of noisy ranges the uncertainty is visualized as the two concentrical circles, with the true range lying in between. The intersection of the two circles, in the noisy case, provides an area in which the receiver is estimated to be. Comparing Figures 2.8(a) and 2.8(b) it becomes evident that the geometrical situation of the transmitters affects the size of this area, which is indeed quantified by the GDOP.

It was proved that GDOP is a monotonically decreasing function with the number of anchor nodes [3]. In other words, no matter the resulting geometry seen by the node, including a new anchor node in matrix $\mathbf{H}$ will always reduce (or at most leave unaltered) the GDOP value.

As example, in anchor and range based positioning, the GDOP informs about the geometry seen by nodes on the positioning solution. Clearly the GDOP value at the target node depends on the number of visible anchor nodes, which in turn depends on their transmitted powers. For instance, if we focus on the i-th anchor node, higher power values will turn into larger coverage area and the eventual coverage of a target node, thus varying GDOP calculations for the specific target node. It can thus be claimed that GDOP is monotonically decreasing function with anchor transmitters power levels. Increasing the power level of a given anchor node increases its coverage and, potentially, can result into a larger number of anchor nodes seen by a non-empty set of nodes.

2.3.2 GDOP for Received Signal Strength Ranging

There are differences between the Gaussian error model for TOA based ranging and the log-normal model for RSS measurements. In [31], the CRB of variance of the position estimation has been studied for both models. The main difference between TOA and RSS models is that in the case of RSS techniques, the CRB scales with the size of the system even if geometry is unaltered. In [56], the CRB for any unbiased RSS location estimator has been derived and hence, the GDOP is given by

$$\mathrm{GDOP}_j = \frac{\ln(10)}{10} \sqrt{\frac{\sum_{i=1}^{|\mathcal{N}_j|} \rho_{j,i}^{-2}}{\sum_{i=1}^{|\mathcal{N}_j|-1} \sum_{k=i+1}^{|\mathcal{N}_j|} \frac{\sin^2 \phi_{ik}}{\rho_{j,i}^2 \rho_{j,k}^2}}} \tag{2.47}$$

where ϕ_{ik} is the angle between the two vectors from target node j to the i-th and k-th anchor nodes. From (2.47) we can observe that the GDOP depends not only on the angular distribution of reference nodes (geometry), but also on the distances from target node to reference nodes.

3

Introduction to Non-Cooperative Game Theory

IN this chapter we present an introduction to game theory tools and results that will be used throughout this dissertation. In particular, we focus on non-cooperative games.

Game Theory is a collection of models and analytic tools used to study interactive decision processes [2, 60]. Such models are called *games* and address the interaction among individual rational decision makers referred to as *players*. In communications, players are users, devices or operators. As players are rational they try to maximize their payoffs (or *utilities*). The utility or payoff expresses the benefit of a player given a concrete strategy. In order to maximize their utilities, the players act according to a set of *strategies*.

Game theory has been used to model problems in communications systems [2, 61, 62]. In the sequel a review of the types of games as well as their application in communications is provided. A first main classification of the games distinguishes between *cooperative* and *non-cooperative games*. *Cooperative games* require agreements between players, therefore a solution based on them might be more difficult to realize or might require too much information interchange. In *non-cooperative games* players have potentially conflicting interests and they try to maximize their utility or

minimize their cost. For example, in most of the strategic situations in wireless communications the players have to agree on sharing or providing a common resource (e.g., they share the same medium) in a distributed way.

Non-cooperative games can be classified in static and dynamic games. In *static games*, it is assumed that the players have only one move as a strategy. Players make their moves simultaneously without knowing what the other players do (i.e., Multiple Access Game, where players share the same medium). Conversely, in *dynamic games* the players make their moves in a sequential manner, thus the move of one player is conditioned by the move of the other player. In a game with *complete information* each player knows the game, the set of players, the set of strategies and the set of payoff functions. Alternatively, a game with *incomplete information* is one in which information about characteristics of the other players (i.e. payoffs) is incomplete. The players may have certain beliefs about the payoffs of other players. Bayesian games aim at solving the game on their basis. Moreover, in a game with *perfect information* the players have knowledge of all previous moves in the game at any moment they have to play.

A game can be represented in strategic or extensive form. When a game is represented in strategic form, it is usually assumed that each player plays simultaneously without knowing the strategies chosen by the other players. Typically, static games are represented with strategic form. If the players have a sequential interaction, with perfect information or imperfect information, the game is usually presented in extensive form. In the extensive form, the game is represented as a tree, where the root of the tree is the start of the game, the circles are the players and the paths between the circles are the strategies [63]. A path on the tree defines a sequence of movements of the players. Extensive form is usually used to represent dynamic games. However, strategic form might be also used to represent dynamic games.

3.1 Strategic Form Representation

Definition 3.1. *A game can be defined in strategic form as* $\Gamma(\Omega, \mathcal{A}, u)$ *which has three main components: i)* Ω *is the set of* N *players; ii)* $\mathcal{A}$ *is the set of pure strategies and* $\mathbf{a} = [a_1, \ldots, a_N]^T \in \mathcal{A} \subseteq \mathbb{R}^N$ *the chosen strategies, where* $a_i \in \mathcal{A}_i$ *represents the strategy of the* i*-th player over the set of its possible strategies* $\mathcal{A}_i$*. Thus,* $\mathcal{A} = \times_{i=1}^{N} \mathcal{A}_i$*, and* $\mathbf{a}_{-i} \in \mathcal{A}_{-i} = \times_{j \neq i}^{N} \mathcal{A}_j$ *represents the strategies of all players but the* i*-th; iii)* $u_i : \mathcal{A} \mapsto \mathbb{R}$ *is the utility function of the* i*-th player. The utility function (or payoff) quantifies the preferences of each player to a given strategy.* $u \triangleq \{u_i\}_{i \in \Omega}$ *is the set of all* N *utility functions.*

Players can use pure or mixed strategies.

Definition 3.2. *A pure strategy assigns zero probability to all moves, except one that clearly determines the move to make.* a_i *corresponds pure strategy space of player* i*.*

Alternatively, the players can also use *mixed strategies*, meaning that different probabilities are assigned for each strategy. It is considered that the set of strategies $\mathcal{A}_i$ is the same for all players.

As an illustrative example of pure strategy consider the Forwarder's Dilemma. This game is a version of the well known Prisoner's Dilemma [60] of the Game Theory literature. Prisoner's Dilemma considers that two members of a criminal gang are arrested and imprisoned in solitary confinement. The police tell each suspect that if he testifies against with the other, i.e. he does not cooperate, he will receive a reward (the other suspect does not testify against him) and will be released. If neither suspect testifies, i.e. they both cooperate, all will be released. If only one testifies, the other one will go to prison. If both testify, both will go to prison, but they will collect rewards. The idea is that although cooperating would give each player a payoff, self-interest leads to an inefficient outcome. Forwarders Dilemma is characterized as static game [63] in Table 3.1. In Forwarders Dilemma the strategies of the players are to forward (F) the packet of the other player or to drop it (D). C is a transmission cost. Player 1 is the row player and player 2 is the column player. In each cell, the first value is the payoff of player 1, whereas the second is the payoff of player 2.

		Player 2	
		F	D
Player 1	F	(1-C,1-C)	(-C,1)
	D	(1,-C)	(0,0)

Table 3.1: Forwarders Dilemma.

This is a *nonzero-sum game*, because the players can mutually increase their payoffs by cooperating, by helping each other to forward (1-C,1-C), which is a better outcome for both players than mutual dropping (0,0). In a *zero-sum game* the gain of one player represents the loss of the other player.

3.2 Game Strategies

The simplest way to solve a game is based on *iterated strict dominance*.

Definition 3.3. *A strategy a_i of player i strictly dominates the strategy a_i' if $u_i(a_i, a_{-i}) > u_i(a_i', a_{-i})$, for all $a_{-i} \in \mathcal{A}_{-i}$.*

From Table 3.1, for player 1 the best option is to choose strategy D regardless of what the other player chooses: $u_1(D, F) > u_1(F, F)$ and $u_1(D, D) > u_1(F, D)$. Thus, strategy F is strictly dominated by strategy D. We can eliminate the first row of the matrix. For player 2, $u_2(D, F) > u_2(F, F)$ and $u_2(D, D) > u_2(F, D)$, F strategy is strictly dominated by strategy D, too. The first column of the matrix can be eliminated. As a result, the solution of the game is (D, D) and the payoffs are (0, 0). The pair (F, F) would have led to a better payoff for each of the players, but because of the lack of trust between the players the game leads to this suboptimal solution.

The technique of iterated strict dominance cannot be used to solve a game in which none of the strategies strictly dominates the other. For example, in the Joint Packet Forwarding Game [63] of Table 3.2, the two devices have to decide whether to forward the packet simultaneously before the source sends it. A source wants to send a packet to the destination with the multi-hop communication link: source - player 1 - player 2 - destination. To this end, source needs both devices player 1 and player 2 to forward for it. Both players obtain benefit if they forward the packet. If player 1 drops the packet, then the player 2 strategy is indifferent and thus we cannot eliminate strategy D based on strict dominance. This game can be solved with *iterated weak dominance*.

		Player 2	
		F	D
Player 1	F	(1-C,1-C)	(-C,0)
	D	(0,0)	(0,0)

Table 3.2: Joint Packet Forwarding Game.

Definition 3.4. *A strategy a_i of player i weakly dominates the strategy a_i' if $u_i(a_i, a_{-i}) \geq u_i(a_i', a_{-i})$, for all $a_{-i} \in \mathcal{A}_{-i}$ and if $u_i(a_i, a_{-i}) > u_i(a_i', a_{-i})$ for at least one $a_{-i} \in \mathcal{A}_{-i}$.*

From Table 3.2, strategy F of player 2 weakly dominates strategy D: $u_2(D, F) \geq u_2(D, D)$ and $u_2(F, F) > u_2(F, D)$. The solution with the elimination based on iterated weak dominance is (F, F). However, while the solution of the game with iterated strict dominance technique is unique (Table 3.1), the solution of the iterated weak dominance technique depends on the sequence of the strategies: if player 2 starts playing D, player 1 will choose D, too.

3.3 Nash Equilibrium

In general, most of the games cannot be solved by the iterated dominance techniques. In the Multiple Access Game (Table 3.3) each of the players have two strategies: access the channel to transmit (A) or wait (W). The channel is shared, therefore a simultaneous transmission of both players causes a collision with the cost C of transmission without the benefit 1. This game is a version of the classical Hawk-Dove game. In this game there is no dominating strategy, therefore the game should be solved with *best response* procedure.

		Player 2	
		W	A
Player 1	W	(0,0)	(0,1-C)
	A	(1-C,0)	(-C,-C)

Table 3.3: Multiple Access Game.

Definition 3.5. *The* best response $br_i(a_{-i})$ *of player* i *to the profile of strategies* a_{-i} *is a strategy* a_i *such that*

$$br_i(a_{-i}) = \arg\max_{a_i \in \mathcal{A}_i} u_i(a_i, a_{-i}). \tag{3.1}$$

From Table 3.3, (W, A) and (A, W) are mutual best responses, players do not have a reason to deviate from the given strategy profile. A Nash equilibrium (NE) is a strategy profile comprised of mutual best responses of the players. The *Nash equilibrium* (NE) is a stable solution of the game in which no player may improve its utility function by unilaterally deviating from it.

Definition 3.6 (Nash Equilibrium)**.** *A strategy profile* $\mathbf{a}^*$ *is a Nash equilibrium if,* $\forall i \in \Omega$ *and* $\forall a_i \in \mathcal{A}$*,*

$$u_i(\mathbf{a}^*) \geq u_i(a_i, \mathbf{a}^*_{-i}). \tag{3.2}$$

The existence of a Nash equilibrium is the first step to solve a game. Although in some cases a pure strategy Nash equilibrium does not exist, there always exists at least one mixed-strategy Nash equilibrium as the next theorem states.

Theorem 3.1 (Nash, 1950)**.** *Every finite strategic-form game has a mixed-strategy Nash Equilibrium.*

A NE may not be unique. Its efficiency can be characterized with the *Price of Anarchy (PoA).*

Definition 3.7 (Price of Anarchy)**.** *The PoA of a game is the ratio between the sum of the payoffs of all players in a globally optimal solution (with strategies* $\mathbf{a}^*$*) and the sum of the payoffs in a worst-case Nash equilibrium (with strategies* $\mathbf{a}^+$*):*

$$PoA = \frac{\sum_{i=1}^{N} u_i(\mathbf{a}^*)}{\sum_{i=1}^{N} u_i(\mathbf{a}^+)} \ . \tag{3.3}$$

When the NE is not unique, equilibrium selection and identification is studied with other methods. One method is the application of the Pareto-optimality concept that compares strategy profiles [63].

Best-Response Dynamics is a local search method where at each step a player i plays its best-response strategy $br_i(a_{-i})$, given the strategies of the others. For potential games (Section 3.4.1), in [64], the rules that each player must follow to reach an equilibrium are explained when the game is played repeatedly. At each round, every player does not know about past or future game events, but it chooses the strategy according to some decision rules that depend on the current state of the game. Best response guarantees the asymptotic stability of (at least some) NE of the game. Given best response different iterative algorithms can be performed by the players. In Gauss-Seidel based scheme the players update their strategy sequentially and in Jacobi method the players update their strategy simultaneously. The authors claim the convergence of the Gauss-Seidel and Jacobi update with the best response. If the utility function of a potential game (potential function) is continuously differentiable and strictly concave on $\mathcal{A}$, and $\mathbf{a} = [a_1, \ldots, a_N]^T$, with each a_i closed and convex, Gauss-Seidel algorithm with best response coincides with the classical nonlinear Gauss-Seidel algorithm of distributed convex optimization theory. Then, it is guaranteed to converge to the maximum of the potential function, and thus to the unique NE of the game.

In [65] the authors relates non-cooperative game theory with distributed algorithms for convex optimization such as Gauss-Seidel and Jacobi methods. In a game every player is trying to optimize his utility. A natural approach is to consider an iterative algorithm based on the Jacobi or Gauss-Seidel schemes. At each iteration every player updates his own strategy by solving his optimization problem, given the strategies of the others. The Gauss-Seidel implementation of the best-response-based algorithm is described in Algorithm 3.1. Algorithm 3.1, as well as its Jacobi version, globally converge to the NE [65].

Algorithm 3.1 Gauss-Seidel best response-based algorithm

1: S0: Choose a starting point $\mathbf{a}^{(0)} = [a_1^{(0)}, ..., a_N^{(0)}]$, set n=0.
2: S1: If $\mathbf{a}^{(n)}$ satisfies a suitable termination criterion: STOP
3: S2: for $i = 1, ..., N$, compute a solution $a_i^{(n+1)}$

$$\begin{aligned} \underset{a_i}{\text{maximize}} \quad & u_i(a_1^{(n+1)}, ..., a_{i-1}^{(n+1)}, a_i, a_{i+1}^{(n)}, ..., a_N^{(n)}) \\ \text{subject to} \quad & a_i \in \mathcal{A}_i \end{aligned}$$

end
4: S3: Set $\mathbf{a}^{(n+1)} = (\mathbf{a}_i^{(n+1)})_{i=1}^N$ and $n \leftarrow n + 1$, go to S1.

3.4 Potential and Supermodular Games

Potential and Supermodular games are two types of non-cooperative games that have interesting characteristics. Therefore in this section, these two games that are used throughout the Thesis are summarized. Potential games are characterized by a global utility function called potential function. The incentives of all players are mapped into the potential function and the set of pure Nash equilibria can be found by locating the local optima of the potential function. Furthermore, the simplicity of Supermodular games and the fact that they have pure strategy NE, led us to study them.

3.4.1 Potential Games

In general, games may have a large number of NE or may not have any. Thus, it is of interest to design the utility function in a way such that the game has at least one equilibrium point. It was proved in [66] that when the utility functions used by the players are concave, the existence and uniqueness of a NE is ensured. However, the utility function may be designed according to criteria which could eventually yield to non-convex functions. In those cases, there is another way for deriving sufficient conditions for existence and uniqueness of the NE in a game based on the so-called *potential games* [67]. This type of games are characterized by a global utility function $V(\mathbf{a})$. We use the name *exact potential game* (EPG) when the game admits an exact potential function, i.e., a player-independent real valued function that measures the marginal payoff when any player deviates unilaterally.

Definition 3.8 (EPG)**.** *A strategic game* $\Gamma(\Omega, \mathcal{A}, u)$ *is an exact potential game if there exists an exact potential function* $V : \mathcal{A} \to \mathbb{R}$ *s.t.* $\forall i \in \Omega, \forall \mathbf{a}_{-i} \in \mathcal{A}_{-i}$ *and*

$\forall a_i, b_i \in \mathcal{A}_i$ *such that*

$$V(a_i, \mathbf{a}_{-i}) - V(b_i, \mathbf{a}_{-i}) = u_i(a_i, \mathbf{a}_{-i}) - u_i(b_i, \mathbf{a}_{-i}) \ . \tag{3.4}$$

An *ordinal potential game* (OPG) is another type of potential game which requires having an ordinal potential function that has the same directional behavior as the individual payoff function.

Lemma 3.1. *Let* $\Gamma(\Omega, \mathcal{A}, u)$ *be an EPG and* $V(\mathbf{a})$ *the corresponding ordinal potential function. If* $\mathbf{a}^* \in \mathcal{A}$ *maximizes* $V(\mathbf{a}^*)$*, then it is a NE.*

If $V(\mathbf{a})$ is continuously differentiable and strictly concave on $\mathcal{A}$, and $\mathbf{a} = [a_1, \ldots, a_N]^T$, with each a_i closed and convex, then the NE of Γ is unique.

3.4.2 Supermodular games

A game $\Gamma(\Omega, \mathcal{A}, u)$ is a supermodular game [68], if it satisfies the conditions of the following definition.

Definition 3.9. *The strategic form game* $\Gamma(\Omega, \mathcal{A}, u)$ *is a supermodular game if for all players i: i)* $\mathcal{A}_i = [A_{min}, A_{max}]$ *is a compact subset of* $\mathbb{R}^+$*, where the set* $\mathcal{A}_i \in [A_{min}, A_{max}]$*, with a minimum strategy value* A_{min} *and the maximum strategy value* A_{max}*; ii)* u_i *is continuous in all player strategies* $\mathbf{a}$*; and iii)* u_i *has increasing differences in* (p_i, p_j)*,* $\forall j \neq i, j \in \Omega$*.*

A function u_i has increasing differences in (a_i, a_j) if for all $a_i' \geq a_i$ and $a_j' \geq a_j$, we have that

$$u_i(a_i', a_j') - u_i(a_i, a_j') \geq u_i(a_i', a_j) - u_i(a_i, a_j) \ . \tag{3.5}$$

In other words, the incremental gain of choosing a higher a_i is greater when a_j is higher. If u_i is twice differentiable, supermodularity is equivalent to [69]

$$\frac{\partial^2 u_i(\mathbf{a})}{\partial a_i \partial a_j} \geq 0 \ . \tag{3.6}$$

Supermodular games exhibit the following interesting properties: i) Pure strategy Nash equilibria (NE) exist. Recall that a NE is a stable solution of the game in which no player may improve its utility function by unilaterally deviating from it; ii) NE can be attained using greedy best-response (BR) type algorithms. Therefore, players can simply update their strategy by maximizing its utility function,

$$BR_i(\mathbf{a}_{-i}) = \arg\max_{a_i \in \mathcal{A}_i} \{u_i(a_i, \mathbf{a}_{-i})\} \ ; \tag{3.7}$$

iii) The equilibrium set has a largest and a smallest element, $\overline{\mathbf{a}^*}$ and $\underline{\mathbf{a}^*}$ respectively. If players start from smallest (largest) element of $\mathbf{a}$ and use the BR algorithm, then the strategies converge to the smallest (largest) NE. For supermodular games, if there exists a unique NE, it is attainable using BR algorithm from any initial strategies and $\overline{\mathbf{a}^*} = \underline{\mathbf{a}^*}$.

In order to prove the uniqueness of NE, we use a framework for convergence of iterative power control algorithms in cellular radio systems presented in [70]. The $BR_i(\mathbf{a_{-i}})$ has to be a *standard* function defined as follow:

Definition 3.10. *Function $BR_i(\mathbf{a_{-i}})$ is standard if for all $\mathbf{a} \geq 0$ the following properties are satisfied:*

- *Positivity:* $BR_i(\mathbf{a}_{-i}) > 0$
- *Monotonicity: if* $\mathbf{a}_{-i} \geq \mathbf{a}'_{-i}$, *then* $BR_i(\mathbf{a}_{-i}) > BR_i(\mathbf{a}'_{-i})$
- *Scalability: for all* $\delta > 1$, $\delta \cdot BR_i(\mathbf{a}_{-i}) > BR_i(\delta \cdot \mathbf{a}_{-i})$

We adopt the convention that the vector inequality $\mathbf{a}_{-i} \geq \mathbf{a}'_{-i}$ is a strict inequality in all components. In [70], if $BR_i(\mathbf{a}_{-i})$ is a standard function, they name the iteration as standard power control algorithm. Moreover from [70], we present the following Proposition:

Proposition 3.1. *If the standard power control algorithm has a NE, then that NE is unique. Then for any initial power vector* $\mathbf{a}$*, the standard power control algorithm converges to the unique NE.*

A more general framework for power control algorithms in wireless communications is presented in [69], where these algorithms and its convergence issues are unified with the theory of S-modular games.

3.5 Game Theory in Communications and Wireless Sensor Networks

In recent years, there has been a growing interest to apply Game Theory to model and solve communications and networking problems ([71]). Game theoretical approaches have been studied for the different layers of the protocol stack.

Physical layer: In the PHY layer, for example, power control problems in wireless and peer-to-peer networks have been addressed with Potential ([64], [65]) and

Supermodular games ([69], [72]). Moreover, resource allocation problems have been modeled with game theoretical solutions [73].

In power control a well known metric to model the problem is the signal-to-interference-and-noise ratio (SINR) γ that depends on the transmit power of the user. Potential games have been widely used in cognitive radio networks for power control ([64], [74]). Players are users that distributively choose their strategies as transmit power to optimize the tradeoff relationship between obtaining high SINR and low energy consumption. Usually, the utility function of the game is defined as some function of the SINR minus a cost C_i associated with power levels to control the power consumption as [74]

$$u_i(p_i, p_{-i}) = f_i(SINR_i(p_i, p_{-i})) - C_i(p_i) \ , \tag{3.8}$$

where p_i is the transmit power of the i-th user and p_{-i} represents the transmit powers of all players but the i-th.

As the SINR depends on other metrics such as waveform, packet size, bit rate or modulation, other non-cooperative games have been studied to optimize the Quality of Service (QoS) of the user ([74],[75]). In [75], a non-cooperative game is proposed in which each user chooses its transmit power (and transmit symbol rate) and constellation size to deal with the trade-off between to maximizing its utility based on energy efficiency and satisfying its QoS based on a delay constraint.

Power management is an important aspect in WSN, thus games to control the energy efficiency have been studied. Some games deals with the activation of radio transceiver. For example, in [76] a non cooperative game theoretic methodology was used for decentralized activation of the radio transceiver for energy efficiency. Moreover, power control has been proposed as one of the methods to save energy as well as for interference avoidance in WSN. As example for power control in [77], a non-cooperative game is presented to balance between maximizing rate and minimizing interference. In [78], cooperative and non-cooperative games have been proposed for power consumption saving taking into account connectivity constraints of the network. Other examples of power control games for energy efficiency can be found in [79] and [80].

MAC layer: In the MAC layer, game theory has been applied to model interaction processes such as spectrum sharing ([81], [74]). Cognitive radio technology allows the utilization of the existing wireless spectrum resources more efficiently. To that end, users have the ability to observe, learn, and make intelligent decisions on their spectrum usage and operating parameters based on the sensed spectrum dynamics and actions adopted by other users. To study, to model and analyze this interaction process between the users, Game theory has been recognized as an important tool [73]. For WSN, game theoretical analysis has been proposed for resource

allocation like spectrum and bandwith allocation as well as energy efficient MAC algorithms which makes the sensor nodes consume their energy efficiently [82].

Upper layers: In network and upper layers, there is a rich literature in flow and congestion control and distributed routing in communication networks with game theoretical approaches [69]. For WSN, routing, QoS, topology issues has been studied mostly with energy consumption constraints [73].

Processing algorithms: In some algorithms, Game Theory has been applied to model user interaction for different purposes. To this end, resources, functionalities and metrics of the other layers are optimized. In the following, some examples are explained for positioning or localization. This problem is less studied in the literature. [83] presents a RSS-based localization and tracking scheme using cooperative game-theoretic tools in which the best anchor coalition is kept active while the other coalitions will be allowed to enter low power mode saving energy. In [84], a non-zero-sum game is presented for tracking in WSN with an adversary target that can use a strategy to maximize the error that is estimated with a minimax filter. Also for tracking in WSN, in [85] a game is proposed that allow to negotiate sensor nodes in clusters formed to track the target. Moreover, [86] focuses on a distributed, cooperative, game-theoretic scheme for energy-efficient data acquisition in bearings-only localization.

4

Potential Game for Energy-Efficient RSS-based Positioning in Wireless Sensor Networks

IN this chapter, we focus on an anchor based positioning scenario with RSS measurements. The goal is to optimize resources at physical layer, transmit power and node selection, of anchor nodes, while using GDOP for positioning error metric as QoS to maintain an adjustable level of accuracy. We present a distributed power control method, that selects and minimizes the number of anchor nodes, with the goal of saving energy. For that aim, non-cooperative Game Theory, concretely a Potential game, is presented with its potential function.

4.1 Introduction

Systems using RSS based positioning exploit RSS measurements from anchor nodes to target nodes to determine the location of the mobile device. The advantage of

the RSS approach with respect to other techniques is that it requires no additional hardware. The main disadvantage is that it is affected by multipath fading and other propagation effects. Typically, RSS measurements are modeled with a log-normal path loss model [24]. In [87], it is shown that the CRB for distance estimation with RSS measurements is proportional to real distance and depends on the channel parameters.

The problem of energy efficiency while maintaining a given accuracy for positioning of WSN has been addressed in the literature. Several works treated energy conservation methods that adapt as a sampling problem the data transmission/reception rates for positioning. In some works, the localization frequency of a mobile target node is optimized to achieve a desired accuracy while reducing the energy consumption. Other works propose the optimization of the communication cost in the ranging phase. In [88], a communication scheme for RSS-based localization is proposed that minimizes the energy that is consumed during RSS measurements. Therefore, for a desired accuracy, the optimum relation between transmission power and packet transmission rate is achieved.

Node selection is also an energy conservation method for positioning because it avoids the use of large number of anchor nodes and hence, it reduces the packet exchange saving energy. Anchor node selection strategies have been addressed with different methods in several works. One approach uses CRB to select nodes. As example, in [89] the authors propose an algorithm in which the anchor nodes are selected based on the lower CRB. Another approach selects the anchor nodes based on a distance metric, based on the fact that the variance of RSS based distance estimation increases with the distance between nodes (Section 2.2.1). In [89], a comparison between distance based and CRB based selection is done. When CRB is used to select cooperating nodes better results are achieved; however, distance based selection is simpler. The major disadvantage of distance based criterion is that the geometry of the selected anchor nodes is not contemplated. For positioning with trilateration method, the geometry of the anchor nodes has an impact on the final position estimation of the receiver. GDOP is a measure of the goodness of a certain geometry for positioning purposes (see Section 2.3 for further details). Thus, GDOP based strategy can also be used for node selection. The simplest selection method that uses GDOP based node selection strategy is an exhaustive search that evaluates the GDOP for all possible size M active sets given a set of possible sensors of size N. However, it leads to a high number of combinations therefore the algorithm is only viable if N is small. Suboptimal approaches have been presented in [90], where the authors compare the global node selection (GNS) algorithm with a modification of spatial split (SS) algorithm. GNS incorporates a greedy strategy in which one sensor node is added at time. First it selects the optimal active subset of two sensors

by exhaustive search based on a cost function based on GDOP. Then, one sensor is added at a time to minimize the cost function. This process is repeated until the active subset contains M sensors. Based on the GDOP metric, the SS algorithm follows a procedure in which a number of partitions of the radio region are created. Then the closest sensor of each sector to the target position estimate is selected and a cost function is calculated with the selected nodes. The authors also present an adaptive sensor selection (ASS) algorithm that adapts the number of active nodes for tracking depending on a local innovations vector.

In the literature, Game Theory has been used in node selection strategies for energy conservation. Note that cooperative Game Theory provides tools for the distributed agreement of the players. Thus, cooperative games have been proposed for anchor selection by means of the formation of the best group of anchor nodes for positioning. For example, [86] focuses on a distributed, cooperative, game-theoretic scheme for energy-efficient data acquisition in bearings-only localization with DOA technique. [83], presents an RSS-based localization and tracking scheme using cooperative game-theoretic tools in which the best anchor coalition is kept while the other coalitions will be allowed to enter low power mode. The utility function is based on distance metric for node selection. The main drawback of cooperative game theory for node selection is the need for information interchange between players that leads to a communication cost.

Besides node selection strategies for power conservation, another power conservation method is power control, which achieves energy saving by minimizing the transmit power expenditure in transmission. From a physical layer perspective, performance is generally estimated as a function of the SINR. When the nodes in a network can adapt their signal depending on changes of the estimated SINR, a process with interactive decisions can occur. Therefore, Game Theory can be applied to the allocation of resources, for example power or spectrum (see Section 3.5). In distributed power control, potential games have been used for avoiding collisions and energy saving. For instance, in [64] a unified framework based on potential games is proposed to deal with power control problems. In general, in power control problems, the QoS requirements are formulated as constraints on the SINR of each user. However, in our case the QoS requirements are formulated using the positioning error.

4.1.1 Contribution

In this chapter, we propose an algorithm that minimizes the power cost of anchor based positioning using RSS. The algorithm minimizes transmit power of anchor

nodes and selects and minimizes the number of anchor nodes that participate in positioning/tracking the target node. Moreover, GDOP is used as error metric. The algorithm is able to maintain an adjustable level of accuracy.

Since we are dealing with a decentralized system, non-cooperative Game Theory provides appropriate models to study such scenarios [60]. In the considered problem the advantage of non-cooperative games, in front of cooperative approaches, is that nodes do not have to reach an agreement and hence the effects derived from cooperation such as communications costs are not present. The problem of power control can be addressed in a distributed fashion with potential games. Taking advantage of the properties of potential games a potential function is derived. Therefore, a NE can be reached when the players play an iterated, distributed algorithm.

Based on a IEEE 802.15.4 compliant WSN that consists of anchor nodes and target nodes, we address the energy cost minimization problem while maintaining a certain quality of the positioning measure at the target nodes. The problem is cast in the form of a potential game. The game performs node selection to use the anchor nodes as close as possible to the target, with the best geometry using GDOP metric. The equilibrium reached with the distributed algorithm based on the potential game is compared to a centrally global solution with exhaustive search. Moreover, the players follow the iterations of a best response algorithm. Thus, the design of the algorithm may allow to add other strategies for energy saving. For example, the optimization of communication costs in the measurements of RSS can be performed while limiting the number of iterations of the algorithm.

Note that although we provide a solution for positioning with WSN, a similar approach may be used with other technologies with higher transmit powers such as WLAN.

The chapter is organized as follows. In Section 4.2, the signal models are described for the static and mobile scenario. The error metric to indicate the QoS is the GDOP. It is explained in Section 4.3. The potential game is described in Section 4.4. In Section 4.5, distributed error metrics to calculate the GDOP are detailed. In Section 4.6 a possible solution to implement the game is explained and analyzed. In Section 4.7, simulation and numerical results are presented to evaluate the performance of the proposed algorithm. Finally, Section 4.8 draws some final remarks and concludes the chapter.

4.2 Signal Models

The problem under study involves the distributed positioning of nodes in a WSN that is applied to two setups. We consider two setups for the positioning problem: a static one, where all nodes are fixed, a dynamic one, where target nodes are mobile.

4.2.1 Static Scenario

The static scenario is composed of a set of M nodes, that aim at estimating their position; and a set of N anchor nodes with known locations, emitting ranging signals to allow positioning of the former nodes. Respectively, we define the two-dimensional coordinates of the nodes as

$$\mathbf{x}^{(j)} = [x^{(j)}, y^{(j)}]^T \qquad j = 1, \ldots, M \tag{4.1}$$

$$\mathbf{x}_a^{(i)} = [x_a^{(i)}, y_a^{(i)}]^T \qquad i = 1, \ldots, N\ . \tag{4.2}$$

We define the set of anchor nodes that provide coverage to the j-th node as $\mathcal{N}_j$, and its dimension as N_j. Similarly, we define the set of target nodes whose messages are received at the i-th anchor node as $\mathcal{T}_i$, with dimension being T_i.

4.2.2 Dynamic Scenario

The dynamic scenario is composed of a set of M mobile nodes, that aim at estimating their positions and a set of N anchor nodes with known locations, emitting ranging signals to allow positioning of the former nodes. Respectively, we define the two-dimensional coordinates of the nodes at time t as

$$\mathbf{x}^{(j)}(t) = [x^{(j)}(t), y^{(j)}(t)]^T \qquad j = 1, \ldots, M \tag{4.3}$$

$$\mathbf{x}_a^{(i)} = [x_a^{(i)}, y_a^{(i)}]^T \qquad i = 1, \ldots, N\ . \tag{4.4}$$

The geometrical distance between the j-th node and the i-th anchor is defined as

$$\rho_{j,i} = \| \mathbf{x}^{(j)}(t) - \mathbf{x}_a^{(i)} \| \ , \tag{4.5}$$

with $\| \cdot \|$ being the Euclidean norm on $\mathbb{R}^2$.

We define the set of anchor nodes that provide coverage to the j-th node as $\mathcal{N}_j$, and its dimension as $|\mathcal{N}_j|$. Similarly, we define the set of target nodes whose messages are received at the i-th anchor node as $\mathcal{T}_i$, with dimension being T_i.

4.2.3 Ranging Model

We further assume that for both scenarios the physical layer of the nodes is capable of estimating the RSS of an incoming signal. In particular, the IEEE 802.15.4 physical layer has this capability.

The target node uses the RSS value to estimate $\rho_{j,i}$. The RSS-based ranging measures are commonly modeled using the log-normal path loss model [24], defined in Section 2.2.1 as

$$P_{Rx,j} = P_{Tx,i} - L_o + 10p \log_{10}\left(\frac{\rho_{j,i}}{\rho_o}\right) + \upsilon_{j,i} \ , \tag{4.6}$$

where ρ_o is a reference distance, L_o is the attenuation at such reference distance in dB, $\rho_{j,i}$ is the distance between nodes j and i and p the path loss exponent. The random contribution is modeled in dBm by $\upsilon_{j,i} \sim \mathcal{N}(0, \sigma^2_{j,i})$, where $\sigma_{j,i}$ is due to the fading effects in static and dynamic environments (node movement or environment changes, e.g. people movement). The averaging of the RSS values reduces its standard deviation when samples are collected over different frequency channels in a short time period, rather than on a single channel but over a longer time interval (see Section 2.2.1).

Rearranging terms from (4.6) (see Section 2.2.1 for details), the distance estimate for RSS-based ranging may be

$$\hat{\rho}_{j,i} = \rho_{j,i} \cdot 10^{\frac{\upsilon_{j,i}}{10 \cdot p}} \ . \tag{4.7}$$

The variance of the distance estimation $\hat{\rho}_{j,i}$ may be (see Section 2.2.1)

$$\sigma^2_{\hat{\rho}_{j,i}} = \rho^2_{j,i} \cdot (e^{\sigma^2_\xi} - 1) e^{\sigma^2_\xi} \ . \tag{4.8}$$

From the previous equation, it can be noticed that the variance of the distance estimation $\hat{\rho}_{j,i}$ between target j and anchor node i is proportional to the distance between both nodes. Therefore, larger distances cause higher error in distance estimation.

4.2.4 Positioning Equations

In the static scenario, a target node could estimate its position with linear Least Squares estimator defined in Section 2.2.6.

Considering the mobile setup, a mobile target node could estimate its position with an EKF. Following [91], we assume that the position $\mathbf{x}^{(j)}$ and velocity $\mathbf{v}^{(j)} = [v_{x^{(j)}}, v_{y^{(j)}}]^{\mathrm{T}}$ evolve in time as

$$\mathbf{s}_j(t) = \mathbf{A}\ \mathbf{s}_j(t-1) + \mathbf{G}\ \mathbf{w}_j(t)\ , \tag{4.9}$$

where

$$\mathbf{s}_j(t) = \begin{pmatrix} x^{(j)}(t) \\ y^{(j)}(t) \\ v_{x^{(j)}}(t) \\ v_{y^{(j)}}(t) \end{pmatrix}\ , \tag{4.10}$$

$$\mathbf{A} = \begin{pmatrix} 1 & 0 & \Delta & 0 \\ 0 & 1 & 0 & \Delta \\ 0 & 0 & 1 & 0 \\ 0 & 0 & 0 & 1 \end{pmatrix}\ , \tag{4.11}$$

$$\mathbf{G} = \begin{pmatrix} \Delta^2/2 & 0 \\ 0 & \Delta^2/2 \\ \Delta & 0 \\ 0 & \Delta \end{pmatrix}\ , \tag{4.12}$$

$$\mathbf{w}_j \sim \mathcal{N}(0, \sigma_{\mathrm{w}}^2 \cdot \mathbf{I}) \tag{4.13}$$

and Δ is the time interval between samples. The covariance matrix of the driving and observation noise is given by

$$\mathbf{Q}_j = \sigma_{\mathrm{w}}^2 \cdot \mathbf{G}\mathbf{G}^{\mathrm{T}}\ . \tag{4.14}$$

We consider the measurements are the received powers $P_{Rx,j}$ at the j-th node from the set of anchor nodes within range, $\mathcal{N}_j$. The measurements are related to the unknown parameters $\mathbf{s}_j(t)$ according to (2.7), where

$$\rho_{j,i} = \sqrt{(x^{(j)}(t) - x_a^{(i)})^2 + (y^{(j)}(t) - y_a^{(i)})^2}\ . \tag{4.15}$$

Then the observation equation is

$$\mathbf{y}_j(t) = \mathbf{h}(\mathbf{s}_j(t)) + \mathrm{v}_j(t)\ , \tag{4.16}$$

with

$$\mathbf{h}(\mathbf{s}_j(t)) = \begin{pmatrix} P_{Tx,1} - L_o + 10p\log_{10}\left(\frac{\rho_{j,1}}{\rho_o}\right) \\ \vdots \\ P_{Tx,|\mathcal{N}_j|} - L_o + 10p\log_{10}\left(\frac{\rho_{j,|\mathcal{N}_j|}}{\rho_o}\right) \end{pmatrix} \tag{4.17}$$

and

$$\mathrm{v}_j(t) = \begin{pmatrix} \upsilon_{j,1} \\ \vdots \\ \upsilon_{j,|\mathcal{N}_j|} \end{pmatrix} , \tag{4.18}$$

with covariance matrix given by

$$\mathbf{C}_j(t) = \begin{pmatrix} \sigma^2_{j,1} & 0 & \cdots & 0 \\ 0 & \sigma^2_{j,2} & \ddots & \vdots \\ \vdots & \ddots & \ddots & 0 \\ 0 & \cdots & 0 & \sigma^2_{j,|\mathcal{N}_j|} \end{pmatrix} . \tag{4.19}$$

Since the measurement function is nonlinear in the signal parameters, to estimate the state vector with the EKF we apply a linearization. The Jacobian, $\mathbf{H}(t)$, is given by

$$\mathbf{H}_j(t) = \begin{pmatrix} H_j^{(1,1)}(t) & H_j^{(1,2)}(t) & 0 & 0 \\ \vdots & \vdots & \vdots & \vdots \\ H_j^{(|\mathcal{N}_j|,1)}(t) & H_j^{(|\mathcal{N}_j|,2)}(t) & 0 & 0 \end{pmatrix} \Bigg|_{\mathbf{s}=\hat{\mathbf{s}}(t|t-1)} , \tag{4.20}$$

where

$$\begin{aligned} H_j^{i,1}(t) &= \frac{10p\ (x^{(j)}(t) - x_a^{(i)})}{\ln 10 \cdot \rho_{j,i}^2} \\ H_j^{i,2}(t) &= \frac{10p\ (y^{(j)}(t) - y_a^{(i)})}{\ln 10 \cdot \rho_{j,i}^2} . \end{aligned}$$

In summary, with the above definitions, the EKF equations [51] for our problem are given by

$$\hat{\mathbf{s}}_j(t|t-1) = \mathbf{A}\hat{\mathbf{s}}_j(t-1|t-1) ; \tag{4.21}$$

$$\mathbf{M}_j(t|t-1) = \mathbf{A}\mathbf{M}_j(t-1|t-1)\mathbf{A}^T + \mathbf{Q}_j ; \tag{4.22}$$

$$\begin{aligned} \mathbf{K}_j(t) &= \mathbf{M}_j(t-1|t-1)\mathbf{H}_j(t)^T(\mathbf{C} \\ &+ \mathbf{H}_j(t)\mathbf{M}_j(t|t-1)\mathbf{H}_j(t)^T)^{-1} ; \end{aligned} \tag{4.23}$$

$$\begin{aligned} \hat{\mathbf{s}}_j(t|t) &= \hat{\mathbf{s}}_j(t|t-1) + \mathbf{K}_j(t)(\mathbf{y}_j(t) \\ &- \mathbf{h}(\hat{\mathbf{s}}(t|t-1))) ; \end{aligned} \tag{4.24}$$

$$\mathbf{M}_j(t|t) = (\mathbf{I} - \mathbf{K}_j(t)\mathbf{H}_j(t))\mathbf{M}_j(t|t-1) , \tag{4.25}$$

where $\mathbf{y}_j(t)$ are the measurements of the received power.

4.3 Error Metric: Geometric Dilution of Precision

The GDOP metric is the error metric of the proposed game. It was presented previously in Section 2.3. As commented previously, the CRB for RSS ranging technique scales with the size of the system even if geometry is kept the same [31]. In [56], the GDOP expression has been derived for the RSS log-normal model as

$$\mathrm{GDOP}_j = \frac{\ln(10)}{10}\sqrt{\frac{\sum_{i=1}^{|\mathcal{N}_j|}\rho_{j,i}^{-2}}{\sum_{i=1}^{|\mathcal{N}_j|-1}\sum_{k=i+1}^{|\mathcal{N}_j|}\frac{\sin^2\phi_{ik}}{\rho_{j,i}^2\rho_{j,k}^2}}} \tag{4.26}$$

where ϕ_{ik} is the angle between the two vectors from target node j to the ith and kth anchor nodes. From (5.10) we can observe that the GDOP depends not only on the angular distribution of reference nodes (geometry), but also on the distances of the target node to the reference nodes.

Notice that anchor nodes in (5.10) are those of the set $\mathcal{N}_j$. $\mathcal{N}_j$ depends on the number of anchor nodes whose beacons are received with enough power by node j. Therefore, it depends on the transmit powers of the anchor nodes. For a given receiver sensitivity s and distance-dependent path loss function $f_L(d)$, an anchor node with transmit power p_a at distance d_a from node j belongs to set $\mathcal{N}_j$ if $p_a > s/f_L(d_a)$. Therefore, given the dependence of GDOP_j on $\mathcal{N}_j$, we may in turn express the GDOP as a function of the power vector of the anchor nodes $\mathbf{p}$ explicitly as $\mathrm{GDOP} \triangleq \mathrm{GDOP}(\mathbf{p})$. Due to the dependence of $\mathcal{N}_j$ on $\mathbf{p}$, we can observe that any error metric based on the covariance of the estimator for RSS model will be a non convex function on $\mathbf{p}$. In particular, the $\mathrm{GDOP}(\mathbf{p})$ shows discontinuities because of the inclusion or exclusion of a node in $\mathcal{N}_j$.

Moreover, let us define the mean GDOP over the entire network as

$$\overline{\mathrm{GDOP}}(\mathbf{p}) = \frac{1}{M}\sum_{j=1}^{M}\mathrm{GDOP}_j(\mathbf{p}) \ , \tag{4.27}$$

where, rearranging terms in (5.10) for convenience, we obtain

$$\mathrm{GDOP}_j = \frac{\ln(10)}{10}\sqrt{\frac{\sum_{i=1}^{|\mathcal{N}_j|}\prod_{\substack{k=1\\k\neq i}}^{|\mathcal{N}_j|}\rho_k^2}{\sum_{i=1}^{|\mathcal{N}_j|-1}\sum_{k=i+1}^{|\mathcal{N}_j|}(\prod_{\substack{l=1\\l\neq i,k}}^{|\mathcal{N}_j|}\rho_l^2)\sin^2\phi_{ik}}} \ . \tag{4.28}$$

4.4 Potential game for energy efficient positioning

A strategic non-cooperative game $\Gamma(\Omega, \mathcal{A}, u)$ has three main components: *i*) Ω is the set of N players; *ii*) $\mathcal{A}$ is the set of pure strategies and $\mathbf{a} = [a_1, \ldots, a_N]^T \in \mathcal{A} \subseteq \mathbb{R}^N$ the chosen strategies, where $a_i \in \mathcal{A}_i$ represents the strategy of the i-th player over the set of its possible strategies $\mathcal{A}_i$. Thus, $\mathcal{A} = \times_{i=1}^{N} \mathcal{A}_i$ and $\mathbf{a}_{-i} \in \mathcal{A}_{-i} = \times_{j \neq i}^{N} \mathcal{A}_j$ represents the strategies of all players but the i-th; *iii*) $u_i : \mathcal{A} \mapsto \mathbb{R}$ is the utility function of the i-th player. The utility function (or payoff) quantifies the preferences of each player to a given strategy, provided the knowledge of other's strategies. Then, $u \triangleq \{u_i\}_{i \in \Omega}$ is the set of all N utility functions.

In our problem, players are the anchor nodes and the game is that of finding a NE such that each anchor node is transmitting at a minimal power while maintaining a certain positioning quality for the M target nodes. As a metric to assess such quality we use the GDOP. With this setup, Ω is the set of anchor nodes in the network. The set of strategies that the i-th reference node can choose are the set of its possible discrete power levels $\mathcal{P}_i$. We define $\mathbf{p} = [p_1, \ldots, p_N]^T \in \mathcal{P} = \times_{i=1}^{N} \mathcal{P}_i$ as the vector containing the strategies of each node. We also assume that, at the beginning of the game, anchor nodes transmit with their maximum power level in order to gather information and allow initial positioning of nodes.

We adopt an iterative *best response* algorithm to achieve a NE of the game defined by $\Gamma(\Omega, \mathcal{P}, u)$. Anchor nodes decide iteratively its power transmission by maximizing its utility function (see Section 3.3 for further details),

$$\hat{p}_i = \arg \max_{p_i \in \mathcal{P}_i} \{u_i(p_i, \hat{\mathbf{p}}_{-i})\} \ . \tag{4.29}$$

After each iteration, the selected power level may modify the geometry of the network, thus impacting on the maximization of other players' utility.

The design of a utility function and the existence of a potential function is crucial for the task of identifying NE in the game. In our algorithm the goal is to attain a desired positioning quality for the M target nodes, as well as reducing the total power of the N anchor nodes. As presented in Section 2.3.2, the GDOP provides an appealing metric to assess such quality. Therefore, the algorithm accepts a strategy if condition $\overline{\text{GDOP}}(\mathbf{p}) \leq \gamma$ is fulfilled, with γ being a design parameter. Recall that the initial topology is such that all nodes transmit at maximum power. Following the result in [62], the utility function stated in Proposition 4.1 is considered.

Proposition 4.1. *The game $\Gamma(\Omega, P, u)$ where the individual utilities are given by*

$$u_i(p_i, \mathbf{p}_{-i}) = \begin{cases} p_{init} - p_i & \text{if} \quad \overline{\text{GDOP}}(p_i, \mathbf{p}_{-i}) \leq \gamma \\ -p_i & \text{otherwise} \end{cases} \tag{4.30}$$

is an EPG and the exact potential function is

$$V(\mathbf{p}) = \begin{cases} p_{init} - \sum_{i\in\Omega} p_i & \text{if} \quad \overline{\text{GDOP}}(p_i, \mathbf{p}_{-i}) \leq \gamma \\ -\sum_{i\in\Omega} p_i & \text{otherwise,} \end{cases} \tag{4.31}$$

where $p_{init} = p_{max}$ is the maximum power of the sensor node.

Proof. We prove it by applying the concept of EPG in Definition 3.6. Consider $p_i, p_i' \in \mathcal{P}_i \mid p_i < p_i'$, therefore

$$\Delta u_i = u_i(p_i, \mathbf{p}_{-i}) - u_i(p_i', \mathbf{p}_{-i}) = p_i' - p_i \tag{4.32}$$

regardless $\overline{\text{GDOP}}(p_i, \mathbf{p}_{-i}) \leq \gamma$ or $\overline{\text{GDOP}}(p_i, \mathbf{p}_{-i}) > \gamma$. Similarly, the potential variational may be

$$\begin{aligned} \Delta V &= V(p_i, \mathbf{p}_{-i}) - V(p_i', \mathbf{p}_{-i}) \\ &= -\left(p_i + \sum_{j\in\Omega; j\neq i} p_j\right) + \left(p_i' + \sum_{j\in\Omega; j\neq i} p_j\right) \\ &= p_i' - p_i \ . \end{aligned} \tag{4.33}$$

Thus, $\Delta u_i \equiv \Delta V$ therefore V is an exact potential function and the game $\Gamma(\Omega, \mathcal{P}, u)$ is an EPG. □

The designed game falls into the category of EPG games, and thus finding the NE point of (5.12) is equivalent to maximizing the potential function in (4.31). We note that GDOP is not a convex function on $\mathbf{p}$. Therefore, we cannot claim that $V(\mathbf{p})$ has a single optimum, and thus the game might have several NE that satisfy $\overline{\text{GDOP}}(\mathbf{p}) \leq \gamma$. However, simulations of Section 4.7.1 reveal that the distributed algorithm obtains results which are comparable to a global approach.

4.5 Distributed error metrics

The game presented above has several challenges when it comes to implementation. A major concern relates to the amount of information exchange required in the networks, as anchor nodes require knowledge of global information of target nodes in order to calculate $\overline{\text{GDOP}}(\mathbf{p})$. The main goal here is to minimize the information exchange requirements in order to preserve the benefits from power savings, due to reduced transmission power at the reference nodes. To that aim other metrics are

proposed, instead of $\overline{\text{GDOP}}(\mathbf{p})$, that only require transmission of information from in-range target nodes to anchors at each game iteration. This information includes the target's own position estimate and the corresponding set $\mathcal{N}_j$.

We propose to modify the discontinuity condition in (5.12)-(4.31) so as to use only local GDOP estimates. Two alternatives are presented. Similarly to the game using global information, it is consider that at the beginning of both games players transmit with maximum power in order to allow initial positioning of target nodes and information gathering. The algorithms proceed in an iterative best response fashion until convergence.

4.5.1 Local GDOP Average

In this case a local estimate of the average GDOP is considered, defined as $\overline{\text{GDOP}}_{\mathcal{T}_i}(\mathbf{p})$ in (4.34) for the i-th anchor node. Recall that $\mathcal{T}_i$ is the set of target nodes from which the i-th anchor nodes receives status information, as they are within its range. Then, each anchor can compute

$$\overline{\text{GDOP}}_{\mathcal{T}_i}(\mathbf{p}) = \frac{1}{T_i} \sum_{j \in \mathcal{T}_i} \text{GDOP}_j(\mathbf{p}) \ . \tag{4.34}$$

The resulting utility function for the i-th player is then modified to take values as $p_{\max} - p_i$ if $\overline{\text{GDOP}}_{\mathcal{T}_i}(p_i, \mathbf{p}_{-i}) \leq \gamma$. With this setup, it is possible that the overall $\overline{\text{GDOP}}$ value exceeds the threshold eventually, since the average used by each player is local. In other words, a certain strategy might lead to $\overline{\text{GDOP}}_{\mathcal{T}_i}(\mathbf{p}) \leq \gamma$ but $\overline{\text{GDOP}}_{\mathcal{T}_{i'}}(\mathbf{p}) > \gamma$, forcing the i'-th node to increase its power in next game iteration.

Notice that this distributed solution approximates the previous game when transmission powers of target nodes are such that one can consider $\overline{\text{GDOP}} \simeq \overline{\text{GDOP}}_{\mathcal{T}_i}, \forall i$. For the static scenario, Figure 4.1 shows the RMSE between $\overline{\text{GDOP}}$ and $\overline{\text{GDOP}}_{\mathcal{T}_i}$, defined as

$$\xi(\text{GDOP}) = \sqrt{\frac{1}{N} \sum_{i=1}^{N} |\overline{\text{GDOP}} - \overline{\text{GDOP}}_{\mathcal{T}_i}|^2} \ , \tag{4.35}$$

versus the ratio range of target nodes over the maximum distance in the network (thus being independent of a particular node's power levels). The approximation is valid for increasing target node's power and density.

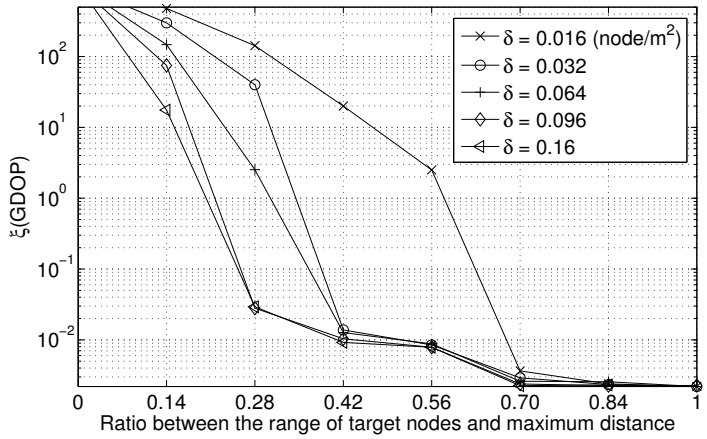

Figure 4.1: RMSE in (4.35) for a number of target node densities δ (node/m^2) and 100 Monte Carlo trials.

4.5.2 Worst Case GDOP

An alternative design is presented where worst-case is addressed. In this configuration, the condition to maximize $u_i(p_i, \mathbf{p}_{-i})$ is to ensure that all target nodes have the specified GDOP. That is, the condition for the i-th player can be formulated as

$$\mathrm{GDOP}_j(\mathbf{p}) \leq \gamma, \forall j \in \mathcal{T}_i \ , \tag{4.36}$$

and the utility in (5.12) should be modified accordingly. It can be easily seen that a game implementing such utility yields to a steady state solution. Remember that game starts with all players transmitting with maximum power. Notice that a player has no incentives to decrease its power if it causes at least one target node increase its GDOP. Same applies to the rest of players when iterating, and thus a stable solution is eventually achieved when no player can modify further its strategy.

Although the achieved solution is not optimal (from an energy-efficient point of view), it provides a strategy set which ensures the specified target GDOP. This might be useful in applications where this is the most restrictive issue, rather than proper power control.

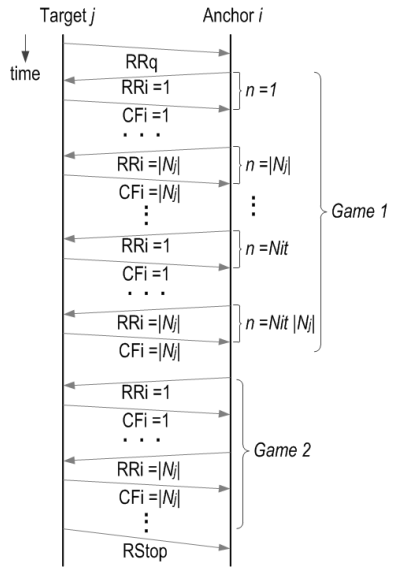

Figure 4.2: Time diagram of the algorithm.

4.6 Computational complexity analysis

4.6.1 Potential Game with Positioning Algorithm

In this section, implementation challenges of the proposed game theoretical algorithm are addressed. A possible solution to implement the proposed game is presented, which minimizes the information exchange required between target and anchor nodes, as well as the number of operations.

On one hand, the information exchange required between target and anchor nodes is presented in Figure 4.2 for the moving scenario. The algorithm starts when one or more target nodes broadcast a ranging request ($\overrightarrow{\text{RRq}}$). Then, $|\mathcal{N}_j|$ iterations of the game are performed: a ranging reply $\overleftarrow{\text{RRi}}$ and a confirmation frame $\overrightarrow{\text{CFi}}$ are interchanged between a target and the corresponding anchor nodes from $i = 1$ to $i = |\mathcal{N}_j|$. Following iterations of the game can be performed until $n = N_{it}|\mathcal{N}_j|$ iteration, in which the game reaches NE. Therefore, we consider that the number of best response iterations is N_{it} and the total number of algorithm iterations is $N_{it}|\mathcal{N}_j|$. The iterations of the best response algorithm are executed by anchor nodes iteratively. Once a game is finished, the target moves and after a while another game can start. Note that the right arrow ($\rightarrow$) over the frame name indicates a frame transmission from target to anchor i and the left arrow ($\leftarrow$) a frame transmission from anchor i to target.

On the other hand, algorithm 4.1 shows the detailed pseudo-code description of the proposed algorithm for the moving scenario. It shows the operations performed by target and anchor nodes in each iteration of the game. Once the algorithm starts when one or more target nodes broadcast a ranging request ($\overrightarrow{\text{RRq}}$), then the prediction phase of the EKF is performed in the target node. Therefore the prediction for the position of the target node is known. Based on this prediction, the game runs and the GDOP can be calculated. In each iteration of the game, the following information exchange is required between the corresponding anchor node and target node:

- $\overleftarrow{\text{RRi}}$: the ranging reply with the chosen transmit power p_i is transmitted from anchor to target node, then the target nodes estimates the distance with RSS-based technique and an averaging can be done with previous RSS measurements.
- $\overrightarrow{\text{CFi}}$: the target nodes respond to the anchor node with the confirmation frame or acknowledgement that contains needed information for the game ($\hat{\rho}_{j,i}$, $i = 1...|\mathcal{N}_j|$). Once the corresponding anchor i receives this $\overrightarrow{\text{CFi}}$, it plays choosing a new p_i maximizing its utility function depending on the used GDOP metric. To analyze the maximization of its utility function, the corresponding anchor i analyzes the condition GDOP $\leq \gamma$ for each value p_i of the set of transmit powers $P_{Tx,i}$ with the following steps: i) Anchor i estimates GDOP metric for p_i. Therefore anchor i analyzes if its contribution to GDOP estimation is required for p_i. Anchor i contributes when $P_{Rx,j}(p_i, \hat{\rho}_{j,i}) > s$, where s is the sensibility and $P_{Rx,j}$ is estimated with (2.7). ii) For p_i, the condition GDOP $\leq \gamma$ is analyzed. iii) Once steps i) and ii) are performed for the set $P_{Tx,i}$, anchor i chooses the p_i. If the contribution is required, anchor i chooses p_i minimum such that GDOP $\leq \gamma$; but if the contribution is not required, anchor i does not help to track any more saving energy.

Once the game is over each target has the information to execute the update phase of the EKF. Then the target estimates its position. The algorithm can start again with the prediction phase and the process runs again. The time interval between game performances could be controlled by parameters as battery and error metric of the target node.

For the static scenario, the same information exchange may apply but only for one game in Figure 4.2. Moreover, in Algorithm 4.1 the positioning procedure may be performed with linear Least Squares algorithm.

Algorithm 4.1 Potential game for energy efficient positioning for $M = 1$ and mobile setup

Target node j computes the predicted position with the Extended Kalman Filter.
Initialization: $\overrightarrow{\text{RRq}}$.
Set $\mathbf{p} = \mathbf{P}_{max}$.
Game iterations phase: $n = 1$, $i = 1$.
while $n < (N_{it}|\mathcal{N}_j|)$ **do**
  $\overleftarrow{\text{RRi}}$ is sent from anchor i to target node j:
  · It contains: if $n = 1$, $\mathbf{x}_a^{(i)}$ and initial $\mathbf{p}$.
  · Operations of target node: distance estimation $\hat{\rho}_i$.
  $\overrightarrow{\text{CFi}}$ is sent from target j to anchor node i:
  · It contains: $\hat{\rho}_i$, $i = 1...|\mathcal{N}_j|$.
  · Operations of anchor node: if $i > 1$, update $p_i \mid \text{GDOP}(p_i, \mathbf{p}_{-i}) \leq \gamma$.
  if $i = |\mathcal{N}_j|$ **then**
    $i = 1$
  else
    $i = i + 1$ {Next anchor node}
  end if
  $n = n + 1$
end while
$\overleftarrow{\text{RStop}}$.
Target node j computes the update phase of the EKF: position $\hat{\mathbf{x}}$.

Table 4.1: Complexity of Algorithm 4.1

Node	**Computation**	**Operation**	**Size**	**Cost**
Target j	Prediction phase of EKF: $\hat{\mathbf{s}}(t\|t-1) = \mathbf{A}\hat{\mathbf{s}}(t-1\|t-1)$ $\mathbf{M}(t\|t-1) = \mathbf{A}\mathbf{M}(t-1\|t-1)\mathbf{A}^T + \mathbf{Q}$	 Matrix product Matrix products, addition	 $4\times\|\mathcal{N}_j\|\times 1$ $4\times 4\times 4$	$\leq \mathcal{O}(5N+84)$ $\mathcal{O}(5\|\mathcal{N}_j\|+4)$ $\mathcal{O}(4^3+16)$
Target j	Update phase of EKF: $\mathbf{H}(t)$, see (4.20) $\mathbf{M}(t\|t) = (\mathbf{I}-\mathbf{K}(t)\mathbf{H}(t))\mathbf{M}(t\|t-1)$ $\mathbf{K}(t) = \mathbf{M}(t-1\|t-1)\mathbf{H}(t)^T$ $\cdot (C + \mathbf{H}(t)\mathbf{M}(t\|t-1)\mathbf{H}(t)^T)^{-1}$ $\hat{\mathbf{s}}(t\|t) = \hat{\mathbf{s}}(t\|t-1)$ $+ \mathbf{K}(t)(\mathbf{x}(t) - \mathbf{h}(\hat{\mathbf{s}}(t\|t-1)))$	 Additions, products Matrix products and addition Matrix products, addition and inverse Matrix product and additions	 $26\|\mathcal{N}_j\|$ $4\times\|\mathcal{N}_j\|\times 1$	$\leq \mathcal{O}(N^3+8N^2$ $+38N+132)$ $\mathcal{O}(26\|\mathcal{N}_j\|)$ $\mathcal{O}(16\|\mathcal{N}_j\|+4^3)$ $\mathcal{O}(\|\mathcal{N}_j\|^3+8\|\mathcal{N}_j\|^2$ $+17\|\mathcal{N}_j\|+4^3)$ $5\|\mathcal{N}_j\|+4$
Anchor i	Compute $N_{Tx}^{(*)}$ $P_{Rx,j}$: $P_{Rx,j} = P_{Tx,i} - L_o + 10p\log_{10}\left(\frac{\hat{\rho}_{j,i}}{\rho_o}\right)$	$N_{Tx}^{(*)}$ (2 Additions, $\log_{10}$, 2 products, division)	6	$\mathcal{O}(6)$
Anchor i	Compute GDOP (see 4.28) with and without i contribution $\sum_{i=1}^{\|\mathcal{N}_j\|}\prod_{\substack{k=1\\k\neq i}}^{\|\mathcal{N}_j\|}\rho_k^2$; (a) $\sum_{i=1}^{N-1}\sum_{k=i+1}^{N}(\prod_{l\neq i,k}^{N}\rho_{j,l}^2)\sin^2\phi_{ik}$; (b) Choose minimum $P_{Tx,i}$ | GDOP $\leq \gamma$	Operations: 2·(a, b, c) (a) Product, addition (b) Product, addition, sin (c) Product, division, root	1 $2(\|\mathcal{N}_j\|-1)\|\mathcal{N}_j\|$ $\frac{(2\|\mathcal{N}_j\|-3)\|\mathcal{N}_j\|!}{(\|\mathcal{N}_j\|-2)!(2!)}$ 3	$\leq \mathcal{O}\left(\frac{2N^3+3N^2-5N}{4}\right)$ $\mathcal{O}\left(2\|\mathcal{N}_j\|^2-2\|\mathcal{N}_j\|\right)$ $\mathcal{O}\left(\frac{(2\|\mathcal{N}_j\|^3-5\|\mathcal{N}_j\|^2)}{4}\right)$ $+\left(\frac{3\|\mathcal{N}_j\|)}{4}\right)$ $\mathcal{O}(3)$

(*) Number of transmit powers.

4.6.2 Computational Resources

In this section the required computational resources of the presented solution are analyzed. From Algorithm 4.1, the computational complexity can be obtained by calculating the number of basic operations involved. In Table 4.1 the number of operations is summarized for $M = 1$ target node. The operations are shown with respect to the number of anchor nodes $|\mathcal{N}_j|$. Taking into account that the upper bound is $|\mathcal{N}_j| \leq N$, then $\mathcal{O}(|\mathcal{N}_j|) \leq \mathcal{O}(N)$.

From Table 4.1, we calculate the total asymptotical computational cost for the target node $\mathcal{C}_j$ and we obtain

$$\begin{aligned} \mathcal{C}_j &= \mathcal{O}((N_{it}|\mathcal{N}_j| - 1)(|\mathcal{N}_j|^3 + 8|\mathcal{N}_j|^2 + 43|\mathcal{N}_j| + 216)) \\ &\leq \mathcal{O}(N_{it}N^4). \end{aligned} \tag{4.37}$$

The cost for the anchor node i, $\mathcal{C}_i$, is

$$\begin{aligned} \mathcal{C}_i &= \mathcal{O}\left((N_{it}|\mathcal{N}_j| - 1)\left(\frac{2|\mathcal{N}_j|^3 + 3|\mathcal{N}_j|^2 - 5|\mathcal{N}_j| + 24}{4}\right)\right) \\ &\leq \mathcal{O}\left(\frac{N_{it}N^4}{2}\right) . \end{aligned} \tag{4.38}$$

Note from (5.20) that $\mathcal{C}_{\text{target}}$ scales with $|\mathcal{N}_j|^4$. One of the most demanding operations is the inverse matrix for $\mathbf{K}(t)$, because the size of the matrix is $|\mathcal{N}_j| \times |\mathcal{N}_j|$. For the anchor node i, the most complex operations are part of the GDOP computation (see (b) operations in Table 4.1) that scales with $|\mathcal{N}_j|^4$.

For the case $M > 1$ each target node has to execute the same operations detailed in Table 4.1 while the anchor node i has to calculate the operations of Table 4.1 for each target node. Therefore, the computational complexity also scales with M and is given by

$$\begin{aligned} \mathcal{C}_i &= \mathcal{O}\left(M(N_{it}|\mathcal{N}_j| - 1)\left(\frac{2|\mathcal{N}_j|^3 + 3|\mathcal{N}_j|^2 - 5|\mathcal{N}_j| + 24}{4}\right)\right) \\ &\leq \mathcal{O}\left(\frac{MN_{it}N^4}{2}\right). \end{aligned} \tag{4.39}$$

The quartic relation of the computational complexity with the number of anchor nodes might be an issue in large-scale networks, mostly in sensor networks due to the limited power processing of the motes. A possible workaround is to limit the total number of anchor nodes used for positioning at the target nodes.

4.7 Simulation Results

The proposed algorithm was tested in the static and dynamic scenarios that were introduced in sections 4.2.1 and 4.2.2. Each node had a 2.4GHz IEEE 802.15.4 ready RF Transceiver based on a CC2420 from Texas Instruments. The set of transmit powers of the CC2420 is $P_{Tx,i} = \{1, 0.79, 0.50, 0.31, 0.1, 0.032, 0.0015, 0\}$ mW.

While the static scenario aims to show the convergence to a NE for one game, the mobile scenario shows the convergence of several games together with the tracking operation of the target nodes. In both cases, target nodes estimated its position with the set of RSS values. In the static scenario, target nodes estimated its position by a LS algorithm whereas in the mobile scenario an EKF was used for tracking. The density of target nodes is higher for the static scenario than for the mobile scenario. In both cases, we compare the performance of the distributed $\text{GDOP}_j(\mathbf{p})$ and $\overline{\text{GDOP}}_{\mathcal{T}_i}(\mathbf{p})$ metrics with the global metric $\overline{\text{GDOP}}(\mathbf{p})$.

4.7.1 Static Scenario

The considered static scenario was composed of $M = 20$ nodes that aim at locating themselves using RSS signal to a set of $N = 8$ anchor nodes (Figure 4.3). Anchor nodes (big dots) were distributed at known positions in a 25×25 meters area, whereas the M target nodes (black crosses) were placed randomly in the space. Position estimates (grey crosses) are also shown for the last iteration of the game.

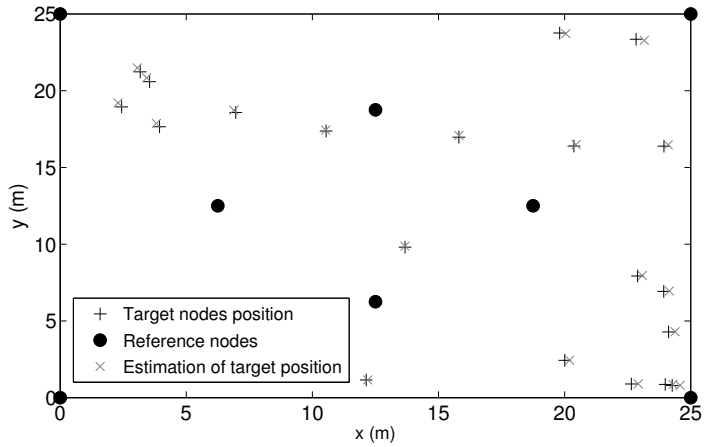

Figure 4.3: Static scenario of simulation.

In one game, anchors play N_{it} rounds (best response iterations). In each round all anchors play in an ordered sequential fashion. Thus, once all anchors have played the first round, they play again another round and successively. The number of rounds is N_{it}, therefore each player plays N_{it} times or iterations. At each iteration, the corresponding anchor node has to compute GDOP values, which depend on the estimated positions of the target nodes within range. Such position estimate is performed at target nodes using the set of RSS values. At each iteration, the random error $\upsilon_{j,i}$ is different in each RSS measurement, it affects the distance estimation $\hat{\rho}_{j,i}$. Thanks to the game iterations, the RSS values are averaged N_{it} times, thus decreasing its error. Therefore, for each iteration of the game the RMSE of position estimate decreases in this phase of refinement of the error.

We considered $N_{it} = 5$ iterations of the game as stopping rule and the mean GDOP value was $\gamma = 1.3$. For RSS based range model we considered $p = 3$ and $\sigma_{j,i} = 0.1$ dB for all possible $\{i, j\}$ pairs.

Recall that initially all nodes transmit at their maximum power. Results of the proposed algorithm were averaged over 100 Monte Carlo independent trials and compared to those obtained by an algorithm that globally optimizes the set of power levels $\mathbf{p}$. That is, the solution of the coordination game that finds the global optima of the potential function $V(\mathbf{p})$. This solution, implemented by exhaustive search, explores all combinations of power levels for the N nodes ($\dim\{\mathcal{P}\}^N$) and obtains the set of strategies with lower mean power ($\bar{\mathbf{p}}_{\min}$) over the network, with the condition on the GDOP holding. In the simulation results, we compare the average results of our method with the GDOP average of all the target nodes $\overline{\text{GDOP}}(\mathbf{p})$, the distributed game with local GDOP average $\overline{\text{GDOP}}_{\mathcal{T}_i}(\mathbf{p})$ and the distributed game with worst case GDOP, as well as $\bar{\mathbf{p}}_{\min}$.

Figure 4.4 shows the evolution of the mean power of the network versus the iterations of the game. We can observe that this value decreases and tends to $\bar{\mathbf{p}}_{\min}$. Of interest is the comparison of these results with those in Figure 4.5, where we can identify that although our algorithm might yield larger mean power values, we experience a tradeoff in the final GDOP achieved. Results of the case with local GDOP average come closer to $\bar{\mathbf{p}}_{\min}$ than for worst case GDOP. This is because worst case GDOP assures that each GDOP is below the threshold.

4.7.2 Dynamic Scenario

The proposed algorithm was tested in a scenario composed of $M = 2$ mobile target nodes that aim at locating themselves using the RSS from a set of anchor nodes (Figure 5.1). The considered nodes are IEEE 802.15.4 compliant. Anchor nodes are

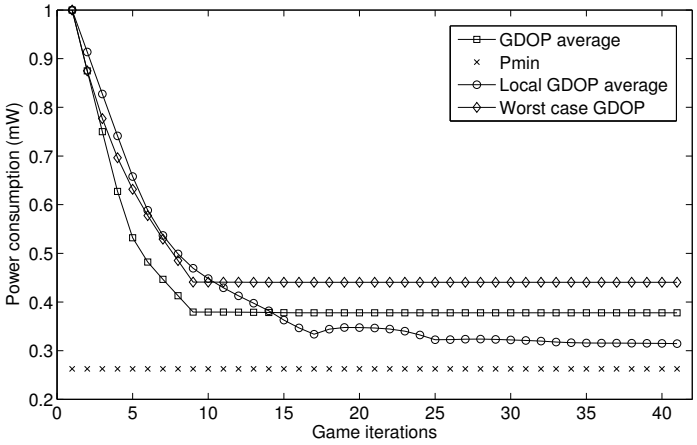

Figure 4.4: Mean power of anchor nodes versus iterations of the game.

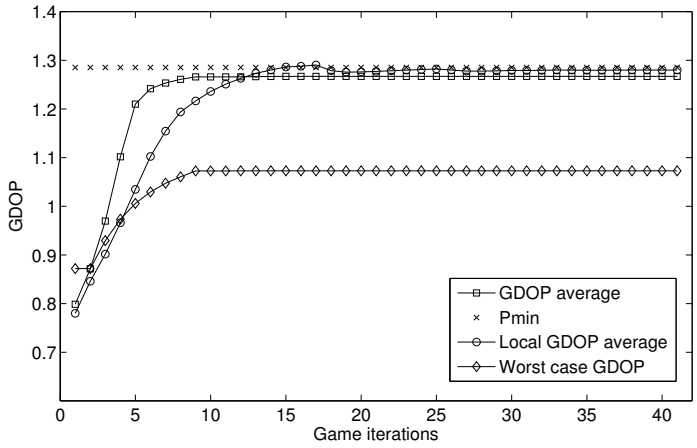

Figure 4.5: $\overline{\text{GDOP}}$ versus iterations of the game.

distributed at known, regular positions every 15m in a $800 \times 450\text{m}^2$ region. They are numbered starting at origin in Figure 5.1. The $M = 2$ target nodes are placed in a close position initially, but their trajectories diverge. Target nodes are mobile and they send requests to receive ranging signals at intervals of $\Delta = 0.8$s. In each request the game starts until the NE is achieved. In order to show how the algorithm works, Δ equals for each node is considered. The playing anchor nodes compute the GDOP of the target nodes for the three cases previously presented: $\overline{\text{GDOP}}(\mathbf{p})$, $\overline{\text{GDOP}}_{\mathcal{T}_i}(\mathbf{p})$ and $\text{GDOP}_j(\mathbf{p})$. Therefore, as a game is executed every Δ s and the number of games is $N_{games} = 120$, the simulation duration in time is $\Delta \cdot N_{games} = 96$ s. Results of the proposed algorithm were averaged over 200 Monte Carlo independent trials.

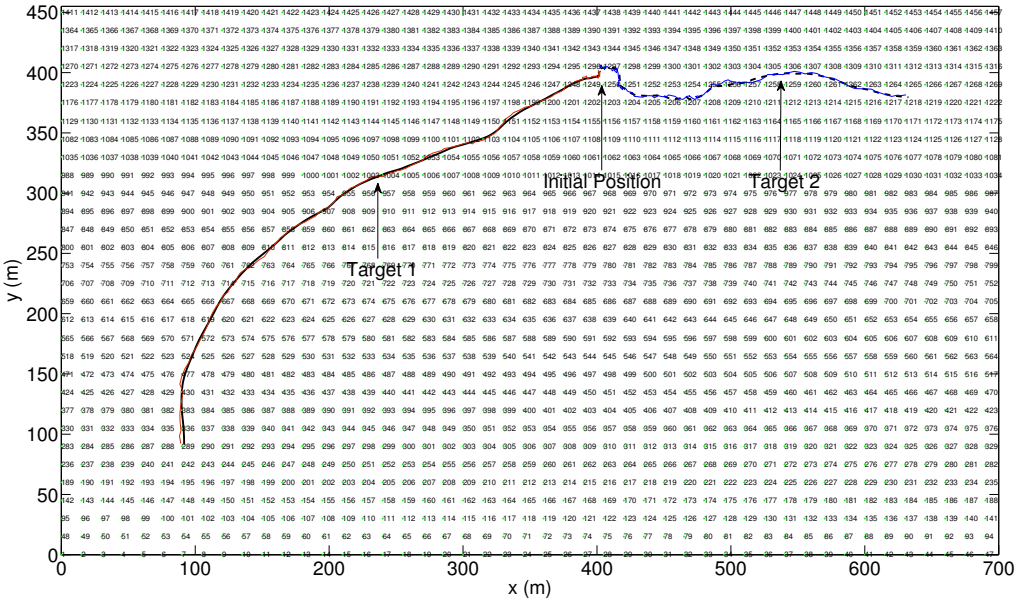

Figure 4.6: Scenario consisting of anchor nodes (green points) and M=2 target nodes with different trajectories. The initial position of target 1 is (401, 401) and for target 2 (403, 403). The anchor nodes are numbered with and ID number starting from the origin. The trajectory of target node 1 is represented with a solid line (black color for real trajectory and red for estimated one). The trajectory of target node 2 is represented with a dashed line (black: real trajectory; blue: estimated trajectory).

For the simulations, the used values of channel model parameters are from [23]. These parameters values have been obtained from an experimental campaign to collect the RSS measurements with sensor nodes equipped with CC2420 transceiver. Thus, we consider $L_0 = -20$ dB, $\rho_0 = 0.1$ m, $p = 3$ and $\sigma_{j,i} = 4$ dB. The initial conditions of the first target node were the following: the position was $x^{(1)}(0) = y^{(1)}(0) = 401$ m and the velocity was $v_x^{(1)}(0) = v_y^{(1)}(0) = 0$ m/s. While for the second node the position was $x^{(2)}(0) = y^{(2)}(0) = 403$ m and the velocity was $v_x^{(2)}(0) = v_y^{(2)}(0) = 0$ m/s. Also, $\sigma_{\mathrm{w}}^2 = 5$ for both target nodes.

On one hand, the evolution towards the NE for a game is explain. In one game, anchors play N_{it} rounds. In each round all anchors play in an ordered sequential fashion. Thus, once all anchors have played the first round, they play again another round and successively. The number of rounds is $N_{it} = 4$, therefore each player plays $N_{it} = 4$ times or iterations. At each iteration, the corresponding anchor node has to compute GDOP values, which depend on the estimated positions of the target nodes within range. Such position estimate is performed at target nodes using the

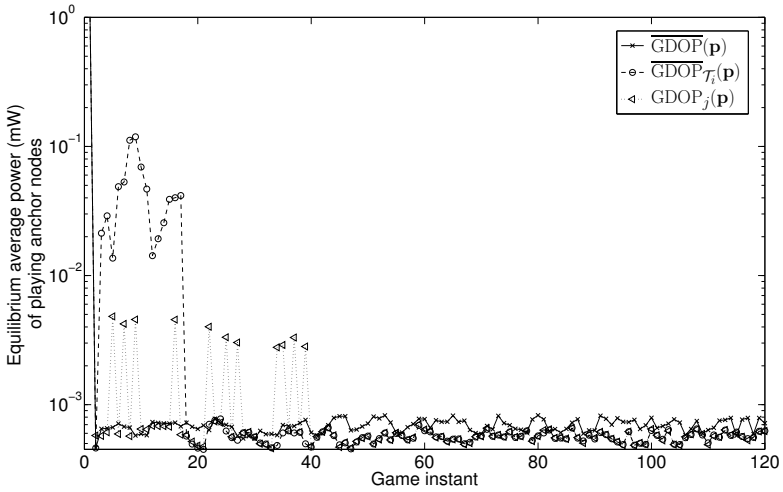

Figure 4.7: Average power of playing anchors in Nash equilibrium of the games for metrics $\overline{\text{GDOP}}(\mathbf{p})$, $\overline{\text{GDOP}}_{\mathcal{T}_i}(\mathbf{p})$ and $\text{GDOP}_j(\mathbf{p})$.

set of RSS values by EKF procedure. During the evolution towards the NE, transmit powers are minimized from maximum (1 mW) to smallest value that maintains the $\text{GDOP}_j(\mathbf{p}) < \gamma$, which is set to $\gamma = 4$. Thanks to the game iterations, the RSS values are averaged $N_{it} = 4$ times decreasing its error. See previous Section 4.7.1 for more information about the evolution of one game towards the NE. In Figure 4.9 is plotted the resulting RMSE on the positioning solution after the power control games were executed, with consistent results.

On the other hand, the results at the NE of each played game while target nodes move along the trajectories are shown in the scenario of Figure 5.1. Every game is run every Δ s. As targets move, the different games may be played by different anchors. In Figure 4.7, the mean power of anchor nodes at the NE of the played games ($N_{games} = 120$) is showed. The power value is minimized to values close to 0.001mW. Of interest is the comparison of these results with Figure 4.8. We can identify that, for each played game, the proposed algorithm maintains the global metric $\overline{\text{GDOP}}(\mathbf{p}) < \gamma$ as well as the distributed metric $\text{GDOP}_j(\mathbf{p}) < \gamma$, ($\gamma = 4$). The differences with the threshold are due to the errors in the RSS measurements. For the less restrictive case $\overline{\text{GDOP}}_{\mathcal{T}_i}(\mathbf{p})$ of Figure 4.8 the values are clearly different to the other two metrics, when the two trajectories of the target nodes are close and anchor nodes performs the GDOP averaging $\overline{\text{GDOP}}_{\mathcal{T}_i}(\mathbf{p})$.

As previously commented, in Section 4.5.1, the RMSE between $\overline{\text{GDOP}}_{\mathcal{T}_i}(\mathbf{p})$ and $\overline{\text{GDOP}}(\mathbf{p})$ depends on target node density. The approximation $\overline{\text{GDOP}}_{\mathcal{T}_i}(\mathbf{p}) \simeq \overline{\text{GDOP}}(\mathbf{p})$ is valid for increasing density of target nodes (considering maximum

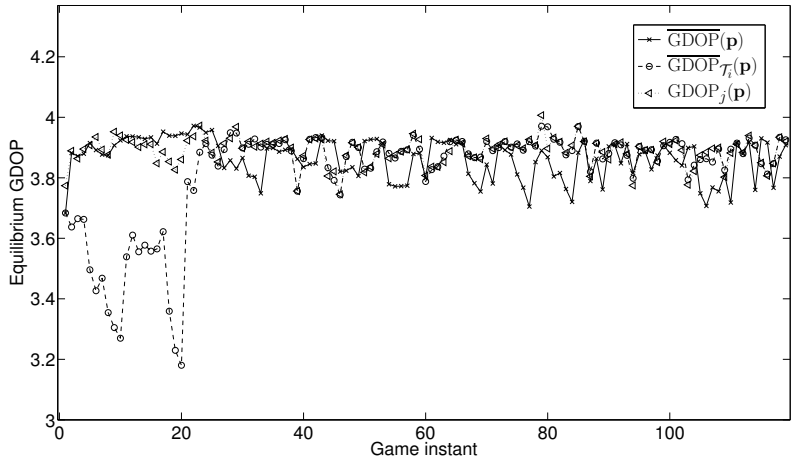

Figure 4.8: Real GDOP in Nash equilibrium of the games for metrics $\overline{\text{GDOP}}(\mathbf{p})$, $\overline{\text{GDOP}}_{\mathcal{T}_i}(\mathbf{p})$ and $\text{GDOP}_j(\mathbf{p})$.

transmit power for target nodes). In the mobile scenario there are $M = 2$ target nodes. Thus, effect due to low density of target nodes for $\overline{\text{GDOP}}_{\mathcal{T}_i}(\mathbf{p})$ can be observed, mostly in the part of the figures that corresponds to close trajectories of the target nodes (from 1st to 25th games). As earlier mentioned, in this part of Figure 4.8 the estimated GDOP metric $\overline{\text{GDOP}}_{\mathcal{T}_i}(\mathbf{p})$ is less accurate than the other metrics. Also, target trajectories are close and share anchor nodes, however the number of target nodes within range τ_i is different for each anchor node i. In Figure 4.10, the percentage of anchor nodes with $\tau_i = 1$ is shown (before playing the game). At the beginning, target nodes share the majority of anchor nodes, but when target trajectories separate, the number of anchor nodes that have one target node within range increases. For example in game 17th, 50% of anchor nodes have $\tau_i = 1$. Thus, the playing anchor nodes decide the new transmit power taking into account the GDOP average of τ_i, but this average $\overline{\text{GDOP}}_{\mathcal{T}_i}(\mathbf{p})$ can change for each player i as τ_i is different for each player. Comparing Figures 4.8 and 4.10, we can observe that the difference between $\overline{\text{GDOP}}_{\mathcal{T}_i}(\mathbf{p})$ and γ is low when the percentage of anchor nodes with $\tau_i = 1$ is $< 15\%$, meaning that the local metric approximates properly the global metric. The difference increases with larger percentages up to approx. 50% (corresponding to the 10th to 20th games). Then, the difference decreases again for larger percentages since, once the trajectories of target nodes are distant enough, $\text{GDOP}_j(\mathbf{p})$ and $\overline{\text{GDOP}}_{\mathcal{T}_i}(\mathbf{p})$ values are similar (Figure 4.8). This is because target nodes use different set of anchor nodes and thus the GDOP averaging $\overline{\text{GDOP}}_{\mathcal{T}_i}(\mathbf{p})$ ($\tau_i = 1$ for all i) is equivalent to the worst-case GDOP.

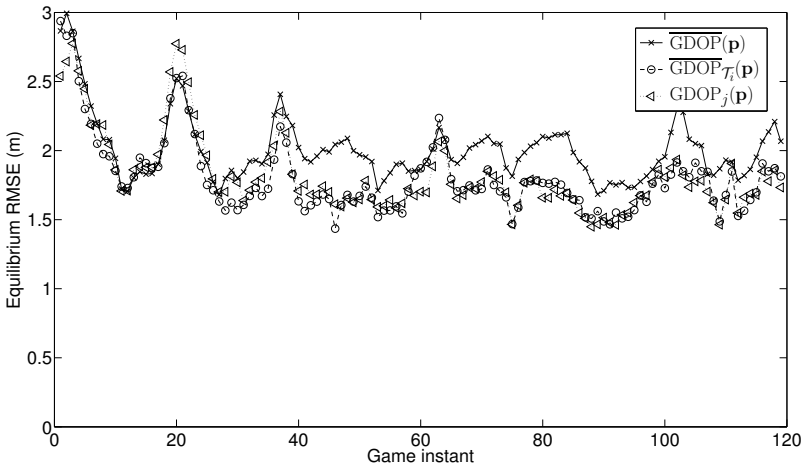

Figure 4.9: RMSE (m) in Nash equilibrium iterations of the games for metrics $\overline{\text{GDOP}}(\mathbf{p})$, $\overline{\text{GDOP}}_{\mathcal{T}_i}(\mathbf{p})$ and $\text{GDOP}_j(\mathbf{p})$.

In conclusion, distributed $\text{GDOP}_j(\mathbf{p})$ and $\overline{\text{GDOP}}_{\mathcal{T}_i}(\mathbf{p})$ metrics are valid quantities, taking into account that the density of target nodes affects its performance. The results show that for low density of target nodes ($M = 2$ in this case), the approximation $\overline{\text{GDOP}}_{\mathcal{T}_i}(\mathbf{p}) \simeq \overline{\text{GDOP}}(\mathbf{p})$ depends on τ_i. Thus, $\text{GDOP}_j(\mathbf{p})$ metric is a better option to approximate to $\overline{\text{GDOP}}(\mathbf{p})$. For $M = 20$ target nodes, the metric $\text{GDOP}_j(\mathbf{p})$ is more conservative than $\overline{\text{GDOP}}_{\mathcal{T}_i}(\mathbf{p})$ as it was shown in Section 4.7.1, being the approximation $\overline{\text{GDOP}}_{\mathcal{T}_i}(\mathbf{p}) \simeq \overline{\text{GDOP}}(\mathbf{p})$ valid for increasing density of target nodes.

Finally, in Figure 4.11 the activity of the anchor nodes depending on the trajectory of the target nodes is showed. The relation between the ID number of each anchor node and its position in the scenario can be checked in Figure 5.1. There are anchor nodes that contribute to positioning at a certain instant and when they are no longer necessary, they do not contribute, thus saving energy. Moreover, the figure shows the set $\mathcal{N}_j$ of anchor nodes that provide ranging signals to target node 1 and target node 2. At the beginning of the trajectories, target nodes share anchor nodes for positioning, however when their trajectories separate, different anchor nodes help in positioning to each target node.

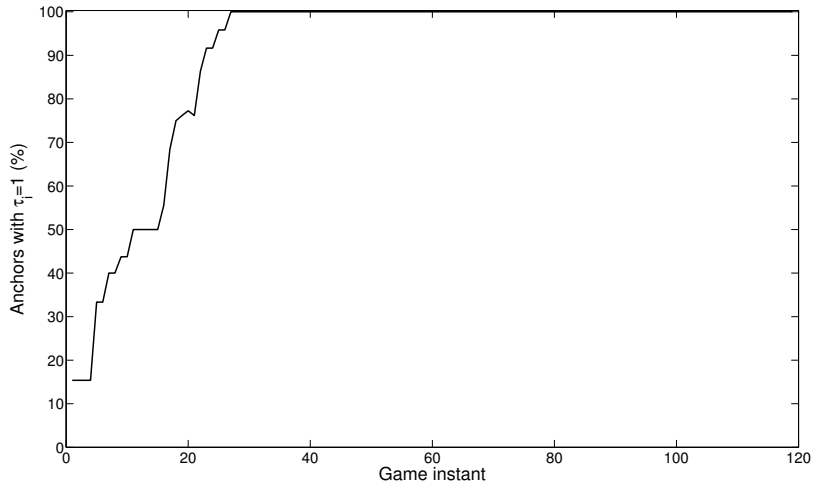

Figure 4.10: When the trajectories of the target nodes depart, the percentage of nodes with $\tau_i = 1$ increase. Case plotted for metric $\overline{\text{GDOP}}_{\mathcal{T}_i}(\mathbf{p})$.

4.8 Chapter Summary and Conclusions

In this chapter, an algorithm for power control in WSN with RSS-based positioning capabilities has been presented. The algorithm performs node selection by means of the anchor nodes that are not necessary for positioning purposes are turned to low power mode. Thus, besides power control, the algorithm minimizes the number of anchor nodes that collaborate in positioning, saving energy. We have used the framework provided by potential games to design and analyze our algorithm. The game falls into the category of Exact Potential Game. The proposed solution provides a distributed approach to select the power levels of anchor nodes such that a predefined positioning quality is ensured, as quantified by the GDOP metric. Two distributed metrics have been proposed to estimate the average GDOP using merely the local information available at each anchor node. A possible solution for a fully-distributed implementation of this game has been explained. This solution has been analyzed in terms of its asymptotical computational complexity.

Performance has been assessed by means of computer simulations in two scenarios, a static setup and a mobile one. For the static scenario, results showed the evolution towards the NE. Transmit powers of anchor nodes were minimized while the accuracy in positioning, measured by the GDOP, is maintained. Results revealed that the distributed algorithm obtains results which are comparable to a global approach, while requiring much less computational resources. The complexity is on the order of $\mathcal{O}(n_p^N)$ and $\mathcal{O}(n_p)$ for the global and proposed solutions, respectively, with

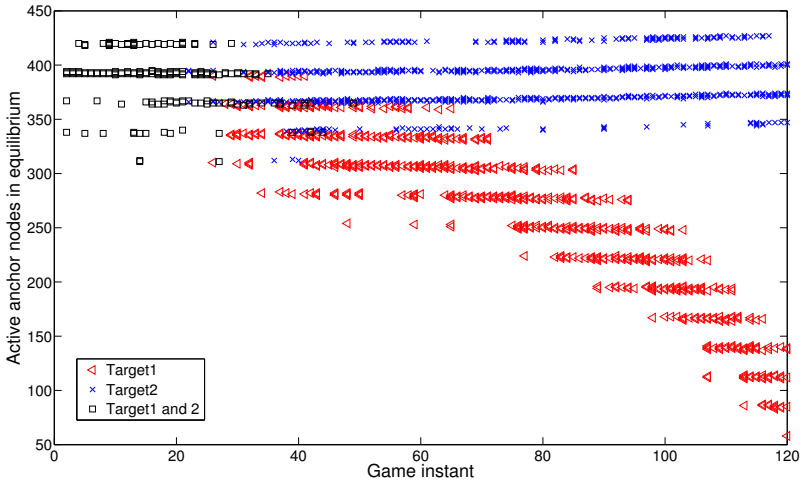

Figure 4.11: Active anchor nodes (ID number) in Nash equilibrium iterations of the games for $\text{GDOP}_j(\mathbf{p})$ case (no Monte Carlo trials).

n_p being the number of available power levels. We have found that the resulting RMSE of the position estimate has consistent results. Moreover, RMSE decreases in each iteration of the algorithm due to the averaging of RSS values that is also a phase of refinement of the error.

For the sake of simplicity in the simulations of the mobile scenario, we have considered that the position of the target node is fixed during a small time window in which the iterations of a game are performed. It is a reasonable approximation since the communications rate is much larger than the velocity of the mobile node. It remains as future work to study the convergence of the game taking into account the change of position between iterations of the algorithm. For the mobile scenario, results showed the evolution towards the NE of each game. The activity of the anchor nodes revealed that the anchor nodes that are not necessary for positioning, do not contribute, thus saving energy.

We have learnt that the distributed error metrics based on GDOP are valid quantities as the global one, taking into account that the density of target nodes affects their performance. For low density, the approximation of the worst case metric as the global metric is the best option. However, the approximation of the local GDOP average as the global metric is valid for increasing density of target nodes, while the worst case metric becomes more conservative.

Finally, while the analysis of our positioning algorithm was made in the context of WSN, we note that it may be applicable to other communications systems using RSS for positioning.

The results presented in this chapter were partially published in:

- Journal:
  [92] Moragrega, A.; Closas, P.; Ibars, C., "Potential Game for Energy-Efficient RSS-based Positioning in Wireless Sensor Networks," *IEEE Journal on Selected Areas in Communications*, Special Issue on Location-Awareness for Radios and Networks, to appear in 2015.

- Conference:
  [93] Moragrega, A.; Closas, P.; Ibars, C., "Energy-Efficient Positioning in Sensor Networks by a Game Theoretic Approach," in Proceedings of 19th European Signal Processing Conference (EUSIPCO 2011), 29-2 September 2011, Barcelona (Spain).

5

Supermodular Game for Power Control in TOA-based Positioning

THIS chapter is a natural extension of previous Chapter 4. In both chapters we address the minimization of power consumption by the anchor nodes in the positioning problem with an anchor based approach using lateration. However, in the current one TOA based ranging is used instead of RSS. Ranging models as well as GDOP metric are different for TOA and RSS techniques. Due to these differences, the game theoretical algorithm presented in this chapter for distributed power control with TOA has a different structure, based on a supermodular game.

5.1 Introduction

Ranging techniques based on TOA with UWB technology can potentially achieve very high indoor position accuracy [32]. Its main advantages are large bandwidth and short pulses, which provide accurate measurements of the TOA with high resolution. The IEEE 802.15.4a standard provides mechanisms for precision ranging using TOA by means of an UWB PHY layer [29]. Typically, cooperative range-based positioning algorithms consist of three phases [48]: a ranging phase, a positioning phase, and

a refinement phase. In the ranging phase, distance estimates between anchor and target nodes are obtained. An interesting technique for distance estimation is RTOA. Although a double transmission is necessary in order to obtain a time measurement, the RTOA method does not rely on clock synchronization among different nodes [38]. Positioning can be done with different algorithms. Trilateration algorithm needs at least three distance measurements (assuming a 2-dimensional scenario) to anchor nodes for each target node. Using lateration, the target node computes its position based on one of the existing algorithms as described in Chapter 2.2 [94]. In this chapter the deterministic simplified LLS algorithm is used. Finally, in the refinement phase, position estimates can be refined using information about the range (distance) to neighboring nodes.

In this chapter, a WSN consisting of anchor nodes and target nodes is considered. Target nodes are self-positioned using the LS algorithm and range measurements to anchor nodes. The IEEE 802.15.4a standard [29] is assumed for ranging, which obtains distance estimates based on RTOA measurements. Within this context, as in the previous chapter, we address the problem of optimizing in a distributed manner the power consumption of anchor nodes while maintaining a certain quality of positioning at the target nodes. We do so using a distributed algorithm based on game theory, which provides a useful set of analytic tools to model distributed decision processes [60].

As previously commented in Chapter 4.1, in the literature, the problem of energy efficiency for positioning of WSN has been addressed. Some works treated data acquisition conservation methods to achieve energy saving by minimizing the energy expenditure in data transmission/reception rates, sensing by adapting a sampling problem and doing node selection strategies. One approach selects the anchor nodes based on distance metric. For TOA based ranging, the variance of the distance estimation does not depends on the distance between nodes (Section 2.2.2), but on the SNR. As previously explained, the major disadvantage of the distance based criterion is that geometry of the selected cooperating nodes is not taken into account. Thus, GDOP based strategy is also used for node selection. The simplest selection method that uses GDOP based strategy is an exhaustive search that evaluates the GDOP for all the possible active sets of size M given a set of possible sensors of size N. It leads to a high number of combinations be means of the algorithm is only viable if N is small. Otherwise, suboptimal approaches have been presented in [90].

In the literature, Game Theory has been used for node selection strategies. Thus, anchor selection has been dealt with cooperative games, as previously commented in Chapter 4.1. However, the main drawback of cooperative game theory for node selection is the needed information interchange between players until convergence, which incurs to a communication cost.

Besides node selection, game theoretic tools have been proposed extensively for distributed power control mechanisms. In [64] a unified framework based on potential games is proposed to deal with power control problems. Also in [69] centralized or distributed power control algorithms in wireless communications are viewed as S-modular games. In [72] the power control problem is solved using a supermodular game with linear pricing proportional to the power. The price of the system resources is used to achieve a more socially desirable result. In general, in power control problems, the QoS requirements are formulated as constraints of the SINR of each user. However, in our case the QoS requirements are formulated using the positioning error.

5.1.1 Contribution

In this chapter, an algorithm for distributed power control in anchor based positioning is proposed. In particular, we propose to minimize the transmit power of anchor nodes that help in positioning/tracking the target node (nodes selection), while using GDOP for positioning error metric as QoS to maintain an adjustable level of accuracy.

The distributed nature of the problem can be observed considering that there may be several target nodes within range of an anchor node. Since we are dealing with a decentralized problem, non-cooperative game theory provides appropriate models to study such a system [60]. The problem of power control can be addressed in a distributed fashion with non-cooperative games. Under a non-cooperative game model, service preferences for each user are represented by a utility function [68]. The utility function quantifies the level of satisfaction a user gets from using the system resources. Each player in the game maximizes the utility function in a distributed fashion. A particular class of non-cooperative games are the supermodular games that were introduced in Chapter 3.4.2. They are characterized by the existence of at least one pure strategy Nash equilibrium. Another characteristic of such games is strategic complementarity, which means that the marginal utility when playing a higher strategy increases when opponents also play higher strategy. In our game setup, when a player plays a higher strategy (i.e., higher transmit power), the positioning error decreases and the utility of the other players increases. In order to penalize power consumption, a linear pricing is included in the utility function.

A deployed, IEEE 802.15.4a compliant, WSN is considered that consists of anchor and target nodes. Within this context, we propose a non-cooperative dynamic game, a supermodular game. The supermodular game is designed by means of transmit power of anchor nodes is minimized and node selection is performed to use the

anchor nodes as close as possible to the target with the best geometry using GDOP metric.

Therefore, the algorithm avoids the exhaustive search that evaluates the GDOP for all the possible active sets of size M that leads to a high number of combinations. Moreover, the players follows the iterations of the best response algorithm. Thus, the design of the algorithm may allow to add other strategies for power saving. As example, the optimization of the communication costs in the measurements of the TOA can be performed controlling the number of iterations of the algorithm.

Although a solution for positioning with WSN is provided, a similar approach may be used with other technologies with higher transmit powers such as WLAN and cellular communications.

5.2 System Model

The scenario of interest consists of a WSN deployed in a certain geographical area (e.g., Figure 5.1). The WSN consists of two types of nodes: anchor nodes, with known position, and target nodes, with unknown position. We define their two-dimensional coordinates as $\mathbf{x}_a^{(i)} = [x_a^{(i)}, y_a^{(i)}]^T,\ i = 1, \ldots, N$, and $\mathbf{x}^{(j)} = [x^{(j)}, y^{(j)}]^T,\ j = 1, \ldots, M$, respectively. The set of anchor nodes that provide coverage to the j-th target node is defined as $\mathcal{N}$. We further assume that the WSN has an air interface capable of accurately estimating the TOA of an incoming signal. In particular, the IEEE 802.15.4a UWB physical layer has this capability. A target node positions itself using trilateration, which requires at least three known distances to three known positions, i.e. anchor nodes. We consider a static setup, therefore assuming that anchor and target nodes remain fixed while they are positioned and the game runs.

The geometrical distance between the target node and the i-th anchor is defined as

$$\rho_i(\mathbf{x}) = \| \mathbf{x} - \mathbf{x}_a^{(i)} \|,\ i = 1, \ldots, N\ , \tag{5.1}$$

with $\| \cdot \|$ being the Euclidean norm in $\mathbb{R}$.

In order to estimate ρ_i, we assume that a TOA estimation technique is used in conjunction with the symmetric double-sided SDS TW-TOA protocol, outlined in the IEEE 802.15.4a standard [29]. The aim of the SDS TW-TOA protocol is to compensate for clock instability, which would affect the accuracy of the distance estimates ([29], p. 126). The SDS TW-TOA protocol needs at least three frame interchanges between the anchor and the corresponding target node. Some of these frame interchanges contain information for the power control algorithm. The positioning algorithm works as follows: first, a target node broadcasts a ranging request

(RRq), which is received by the set of neighboring anchor nodes $\mathcal{N}$. At each iteration of the algorithm one of the anchor nodes sends a ranging reply (RRi) to the target node with power level p_i, $i = 1, \cdots, N$, which is indicated in the reply frame besides information relevant for the power control algorithm. The target node, upon reception of the ranging reply, sends a confirmation frame (CFi) to the anchor node with power p_i, $i = 1, \cdots, N$. Finally, the anchor node sends a confirmation reply (CRi), which allows the target node estimates the distance and to position itself once at least three anchor nodes have participated. Then the target node sends a confirmation frame (CFi2) to the anchor node with power p_i, $i = 1, \cdots, N$ that contains the estimated distance, position and other information relevant for the power control algorithm. Therefore, after this confirmation has been sent, the anchor node updates its power level p_i, $i = 1, \cdots, N$. Further refinements of the node position are carried out iterating this positioning algorithm. The procedure stops when the target node sends a ranging stop (RStop) signal to the anchor node. During the procedure, the target node replies to anchor nodes with the same power level, in order to maintain the same signal-to-noise ratio (SNR) during all phases of the SDS TW-TOA protocol. Therefore, the power control algorithm benefits the target node power consumption as well. Finally, note that this ranging protocol allows anchor nodes to have knowledge of the power levels of other anchor nodes without any additional packet transmissions. The latter is desirable since it allows characterization the problem as a game of perfect information later in the paper.

5.3 Positioning Equations and Error Metric

A target node estimates its position using noisy range measurements

$$\hat{\rho}_i \sim \mathcal{N}(\rho_i(\mathbf{x}), \sigma^2_{\hat{\rho}_i}), \tag{5.2}$$

where the standard deviation of the observations depends on the standard deviation of TOA measurements as [26]

$$\sigma_{\hat{\rho}_i} = \frac{c \cdot \sigma_{TOA_i}}{4} \ , \tag{5.3}$$

with c being the speed-of-light constant, σ_{TOA} the standard deviation of TOA measurements and the factor 4 in the denominator stemming from the fact that two round trip times (with independent TOA error) are used to obtain a distance estimate with the SDS TW-TOA ranging protocol [1].

[1] In this case we assume no deviation from the nominal frequency in the sensor clocks, which would further increase the error.

The position of a target node can be estimated by the Least Squares (LS) algorithm. The LS method provides a simple solution to the trilateration problem, where the coordinates of the target node are those that minimize the squared-error

$$\hat{\mathbf{x}} = \arg\min_{\mathbf{x}} \left\{ \sum_{i \in \mathcal{N}} \left(\hat{\rho}_i - \parallel \mathbf{x} - \mathbf{x}_a^{(i)} \parallel \right)^2 \right\} , \tag{5.4}$$

the optimization admits a closed-form solution [51] based on the Moore-Penrose pseudoinverse

$$\hat{\mathbf{x}} = (\mathbf{H}^T \mathbf{H})^{-1} \mathbf{H}^T \mathbf{b} , \tag{5.5}$$

with the definition of a $|\mathcal{N}|$-vector

$$\mathbf{b} = \left[\hat{\rho}_1 - \rho_1(\mathbf{x}^0), \ldots, \hat{\rho}_{|\mathcal{N}|} - \rho_{|\mathcal{N}|}(\mathbf{x}^0) \right]^T \tag{5.6}$$

and the so-called, $|\mathcal{N}| \times 2$, visibility matrix

$$\mathbf{H} = \left(\begin{array}{cc} \frac{x_a^{(1)} - x}{\rho_1(\mathbf{x})} & \frac{y_a^{(1)} - y}{\rho_1(\mathbf{x})} \\ \frac{x_a^{(2)} - x}{\rho_2(\mathbf{x})} & \frac{y_a^{(2)} - y}{\rho_2(\mathbf{x})} \\ \vdots & \vdots \\ \frac{x_a^{(|\mathcal{N}|)} - x}{\rho_{|\mathcal{N}|}(\mathbf{x})} & \frac{y_a^{(|\mathcal{N}|)} - y}{\rho_{|\mathcal{N}|}(\mathbf{x})} \end{array} \right) \Bigg|_{\mathbf{x}=\mathbf{x}^0} \tag{5.7}$$

where $|\mathcal{N}|$ indicates the cardinality of set $\mathcal{N}$, i.e., the number of ranging measurements at the target node. Notice that the solution in (5.5) requires initialization of the unknown coordinates, which we have defined as $\mathbf{x}^0$.

It is well known that a weighted LS solution has an associated covariance matrix which can be calculated as

$$\mathbf{C}_{\hat{\mathbf{x}}} = (\mathbf{H}^T \mathbf{\Sigma}^{-1} \mathbf{H})^{-1} , \tag{5.8}$$

with

$$\mathbf{\Sigma} = \text{diag} \left(\sigma_{\hat{\rho}_1}^2, \ldots, \sigma_{\hat{\rho}_{|\mathcal{N}|}}^2 \right) \tag{5.9}$$

being a diagonal matrix whose entries are the corresponding variances of each range measurement as in (5.3).

In this work, we are interested in using a scalar metric to assess the *goodness* of a given power allocation strategy (at anchor nodes) for positioning purposes at target nodes. We resort to the GDOP parameter, a dimensionless value, that can be thought of as a value that measures the effect of network geometry on the positioning

solution [55]. Larger GDOP values imply worse positioning solutions, and viceversa. Accounting for the quality of each range measurement, it is defined as

$$\text{GDOP} \triangleq \sqrt{\text{Tr}\{(\mathbf{H}^T\boldsymbol{\Sigma}^{-1}\mathbf{H})^{-1}\}}\ , \tag{5.10}$$

where its relation to the estimation covariance (5.8) is evident. Actually, there is a clear relation between GDOP and the theoretical lower bound on the variance of a position estimator when the correct position $\mathbf{x}$ is used in the calculation of $\mathbf{H}$ [95]. In practice, we build the metric upon position estimates (i.e., $\mathbf{H}(\mathbf{x} = \hat{\mathbf{x}})$) and compute the elements in $\boldsymbol{\Sigma}$ based on the closed-form expression provided by its theoretical lower bound, given by the CRB. The latter is convenient as the CRB relates the minimum estimation variance to some meaningful receiver parameters, including the target p_i. For the considered technology [26], the squared CRB is given by the right-hand side in

$$\sigma_{\hat{\rho}_i} = K_i\sqrt{\frac{c^2N_0}{16\pi^2BT_sf_c^2L_ip_i}} \geq \sqrt{\frac{c^2N_0}{16\pi^2BT_sf_c^2L_ip_i}}\ , \tag{5.11}$$

where B is the signal bandwidth, T_s the signal duration, f_c the center frequency, $L_i = (\lambda/4\pi\hat{\rho}_i)^2$ the path loss, p_i the transmitted power of the i-th anchor node, and N_0 the noise spectral density. Recall that if the range measurement is obtained by the maximum likelihood principle, its variance coincides with the CRB in (5.11). Otherwise, for unbiased estimators of $\hat{\rho}_i$, the variance is always larger or equal. To account for this issue, a constant $K_i \geq 1$ is introduced to quantify the difference between the estimator variance and the CRB. The constant is dependent on the method use to estimate the ranges. The analysis of the game given in Section 5.4 holds for arbitrary K_i, but for the sake of clarity we restrict ourselves to $K_i = 1$ in the simulations.

In conclusion, we have an error metric which depends inversely on the power allocated per anchor node and the geometry of anchor nodes in the network. Thus, GDOP($\mathbf{p}$) is a power-dependent metric of position accuracy.

5.4 Supermodular Game for Power Allocation with Positioning Constraints

In this section the problem of assigning a transmission power to each of the anchor nodes in a distributed fashion is addressed. The objective of such allocation is to use the minimum power at each node while maintaining a certain quality in the positioning solution of target nodes. Due to its distributed nature, game theory

is an excellent tool for the problem at hand [60]. We denote the anchor power allocation problem in strategic form as the tuple $\Gamma(\Omega, \mathcal{P}, u)$, where *i)* Ω is the set of N players, the anchor nodes in our case; *ii)* $\mathcal{P}$ is the set of pure strategies and $\mathbf{p} = [p_1, \ldots, p_N]^T \in \mathcal{P} \subseteq (\mathbb{R}^+)^N$ the chosen strategies, where $p_i \in \mathcal{P}_i$ represents the strategy of the i-th player over the set of its possible strategies $\mathcal{P}_i$. Thus, $\mathcal{P} = \times_{i=1}^{N} \mathcal{P}_i$. Moreover $\mathbf{p}_{-i} \in \mathcal{P}_{-i} = \times_{j \neq i}^{N} \mathcal{P}_j$ represents the strategies of all players but the i-th. Here, players' strategies are the set of all possible power levels $\mathcal{P}_i \in [P_{min}, P_{max}]$, with $P_{min} \geq 0$ and $P_{max} \geq 0$, where P_{min} is the minimum transmit power and P_{max} is the maximum transmit power ; *iii)* $u_i : \mathcal{P} \mapsto \mathbb{R}$ is the utility function of the i-th player. The utility function (or payoff) quantifies the preferences of each player to a given strategy, given the other user strategies. Then, $u \triangleq \{u_i\}_{i \in \Omega}$ is the set of all N utility functions.

The selection of a proper utility function is paramount. In our application, we seek a utility that depends on the power allocated per anchor node which is related to the quality of the positioning solution at the target node. To that aim, we propose to use the GDOP metric in the function as well as using a linear pricing function to avoid the trivial solution of transmitting at maximum power. For the sake of simplicity, in this section we consider the case of $M = 1$ to present the proposed approach, which we generalize to $M \geq 1$ in section 5.4.2. Then, we consider

$$u_i(p_i, \mathbf{p}_{-i}) = (\beta - 1)\sqrt{g(\mathbf{p})} - \beta p_i \ , \tag{5.12}$$

with $0 \leq \beta \leq 1$ and $g(\mathbf{p}) \triangleq (\text{GDOP}(\mathbf{p}))^2$. β determines a trade-off between transmit power and error. Each anchor node i may control this parameter depending on e.g. the state of its battery (β is fixed before the game).

We can prove that $\Gamma(\Omega, \mathcal{P}, u)$ is a supermodular game [68], as it satisfies the conditions in Definition 5.1.

Definition 5.1. *The strategic form game $\Gamma(\Omega, \mathcal{P}, u)$ is a supermodular game if for all players i: i) $\mathcal{P}_i = [P_{min}, P_{max}]$ is a compact subset of $\mathbb{R}^+$; ii) u_i is continuous in all player strategies $\mathbf{p}$; and iii) u_i has increasing differences in (p_i, p_j), $\forall j \neq i, j \in \Omega$.*

The first two conditions can be easily shown to be satisfied by the proposed game. The increasing differences property is also satisfied, although a more involved proof is required. A function u_i has increasing differences in (p_i, p_j) if for all $p_i' \geq p_i$ and $p_j' \geq p_j$, we have that

$$u_i(p_i', p_j') - u_i(p_i, p_j') \geq u_i(p_i', p_j) - u_i(p_i, p_j) \ . \tag{5.13}$$

In other words, the incremental gain of choosing a higher p_i is greater when p_j is higher. To prove that (5.12) satisfies this property, we show in Proposition 5.1 a

more general result stating that the function is supermodular. Recall that, if u_i is twice differentiable, supermodularity is equivalent to

$$\frac{\partial^2 u_i(\mathbf{p})}{\partial p_i \partial p_j} \geq 0 \ . \tag{5.14}$$

Proposition 5.1. *In the game $\Gamma(\Omega, \mathcal{P}, u)$, the utility defined in (5.12) is supermodular.*

Proof. See Appendix 5.8.1 for the proof. □

Supermodular games exhibit the following interesting properties: 1) pure strategy NE exist. Recall that a NE is a stable solution of the game in which no player may improve its utility function by unilaterally deviating from it; 2) NE can be attained using greedy best-response (BR) type algorithms. Therefore, anchor nodes can simply update their transmit power by maximizing its utility function,

$$BR_i(\mathbf{p}_{-i}) = \arg\max_{p_i \in \mathcal{P}_i} \{u_i(p_i, \mathbf{p}_{-i})\} \ ; \tag{5.15}$$

and 3) the equilibrium set has a largest and a smallest element, $\overline{\mathbf{p}^*}$ and $\underline{\mathbf{p}^*}$ respectively. If anchor nodes start from smallest (largest) element of $\mathbf{p}$ and use the BR algorithm, then the strategies converge to the smallest (largest) NE.

It is worth mentioning that the stochastic error effects due to range measures over the game are minimized. This is because at each iteration of the game, once the distance with the target node is estimated, the anchor node i, that is playing, decides the new transmit power for next iteration maximizing its $u_i(p_i, \mathbf{p}_{-i})$. Once each anchor node has played, the game continues to reach the equilibrium and the anchor nodes play again. At each round of iterations the distance estimation $\hat{\rho}_i$ is averaged with previous estimations, which reduces the variance of $\hat{\rho}_i$ and thus the uncertainty in computing $\mathbf{H}$. Such averaging reduces the Gaussian error of the distance estimation $\hat{\rho}_i$ in (5.3), thus improving the position estimation.

Although in this work the game $\Gamma(\Omega, \mathcal{P}, u)$ is applied to positioning with WSN, this game may be applied to TOA-based positioning with other technologies or hybrid ranging techniques, whenever $\sigma_{\hat{\rho}_i}$ is inversely proportional to p_i through σ_{TOA}.

5.4.1 Uniqueness of Nash Equilibrium

For supermodular games, if there exists a unique NE, it is attainable using BR algorithm from any initial strategies and $\overline{\mathbf{p}^*} = \underline{\mathbf{p}^*}$. In Proposition 5.2 we show that

the game $\Gamma(\Omega, \mathcal{P}, u)$ with utility function defined in (5.12) has a unique NE, result which is assessed by computer simulations in Section 5.6.

Proposition 5.2. *The game $\Gamma(\Omega, \mathcal{P}, u)$ satisfies the conditions for uniqueness of NE reported in [70].*

Proof. The proof of uniqueness of NE is shown in Appendix 5.8.2. □

The efficiency of the NE shows the goodness of it. To show the efficiency of the NE, our algorithm is compared with a centralized one. We define

$$f(\mathbf{p}) = \sum_{i=1}^{N} u_i(\mathbf{p}) \ , \tag{5.16}$$

which is usually known as the social welfare function of the game. Moreover the set of equilibrium strategies is defined by $\mathbf{p}^+$.

Proposition 5.3. *(5.16) is a convex function.*

Proof. Convexity of (5.16) is shown in Appendix 5.8.3. □

As $f(\mathbf{p})$ is convex, its maximization can therefore be carried out using numerical methods. $f(\mathbf{p})$ can be maximized centrally and therefore $\mathbf{p}^*$ is defined as the optimal solution. In the results we evaluate the efficiency of the achieved NE computing the PoA [96], defined as

$$PoA = \frac{f(\mathbf{p}^*)}{f(\mathbf{p}^+)} \ . \tag{5.17}$$

5.4.2 Extension to Multiple Target Nodes

The setup involving multiple target nodes $M \geq 1$ can also be formulated as a supermodular game. The strategic form of the game is $\Upsilon(\Omega, \mathcal{P}, u)$ with the following utility function:

$$u_i(p_i, \mathbf{p}_{-i}) = (\beta - 1) \cdot \sqrt{\frac{\sum_{j=1}^{M} g_j(\mathbf{p})}{M}} - \beta p_i \ . \tag{5.18}$$

The claims for the case $M = 1$ can be reproduced in this more general setup. The results are summarized here.

Proposition 5.4. *In this game* $\Upsilon(\Omega, \mathcal{P}, u)$*, the utility defined in (5.18) is supermodular.*

Proof. See Appendix 5.8.1 for this proof. □

Proposition 5.5. $\Upsilon(\Omega, \mathcal{P}, u)$ *satisfies the conditions for uniqueness of NE.*

Proof. The proof of uniqueness of the NE is included in Appendix 5.8.2. □

We also study the efficiency of the NE reached with (5.18). To that aim we compute the PoA as previously (5.17) for the $M = 1$ case. The proof of the convexity of (5.16) is included in the Appendix 5.8.3.

5.5 Distributed Implementation and Computational Resources

The game presented above has challenges when it comes to implementation. A major concern relates to the information exchange required between target and anchor nodes. In this direction, Algorithm 5.1 shows a pseudo-code description of the proposed solution with details of frame exchange and operations performed by target and anchor nodes at each iteration of the game. The number of best response iterations is N_{it} and the total number of algorithm iterations is $N_{it} \cdot |\mathcal{N}|$. The right arrow ($\rightarrow$) over the frame name indicates a frame transmission from target to anchor i and the left arrow ($\leftarrow$) a frame transmission from anchor i to target. As we explained in Section 2.2.2, the SDS TW-TOA ranging protocol uses at least three frame interchanges between the anchor and target node so that the distance can be estimated in the target node. The following frames are involved: RRi, CFi, CRi, and CFi2. These and other frames are explained later in this section. We use two of these frames, RRi and CFi2, to convey information related to the power control algorithm. Once at least three distances to three anchor nodes have been estimated the target node attempts to position itself. The positioning protocol starts with a ranging request (RRq) broadcast by a target node. In the following, the frames of the ranging protocol between the target and anchor nodes in range are examined, as well as a possible solution to minimize their payload:

1. $\overleftarrow{\text{RRi}}$: the corresponding anchor node sends a ranging reply (RRi) to the target node with p_i. RRi contains information for the power control algorithm: p_i and $\mathbf{x}_a^{(i)}$ only in first iteration of the game; and $g_i(\mathbf{p})$ once the target has a first estimation of its position.

2. $\overrightarrow{\text{CFi}}$: then the target node sends a confirmation frame (CFi) to the anchor node.
3. $\overleftarrow{\text{CRi}}$: the anchor node sends a confirmation reply (CRi), which allows the target node to estimate the distance $\hat{\rho}_i$ and to position itself once at least three range estimates are available.
4. $\overrightarrow{\text{CFi2}}$: the target node sends a confirmation frame (CFi2) to the anchor node that contains information for the power control algorithm: $\hat{\rho}_i$, and once the target estimates its position $\hat{\mathbf{x}}$, $\mathbf{H}$ and $g(\mathbf{p})$. After this confirmation frame the anchor node updates its power level p_i maximizing the utility u_i of the game.

Further refinements of node position are carried out iterating this positioning algorithm $N_{it} \cdot |\mathcal{N}|$ times. The procedure stops when the target node sends a ranging stop signal (RStop). As we explained before, our distributed algorithm for positioning uses the frame dialog of the SDS TW-TOA ranging protocol to convey information for the power allocation algorithm. Therefore, anchor node i knows the power allocation of other anchor nodes without further overhead.

On the other hand, another concern for implementation is related to p_i. At each iteration of the game, the i-th anchor node updates p_i maximizing u_i with an optimization algorithm such as gradient ascent (GA). As in a real transceiver the set of transmit powers is not a continuous set, the anchor node will select the transmit power value of the transceiver nearest to this p_i. With respect to the GA algorithm, it estimates the maximum of a function with N_{GA} number of iterations taking steps proportional to the positive of the gradient of the function at the current point.

Algorithm 5.1 Supermodular game for power allocation with positioning constraints for $M = 1$

Initialization: $\overrightarrow{\text{RRq}}$.
Game iterations phase: $n = 1$
while $n < (N_{it}|\mathcal{N}|)$ **do**
  $\overleftarrow{\text{RRi}}$ contains:
  i) p_i.
  ii) For $n = 1$: $\mathbf{x}_a^{(i)}$ with $i = 1, \ldots, |\mathcal{N}|$, and initial $\mathbf{p}$.
  iii) For $i > 3$: $g_i(\mathbf{p})$ updated in previous iteration by anchor node i.
  $\overrightarrow{\text{CFi}}$ frame.
  $\overleftarrow{\text{CRi}}$ frame.
  Operations of target node:
  i) Distance estimation $\hat{\rho}_i$.
  ii) If $i \geq 3$: compute $\mathbf{H}$ and position $\hat{\mathbf{x}}$ with LS.
  iii) For $i = 3$: compute $g(\mathbf{p})$ (only once).
  $\overrightarrow{\text{CFi2}}$ frame contains:
  i) $\hat{\rho}_i$. ii) If $i \geq 3$: $\hat{\mathbf{x}}$, $\mathbf{H}$ and $g(\mathbf{p})$.
  Operations of anchor node $i \geq 3$:
  i) Compute $\mathbf{H}_i$ and $g_i(\mathbf{p})$, substitute in $\mathbf{H}$ and $g(\mathbf{p})$. ii) Update p_i maximizing u_i with an algorithm for optimization.
  if $i = |\mathcal{N}|$ **then**
    $i = 1$
  else
    $i = i + 1$ {Next anchor node}
  end if
  $n = n + 1$
end while
$\overleftarrow{\text{RStop}}$.
End:

Table 5.1: Complexity of Algorithm 5.1

Node	**Computation**	**Operation**	**Size**	**Cost**
Target	$\mathbf{b} = \left[\hat{\rho}_i - \rho_i(\mathbf{x}^0))\right]^T$, $i = 1, \ldots, \lvert\mathcal{N}\rvert$	$\lvert\mathcal{N}\rvert$ sums	$\lvert\mathcal{N}\rvert$	$\mathcal{O}(\lvert\mathcal{N}\rvert) \leq \mathcal{O}(N)$
Target	$\mathbf{H}$	$2\lvert\mathcal{N}\rvert$ sums, $2\lvert\mathcal{N}\rvert$ divisions	$2\lvert\mathcal{N}\rvert$	$\mathcal{O}(4\lvert\mathcal{N}\rvert \leq \mathcal{O}(4N))$
Target	$\hat{\mathbf{x}} = (\mathbf{H}^T\mathbf{H})^{-1}\mathbf{H}^T\mathbf{b}$ Position with LS	N_{LS} evaluations of (a), (b), (c) and (d) (a) matrix-matrix prod. (b) matrix-matrix product (c) matrix-matrix product (d) matrix inverse	N_{LS}(*) 2x$\lvert\mathcal{N}\rvert$x2 2×2×$\lvert\mathcal{N}\rvert$ 2×$\lvert\mathcal{N}\rvert$×2 2x2	Total: $\mathcal{O}(N_{LS}(12\lvert\mathcal{N}\rvert + 8))$ $\leq \mathcal{O}(N_{LS}(12N + 8))$ $\mathcal{O}(4\lvert\mathcal{N}\rvert)$ $\mathcal{O}(4\lvert\mathcal{N}\rvert)$ $\mathcal{O}(4\lvert\mathcal{N}\rvert)$ $\mathcal{O}(2^3)$
Target	$g(\mathbf{p}) = \sum_{i\in\Omega} a_{ii}\frac{1}{p_i}$	$\lvert\mathcal{N}\rvert$divisions, $\lvert\mathcal{N}\rvert$sums, $\lvert\mathcal{N}\rvert$evaluations of a_{ii}	$\lvert\mathcal{N}\rvert$	$\mathcal{O}(2\lvert\mathcal{N}\rvert) + \lvert\mathcal{N}\rvert\mathcal{C}(a_{ii})$ $\leq \mathcal{O}(2N) + N\mathcal{C}(a_{ii})$
Anchor i	$\mathbf{H}_i = \left(\frac{x_a^{(i)} - x}{\rho_i(\mathbf{x})}, \frac{y_a^{(i)} - y}{\rho_i(\mathbf{x})}\right)$	2 sums, 2 divisions	2	$\mathcal{O}(4)$
Anchor i	$a_{ii} = \left(\mathbf{H}\mathbf{H}^T\right)^{-1}_{ii} \cdot \left(\frac{C}{\hat{\rho}_i^2}\right)$, see (5.26) $\left(\mathbf{H}\mathbf{H}^T\right)^{-1}_{ii}$: (e), (f), (g) $\left(\frac{C}{\hat{\rho}_i^2}\right)$: (h)	Operations (e), (f), (g), (h) and 1 product (e) determinant ($\lvert\mathcal{N}\rvert \times \lvert\mathcal{N}\rvert$) (f) determinant (2×2) (g) 1 division (h) 2 products, 1 division	1 $\lvert\mathcal{N}\rvert$ 2 1 1	Total: $\mathcal{O}(\lvert\mathcal{N}\rvert! + 8) \leq \mathcal{O}(N! + 8)$ $\mathcal{O}(\lvert\mathcal{N}\rvert!)$ $\mathcal{O}(2!)$ $\mathcal{O}(1)$ $\mathcal{O}(3)$
Anchor i	$g_i(\mathbf{p}) = \frac{a_{ii}}{p_i}$ and change $g(\mathbf{p})$	1 division, 2 sums	$\lvert\mathcal{N}\rvert$	$\mathcal{O}(3)$
Anchor i	(5.27) $\nabla u_i = -(\beta - 1)\frac{a_{ii}\frac{1}{p_i^2}}{2\sqrt{g(\mathbf{p})}} - \beta$	2sums, 3products, 1division, 1square root	2, 3, 1, 1	$\mathcal{O}(7)$
Anchor i	Maximize u_i Gradient ascent (GA) algorithm: $z_{m+1} = z_m + \alpha\nabla u_i(m)$	N_{GA} evaluations of (i) (i) sum, product	N_{GA}(**) 1, 1	Total: $\mathcal{O}(2N_{GA})$ $\mathcal{O}(2)$

(*) Number of iterations of LS (N_{LS}).
(**) Number of iterations for the GA algorithm (N_{GA}).

From Algorithm 5.1, the computational costs can be obtained by calculating the number of operations involved. In Table 5.1 the number of operations is summarized for $M = 1$. The operations are shown with respect to the number of anchor nodes $|\mathcal{N}|$. Taking into account that the upper bound is $|\mathcal{N}| \leq N$, then $\mathcal{O}(|\mathcal{N}|) \leq \mathcal{O}(N)$. One of the most complex operations is the inverse matrix for the LS, but the size of the matrix is only 2×2. For the anchor node i, also the most complex operation is the calculation of a component of the inverse of the matrix in the computation of a_{ii}, specifically the determinant, that involves a computational cost factorial with $|\mathcal{N}|$. From Table 5.1, we can calculate the total computational cost for the target node $\mathcal{C}_{\text{target}}$ and we obtain

$$\begin{aligned} \mathcal{C}_{\text{target}} &\simeq \mathcal{O}((N_{it}|\mathcal{N}|^2 - 2|\mathcal{N}|)(5 + 12N_{LS})) + |\mathcal{N}|\mathcal{C}(a_{ii}) \\ &\leq \mathcal{O}(N_{it}N^2 - 2N)(5 + 12N_{LS})) + N\mathcal{C}(a_{ii}) \ , \end{aligned} \tag{5.19}$$

where $\mathcal{C}(a_{ii})$ is the computational cost to obtain a_{ii}. Note from (5.19) that $\mathcal{C}_{\text{target}}$ scales with $|\mathcal{N}|^2$, except for the component $\mathcal{C}(a_{ii})$, which is calculated only once in the game. On the other hand, the total computational cost for the i-th anchor node ($\mathcal{C}_i$) is given by

$$\begin{aligned} \mathcal{C}_i &= \mathcal{O}((N_{it}|\mathcal{N}| - 2)(|\mathcal{N}|! + 22 + 2N_{GA})) \\ &\leq \mathcal{O}((N_{it}N - 2)(N! + 22 + 2N_{GA})) \ , \end{aligned} \tag{5.20}$$

which scales with $|\mathcal{N}|!$.

For the case $M \geq 1$, each target node has to execute the same operations detailed in Table 5.1 while the anchor node i has to calculate $\mathbf{H}_i$, a_{ii} and $g_i(\mathbf{p})$ for each target node. Therefore, the total computational cost for the i-th anchor node depends on M and is given by

$$\begin{aligned} \mathcal{C}_i &\simeq \mathcal{O}((N_{it}|\mathcal{N}| - 2)(M|\mathcal{N}|! + 18M + 7 + 2N_{GA})) \\ &\leq \mathcal{O}((N_{it}N - 2)(MN! + 18M + 7 + 2N_{GA})) \ . \end{aligned} \tag{5.21}$$

The factorial relation of the computational complexity with the number of anchor nodes might be an issue in large-scale networks. A possible workaround is to limit the total number of anchor nodes used for positioning at the target nodes. This would bound the cost due to the terms in $|\mathcal{N}|!$. The effects of such limitation are investigated in Section 5.6 by computer simulation, compared to the case of using all available anchors.

5.6 Simulation Results

The proposed algorithm was evaluated in three scenarios. We consider a static setup while the joint power control and positioning algorithm is executed. A pictorial of the three considered scenarios is shown in Figure 5.1. Scenarios consist of a 25×25 m^2 region where a set of anchor sensor nodes (big dot) are distributed at known positions, whereas the target sensor nodes (black star) are placed randomly. Position estimates (grey cross) are shown at the last iteration of the game. A first scenario was composed of $M = 1$ target node and a set of $N = 8$ anchor nodes distributed at regular known positions. The second scenario was also composed of $M = 1$ target nodes and $N = 8$ anchor nodes distributed at random with known positions. Finally, the third scenario was composed of $M = 5$ target nodes and a set of $N = 8$ anchor nodes distributed at regular known positions.

We performed $N_{it} = 10$ best response iterations and the total number of game iterations was $N_{it} \cdot |\mathcal{N}| = 80$. At each iteration, all players updated their strategy sequentially. We considered that sensor nodes were IEEE 802.15.4a compliant. The target nodes estimated ranges with anchor nodes following the TOA-based ranging protocol explained in Section 2.2.2. We considered noisy range measurements $\hat{\rho}_i$ as in (5.2). The standard deviation of range measurements $\sigma_{\hat{\rho}_i}$ depends on TOA standard deviation as in (5.3) and (5.11). For the sake of simplicity we assume that the variance of the range estimator attains the CRB, $K_i = 1$. For channel 7 in the IEEE 802.15.4a standard, we used $B = 1081$ MHz, $f_c = 6489$ MHz, and the maximum transmit power was -12 dBm.

Figure 5.2 shows the transmit power of each anchor node at each iteration of the game for the three scenarios, with $\beta = 0.2$. The results were obtained with a single realization, for the sake of illustrating the operation of the algorithm. Transmit powers are updated until the equilibrium is attained. Note that anchors with higher power are those that minimize the GDOP of the target taking into account the trade-off between transmit power and error. Also, in general, they are those which are closer to the target node since with minimum power can provide sufficient coverage to the target node, in comparison to those anchors that are farthest and thus need higher power levels. For example, in the case of scenario 2, the anchors that minimize the GDOP of the target are 1, 8 and 3. And in the case of scenario 3, the anchors that minimize the average of the GDOPs of the target nodes are 7, 8, 5, 6 and 4. The anchor nodes that are not necessary, which are typically those farther away from the target node, minimize its transmit power.

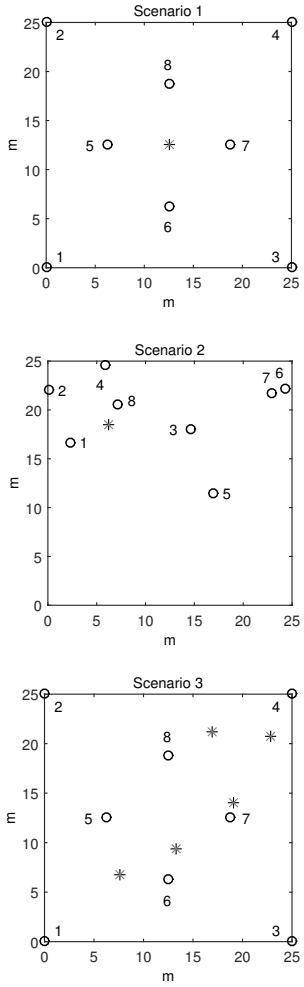

Figure 5.1: Scenarios consisting of a 25×25 m^2 region.

Results of the proposed algorithm were averaged over $N_C = 100$ independent Monte Carlo trials and for different values of β, which determines the trade-off between transmit power and positioning error. We considered the same value of β for each anchor node in the simulations, although each anchor node i could control this parameter depending on e.g. its battery status. In Figures 5.3 and 5.4 the average of transmit power of anchor nodes at each game iteration is shown. Moreover in Figures 5.5 and 5.6 the corresponding RMSE of the target position estimations at each game iteration is shown. The results show the game dynamics for two different initial conditions: all anchors at maximum power, and all anchors at minimum power. Note that the computer simulations verified that NE is unique and it is attainable from smallest and largest elements. The value of the equilibrium depends on β.

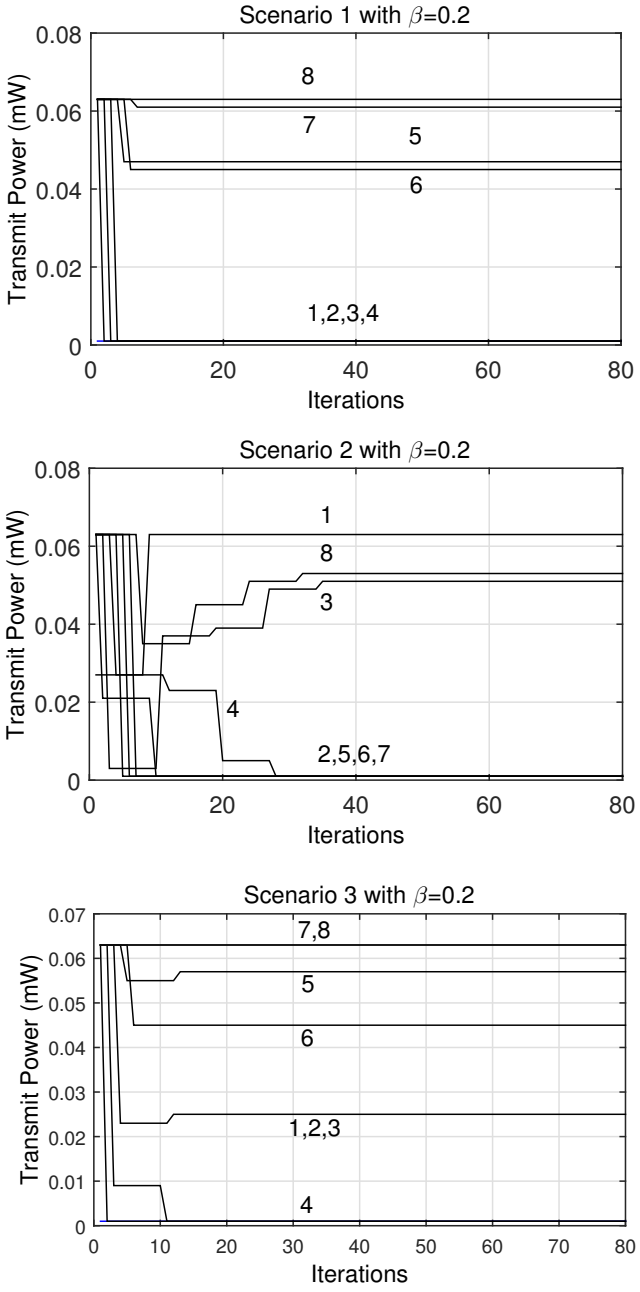

Figure 5.2: Comparison of transmit powers of all anchor nodes vs. game iterations for scenarios 1, 2 and 3.

For small β, the transmit power is higher, but the RMSE of the target position

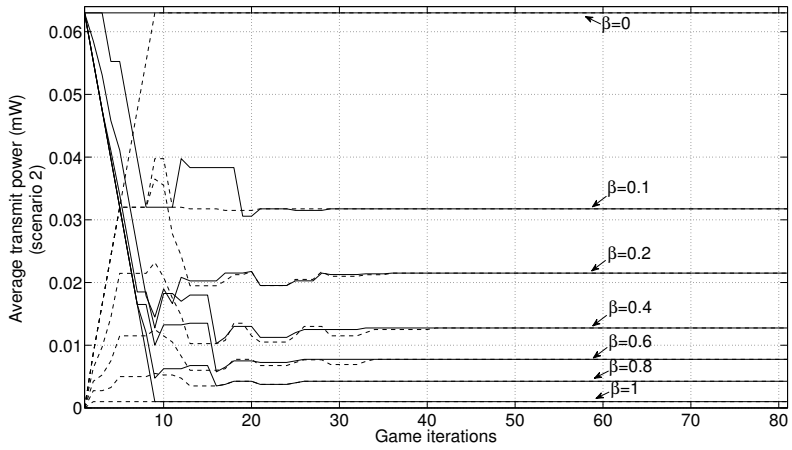

Figure 5.3: Anchor node average transmit power (mW) vs. game iterations for scenario 2. Maximum initial strategies in solid lines and minimum ones in dashed lines.

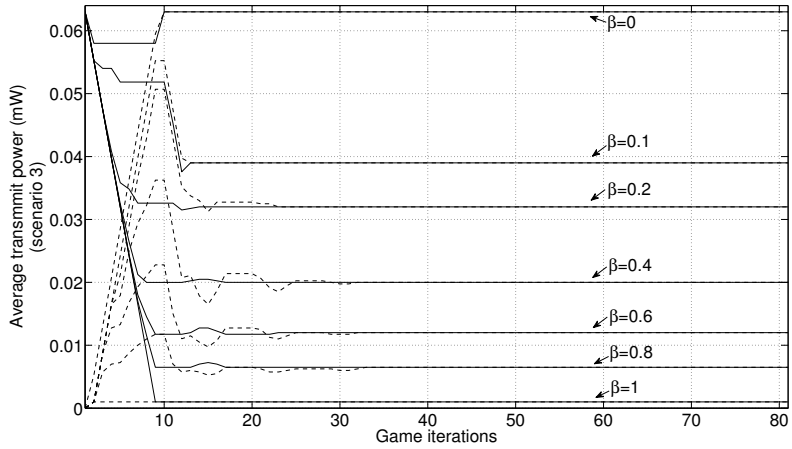

Figure 5.4: Anchor node average transmit power (mW) vs. game iterations for scenario 3. Maximum initial strategies in solid lines and minimum ones in dashed lines.

estimation, defined as

$$RMSE = \sqrt{\frac{\sum_{\ell=1}^{N_C} \sum_{j=1}^{M} \|\hat{\mathbf{x}}_j^{(\ell)} - \mathbf{x}_j\|^2}{2MN_C}} \,, \tag{5.22}$$

is lower, according to the inverse relation given by the CRB in (5.11). Here, $\hat{\mathbf{x}}_j^{(\ell)}$ denotes the position estimation at the l-th Monte Carlo run. For large β, the transmit power is lower, but the RMSE of the target position estimation is higher.

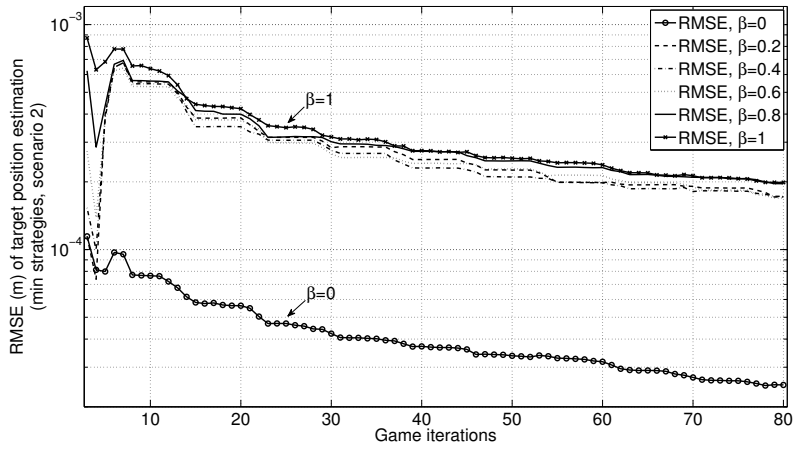

Figure 5.5: RMSE (meters) vs. game iterations for scenario 2.

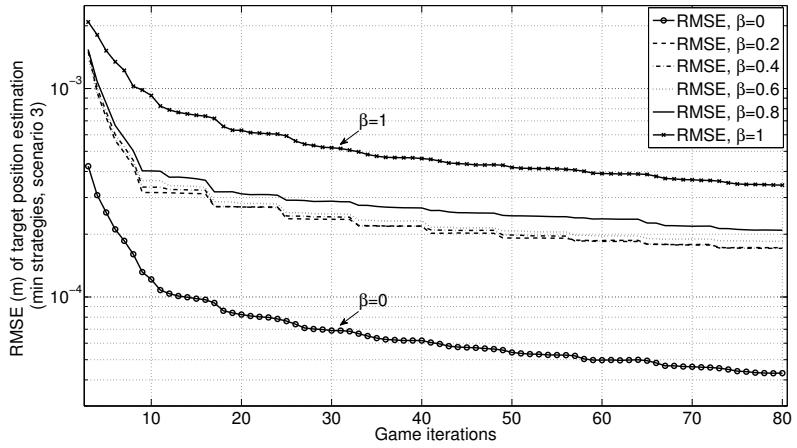

Figure 5.6: RMSE (meters) vs. game iterations for scenario 3.

In Figures 5.7 and 5.8, the resulting average of GDOP over all target nodes is shown for scenarios 2 and 3, respectively. The impact of our game-theoretic solution on the position system can be observed. In case $\beta = 0$, the penalty for power consumption is not taken into account. In this case equilibrium transmit power is maximum and GDOP is minimized without transmit power penalty. Without control power the GDOP and RMSE are minimum, but the transmit power is maximum. With control power ($\beta \neq 0$), a tradeoff between GDOP and transmit power can be established.

While transmit powers of anchor nodes are optimized according to the trade-off between transmitted power and positioning accuracy, at each iteration of the game the distance between the target and the anchor nodes $\hat{\rho}_i$ is estimated at the corresponding target node. The distance is estimated using the ranging protocol explained in Section 2.2.2. The target node performs an average of these distances at each iteration, taking into account the distance estimations of the previous iterations of the game. With this averaging, the error of the distance estimations decreases and so does the position estimation error. This result can be observed in Figures 5.5 and 5.6, where the RMSE decreases as the number of iterations increases. Therefore, the game allows energy efficient positioning (with refinement phase of the position error estimation) thanks to the distributed power control of anchor nodes, according to the trade-off between transmitted power and positioning accuracy.

We calculated the PoA, defined as the value of $\sum_{i=1}^{N} u_i(p_i, \mathbf{p}_{-i})$ for a centrally computed optimum divided by its value at the NE of the game (refer to (5.17)). Table 5.2 reports the PoA for different values of β. The centrally computed optimum was obtained maximizing the sum of utilities using convex optimization tools in Matlab. As it can be seen, the PoA is quite close to 1 for most values of β, which shows that the efficiency of the NE attained with our algorithm is high.

Table 5.2: Price of Anarchy

β	0	0.1	0.2	0.4	0.6	0.8	1
PoA (scenario 1)	1	1.01	1.06	1.31	1.42	1.43	1
PoA (scenario 2)	1	1.06	1.14	1.22	1.32	1.39	1
PoA (scenario 3)	1	1.05	1.08	1.20	1.33	1.39	1

Finally, we investigate the proposed workaround to solve the factorial complexity growth by limiting the number of anchor nodes used at the target. Recall that the idea is to limit this number in order to maintain the complexity bounded to levels that the processor can handle. Therefore, $|\mathcal{N}|$ can be limited considering the complexity constraints of each particular sensor node. For instance, we consider that $|\mathcal{N}|$ can be limited to K, $|\mathcal{N}| \leq K \leq N$. Many possibilities could be considered to select the K nodes; here we consider a simple scheme where the K nearest anchor nodes are selected after the first iteration of the ranging algorithm. Other approaches could be investigated for that purpose [97], but they fall outside the scope of this paper and are left for future work. In this set of simulations, we tested our algorithm in a setup with $N = 16$ anchor nodes and $M = 5$ target nodes in a 30×30 m^2 area. Here we want to compare the case of limiting the positioning of target nodes using the ranges from to $K = 5$ nearest anchor nodes ($|\mathcal{N}| \leq 5$) with the case

of unconstrained complexity ($|\mathcal{N}| \leq N = 16$). In Figures 5.9 and 5.11 the power averages are shown, while in Figures 5.10 and 5.12 the GDOP are shown. Note that a unique equilibrium is attained in both cases and that there are not important differences due to the limitation of $|\mathcal{N}| \leq 5$. In conclusion, our algorithm is functional even when limiting the number of participating anchor nodes; therefore a reduced complexity implementation is possible.

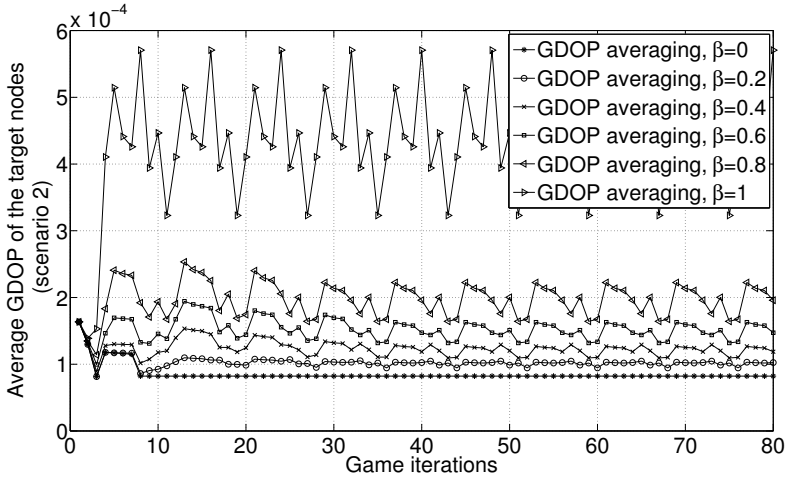

Figure 5.7: Average GDOP over target nodes vs. game iterations for scenario 2.

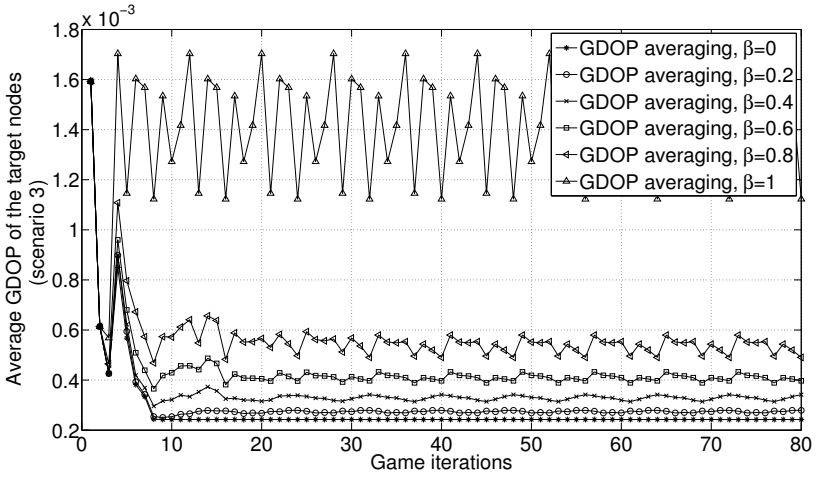

Figure 5.8: Average GDOP over target nodes vs. game iterations for scenario 3.

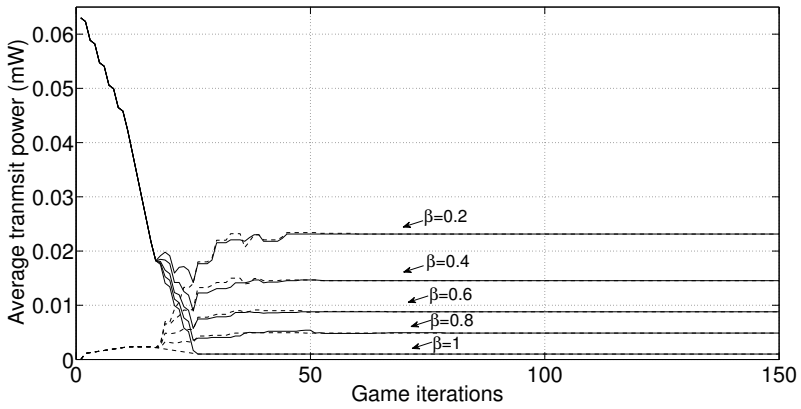

Figure 5.9: Transmit power average (mW) vs. game iterations for $|\mathcal{N}| \leq 5$. Maximum initial strategies in solid lines and minimum ones in dashed lines.

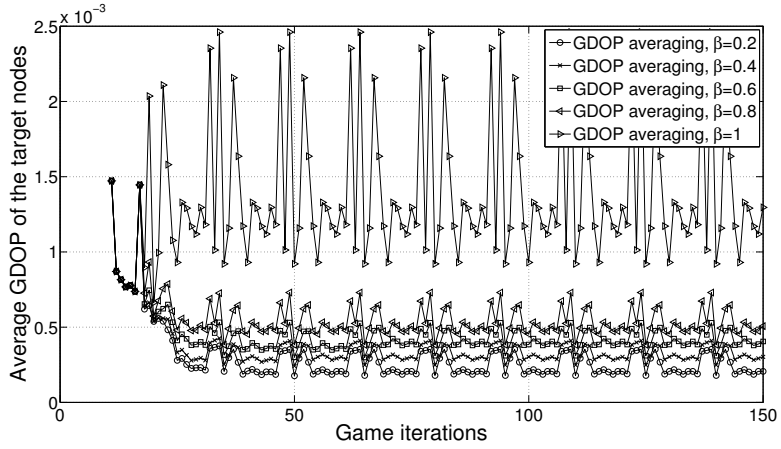

Figure 5.10: Average GDOP over target nodes vs. game iterations for $|\mathcal{N}| \leq 5$.

5.7 Chapter Summary and Conclusions

In this chapter, we have proposed a distributed algorithm for power allocation in WSN with TOA based positioning capabilities using the framework provided by supermodular games. The proposed solution provides a distributed approach to select the power levels of anchor nodes, according to a trade-off between transmitted power and positioning accuracy, quantified by the GDOP parameter. This trade-off may be tuned by a parameter value. It has been proven that the resulting power selection problem is a supermodular game with a unique equilibrium point. Moreover, the

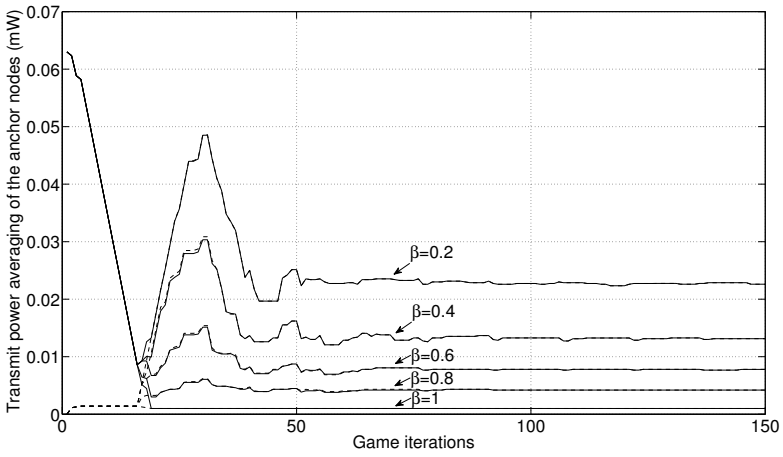

Figure 5.11: Transmit power average (mW) vs. game iterations for $|\mathcal{N}| \leq N = 16$. Maximum initial strategies in solid lines and minimum ones in dashed lines.

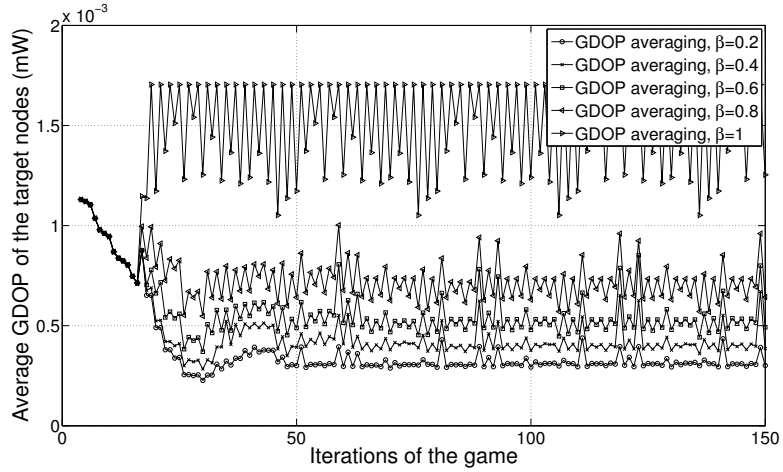

Figure 5.12: Average GDOP over target nodes vs. game iterations for $|\mathcal{N}| \leq N = 16$.

game suffers a small loss with respect to the centrally computed optimum as PoA results show.

A possible solution for the algorithm implementation has been presented as well as its computational complexity and information interchange between nodes. The computational analysis reveals that the computational cost might be an issue in large-scale sensor networks. A possible workaround is to limit the number of anchor nodes used for positioning at the target nodes. The effects of this limitation has

been assessed by means of computer simulations that show that the algorithm is also functional in this case.

The proposed algorithm was applied to WSN, but it can also be applied to other technologies with TOA-based positioning. Moreover, the proposed algorithm can be employed in hybrid positioning with TOA-based ranging and other ranging techniques.

The results presented in this chapter were partially published in:

- Journal:
  [98] Moragrega, A.; Closas, P.; Ibars, C., "Supermodular Game for Power Control in TOA-Based Positioning," Signal Processing, IEEE Transactions on , vol.61, no.12, pp. 3246-3259, June 15, 2013.

- Conference:
  [99] Moragrega, A.; Closas, P.; Ibars, C., "Supermodular game for energy efficient TOA-based positioning," Signal Processing Advances in Wireless Communications (SPAWC), 2012 IEEE 13th International Workshop on , vol., no., pp. 35,39, 17-20 June 2012.

5.8 Appendix

5.8.1 Proof of Proposition 5.1

From (5.12) and (5.10), $g(\mathbf{p})$ can be rearranged applying basic algebra as

$$\begin{aligned} g(\mathbf{p}) &= \mathrm{Tr}\{(\mathbf{H}^T\boldsymbol{\Sigma}^{-1}\mathbf{H})^{-1}\} \qquad (5.23)\\ &= \mathrm{Tr}\{(\boldsymbol{\Sigma}^{-1}\mathbf{H})^{\dagger}(\mathbf{H}^T)^{\dagger}\}\\ &= \mathrm{Tr}\{\mathbf{H}^{\dagger}\boldsymbol{\Sigma}(\mathbf{H}^T)^{\dagger}\}\\ &= \mathrm{Tr}\{\boldsymbol{\Sigma}(\mathbf{H}^T)^{\dagger}\mathbf{H}^{\dagger}\}\\ &= \mathrm{Tr}\{\boldsymbol{\Sigma}\left(\mathbf{H}\mathbf{H}^T\right)^{\dagger}\}\ , \qquad (5.24) \end{aligned}$$

which in the case of diagonal entries in $\boldsymbol{\Sigma}$ is

$$g(\mathbf{p}) = \sum_{i\in\Omega} a_{ii}\frac{1}{p_i}\ , \qquad (5.25)$$

with a_{ii} being the i-th element in the diagonal of $\left(\mathbf{H}\mathbf{H}^T\right)^{-1}$ multiplied by rest of constant terms in the diagonal of $\mathbf{\Sigma}$:

$$\begin{aligned} a_{ii} &= \left(\mathbf{H}\mathbf{H}^T\right)_i^{-1} \cdot \sigma^2_{\hat{\rho}_i} \\ &= \left(\mathbf{H}\mathbf{H}^T\right)_i^{-1} \cdot \left(\frac{K_i^2 C}{\hat{\rho}_i^2}\right) , \end{aligned} \tag{5.26}$$

where $C = \left(\frac{c^2 N_0 (4\pi)^2}{16\pi^2 B T_s f_c^2 \lambda^2}\right)$ and $K_i \geq 1$ from (5.11).

After differentiating w.r.t. p_i we obtain

$$\frac{\partial u_i(\mathbf{p})}{\partial p_i} = -(\beta - 1)\frac{a_{ii}\frac{1}{p_i^2}}{2\sqrt{g(\mathbf{p})}} - \beta \tag{5.27}$$

and the second cross-derivative is given by

$$\frac{\partial^2 u_i(\mathbf{p})}{\partial p_i \partial p_k} = \underbrace{-(\beta - 1)}_{\geq 0} \underbrace{\frac{a_{ii} a_{kk}}{4 p_i^2 p_k^2}}_{\geq 0} \underbrace{\left(\frac{1}{g(\mathbf{p})}\right)^{\frac{3}{2}}}_{\geq 0} , \tag{5.28}$$

which concludes the proof, noting that $p_i, g(\cdot) \geq 0$ by definition. Moreover, we are able to prove that the diagonal terms of (5.24) $a_{ii} > 0$, analyzing the diagonal terms of (5.23). As $\mathbf{\Sigma}^{-1}$ is positive definite and $\mathbf{H}$ is full rank, then $(\mathbf{H}^T\mathbf{\Sigma}^{-1}\mathbf{H})$ is positive definite. The inverse $(\mathbf{H}^T\mathbf{\Sigma}^{-1}\mathbf{H})^{-1}$ is also positive definite and therefore, its diagonal terms are $a_{ii} > 0$ [100], which concludes the proof.

The proof of Proposition 5.1 can be extended for $M \geq 1$ target nodes. In this case for each target node j we define $g_j(\mathbf{p})$ as

$$\sum_{j=1}^{M} g_j(\mathbf{p}) = \sum_{j=1}^{M} \sum_{i \in \Omega} a_{iij} \frac{1}{p_i} , \tag{5.29}$$

were a_{iij} is the i-th element in the diagonal of $\left(\mathbf{H}\mathbf{H}^T\right)^{-1}$ for j-th target node. From (5.18) and following the previous steps, we obtain

$$\frac{\partial u_i(\mathbf{p})}{\partial p_i} = -\frac{(\beta - 1)}{2\sqrt{M}} \cdot \frac{\sum_{j=1}^{M} \frac{a_{iij}}{p_i^2}}{\sqrt{\sum_{j=1}^{M} g_j(\mathbf{p})}} - \beta , \tag{5.30}$$

$$\frac{\partial^2 u_i(\mathbf{p})}{\partial p_i \partial p_k} = \underbrace{\frac{-(\beta - 1)}{4\sqrt{M}}}_{\geq 0} \cdot \sum_{j=1}^{M} \underbrace{\frac{a_{iij}}{p_i^2}}_{\geq 0} \cdot \sum_{j=1}^{M} \underbrace{\frac{a_{kkj}}{p_k^2}}_{\geq 0} \cdot \underbrace{\left(\frac{1}{\sum_{j=1}^{M} g_j(\mathbf{p})}\right)^{\frac{3}{2}}}_{\geq 0} , \tag{5.31}$$

which also concludes the proof, since that $a_{iij}, a_{iik}, p_i, p_k, g(\cdot) \geq 0$ by definition.

5.8.2 Proof of uniqueness of Nash Equilibrium

In order to prove the uniqueness of NE (Proposition 5.2), from [70] we are able to prove that the $BR_i(\mathbf{p_{-i}})$ is a *standard* function with the following definition:

Definition 5.2. *Function $BR_i(\mathbf{p_{-i}})$ is standard if for all $\mathbf{p} \geq 0$ the following properties are satisfied:*

- *Positivity: $BR_i(\mathbf{p}_{-i}) > 0$*
- *Monotonicity: if $\mathbf{p}_{-i} \geq \mathbf{p}'_{-i}$, then $BR_i(\mathbf{p}_{-i}) > BR_i(\mathbf{p}'_{-i})$*
- *Scalability: for all $\delta > 1$, $\delta \cdot BR_i(\mathbf{p}_{-i}) > BR_i(\delta \cdot \mathbf{p}_{-i})$*

When $BR_i(\mathbf{p}_{-i})$ is a standard function, the iteration will be called standard power control algorithm. Moreover from [70], we present the following Proposition:

Proposition 5.6. *If the standard power control algorithm has a NE, then that NE is unique. Then for any initial power vector $\mathbf{p}$, the standard power control algorithm converges to the unique NE.*

For our game, the positivity property of $BR_i(\mathbf{p}_{-i})$ is satisfied since $\mathcal{P} \subseteq \mathbb{R}^+$. If we are able to prove the monotonicity and scalability properties, then from Proposition 5.6 we can prove that the NE is unique. Monotonicity and scalability properties are satisfied with the following reasoning that consists of three steps: in i) we arrange terms of (5.27); in ii) we study $BR_i(\mathbf{p}_{-i})$ and $BR_i(\mathbf{p}'_{-i})$; in iii) we present a graphical method to prove monotonicity and scalability properties.

i) First, from $\frac{\partial u_i(\mathbf{p})}{\partial p_i}$

$$\frac{\partial u_i(\mathbf{p})}{\partial p_i} = -(\beta - 1)\frac{a_{ii}\frac{1}{p_i^2}}{2\sqrt{g(\mathbf{p})}} - \beta = 0 \ , \tag{5.32}$$

we separate terms that depend on p_i and rearrange them as

$$\left(\frac{a_{ii}(1-\beta)}{2\beta}\right) = p_i^2\sqrt{\sum_{k\in\Omega} a_{kk}\frac{1}{p_k}} \ ; \tag{5.33}$$

considering that $\alpha \doteq \left(\frac{a_{ii}(1-\beta)}{2\beta}\right)$ and raising it to the power of two we obtain

$$\alpha^2 = p_i^4\left(a_{ii}\frac{1}{p_i} + \sum_{k\neq i} a_{kk}\frac{1}{p_k}\right) \ . \tag{5.34}$$

Defining

$$\gamma \doteq \sum_{k \neq i} a_{kk} \frac{1}{p_k} \tag{5.35}$$

and applying basic algebra we obtain

$$\gamma p_i^4 + a_{ii} p_i^3 - \alpha^2 = 0 \ . \tag{5.36}$$

ii) We arrange terms and define $x(\mathbf{p}) \doteq p_i^3 \cdot (\gamma p_i + a_{ii})$, then (5.36) can be written as

$$p_i^3 \cdot (\gamma p_i + a_{ii}) = \alpha^2 \ , \tag{5.37}$$

if $\mathbf{p}^*$ is the $BR_i(\mathbf{p}_{-i})$, then it has to satisfy $x(\mathbf{p}^*) = \alpha^2$.

We have to analyze $\delta \cdot BR_i(\mathbf{p}_{-i}) \doteq \delta \cdot \mathbf{p}^*$ and $BR_i(\delta \cdot \mathbf{p}_{-i})$. Regarding the first one, we know that $\delta \cdot \mathbf{p}^* > \mathbf{p}^*$ since $\delta > 1$. With respect to the latter, taking into account (5.35), we obtain

$$\frac{\gamma}{\delta} = \sum_{k \neq i} a_{kk} \frac{1}{\delta \cdot p_k}. \tag{5.38}$$

Applying $BR_i(\delta \cdot \mathbf{p}_{-i})$ to (5.37), we obtain

$$p_i^3 \cdot (\frac{\gamma}{\delta} p_i + a_{ii}) = \alpha^2 \ , \tag{5.39}$$

and define $y(\mathbf{p}) = p_i^3 \cdot (\frac{\gamma}{\delta} p_i + a_{ii})$. In this case, we know that $y(BR_i(\delta \cdot \mathbf{p}_{-i})) = \alpha^2$.

iii) In order to analyze $\mathbf{p}^*$, $\delta \cdot \mathbf{p}^*$ and $BR_i(\delta \cdot \mathbf{p}_{-i})$ we use a graphical method with the functions $x(\mathbf{p})$, α^2 and $y(\mathbf{p})$ shown in Figure 5.13 for node i. The roots of $x(\mathbf{p})$ are 0 and $-a_{ii}/\gamma$, and the roots of $y(\mathbf{p})$ are 0 and $(-a_{ii}\delta)/\gamma$. $\mathbf{p}^*$ is the intersection of $x(\mathbf{p})$ with α^2, being $x(\mathbf{p}^*) = \alpha^2$. While $BR_i(\delta \cdot \mathbf{p}_{-i})$ is the intersection of $y(\mathbf{p})$ with α^2, being $y(BR_i(\delta \cdot \mathbf{p}_{-i})) = \alpha^2$.

With respect to the monotonicity property, if $\mathbf{p}_{-i} \geq \mathbf{p}'_{-i}$, then $\gamma(\mathbf{p}_{-i}) \leq \gamma(\mathbf{p}'_{-i})$, therefore the slope of $x(\mathbf{p}_{-i})$ is lower than the slope of $x(\mathbf{p}'_{-i})$, hence the intersection (corresponding to the best response) of these functions with the constant α^2 satisfies $BR_i(\mathbf{p}_{-i}) > BR_i(\mathbf{p}'_{-i})$.

With respect to the scalability property, we need to show that $\delta \cdot BR_i(\mathbf{p}_{-i}) = \delta \cdot \mathbf{p}^* > BR_i(\delta \cdot \mathbf{p}_{-i})$. For that, we analyze the function $y(\mathbf{p}) = p_i^3 \cdot (\frac{\gamma}{\delta} p_i + a_{ii})$ at the value $\delta \cdot \mathbf{p}^*$. Substituting we obtain $y(\delta \cdot \mathbf{p}^*) = \delta^3 p_i^3 \cdot (\gamma p_i + a_{ii})$ and, using (5.37) then $y(\delta \cdot \mathbf{p}^*) = \delta^3 \alpha^2 > \alpha^2 = y(BR_i(\delta \cdot \mathbf{p}_{-i}))$. Noticing that $y(\mathbf{p})$ is a monotonically increasing function for $p_i > 0$, we have proven that $y(\delta \cdot \mathbf{p}^*) > y(BR_i(\delta \cdot \mathbf{p}_{-i})) \Leftrightarrow \delta \cdot \mathbf{p}^* > BR_i(\delta \cdot \mathbf{p}_{-i})$. This result corresponds to the scalability property.

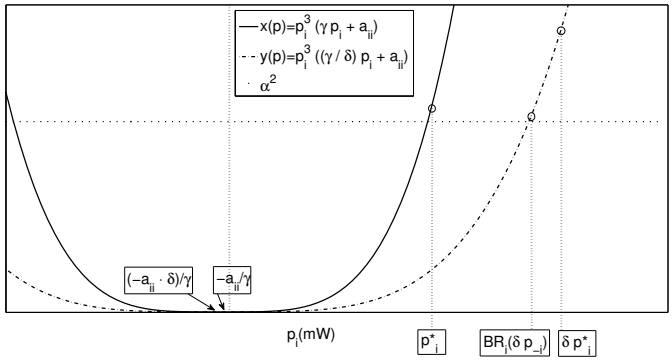

Figure 5.13: Graphical demonstration of the scalability property.

The proof can be extended for $M \geq 1$ target nodes in order to prove Proposition 5.5. From (5.30)

$$\frac{\partial u_i(\mathbf{p})}{\partial p_i} = -\frac{(\beta-1)}{2\sqrt{M}} \cdot \frac{\sum_{j=1}^{M} \frac{a_{iij}}{p_i^2}}{\sqrt{\sum_{j=1}^{M} g_j(\mathbf{p})}} - \beta = 0 \ , \tag{5.40}$$

we follow the previous steps to obtain

$$\left(\frac{(1-\beta)\sum_{j=1}^{M} a_{iij}}{2\sqrt{M}\beta} \right) = p_i^2 \sqrt{\sum_{j=1}^{M} \sum_{k\in\Omega} a_{kkj} \frac{1}{p_k}} \ . \tag{5.41}$$

Arranging terms we obtain

$$\left(\frac{(1-\beta)\sum_{j=1}^{M} a_{iij}}{2\sqrt{M}\beta} \right)^2 = p_i^4 \left(\sum_{j=1}^{M} a_{iij} \frac{1}{p_i} + \sum_{j=1}^{M} \sum_{k\neq i} a_{kkj} \frac{1}{p_k} \right) \ . \tag{5.42}$$

After considering that $\gamma_j = \sum_{k\neq i} a_{kkj} \frac{1}{p_k}$ and applying basic algebra we obtain

$$\sum_{j=1}^{M} \gamma_j p_i^4 + \sum_{j=1}^{M} a_{iij} p_i^3 - \frac{\sum_{j=1}^{M} a_{iij}(1-\beta)}{2\sqrt{M}\beta} = 0 \ . \tag{5.43}$$

Arranging terms we obtain

$$\sum_{j=1}^{M} \gamma_j p_i^4 + a_{iij} p_i^3 - \alpha_M^2 = 0 \ , \tag{5.44}$$

where $\alpha_M \doteq \alpha/\sqrt{M}$. (5.44) is similar to (5.36), therefore the monotonicity and scalability properties hold for (5.44) and then we are able to prove the uniqueness of NE.

5.8.3 Proof of the convexity of the social welfare function

In order to prove that (5.16) is convex it is sufficient to show that the utility function u_i in (5.12), which takes the form

$$u_i(p_i, \mathbf{p}_{-i}) = -(1-\beta)\sqrt{g(\mathbf{p})} - \beta p_i \tag{5.45}$$

is convex for all i.

We start to study the convexity of the following part of the utility function

$$f_i(p_i, \mathbf{p}_{-i}) = -\sqrt{g(\mathbf{p})} = -\sqrt{\sum_{i\in\Omega} a_{ii}\frac{1}{p_i}}. \tag{5.46}$$

For that we consider the following definition of convexity [101]:

Definition 5.3. *A function is convex if and only if it is convex when restricted to any line that intersects its domain. In other words f is convex if and only if for all $x \in dom f$ and all v, the function $g(t) = f(x+tv)$ is convex.*

Taking into account Definition 5.3, p_i is parameterized to $b_i x + c_i$. And f_i can be rewritten as

$$f_i(b_i x + c_i, \mathbf{b}_{-i}x + \mathbf{c}_{-i}) = \\ -\sqrt{\sum_{i\in\Omega} \frac{a_{ii}}{b_i x + c_i}} = -\sqrt{\sum_{i\in\Omega} \frac{d_i}{x + m_i}} \tag{5.47}$$

where $d_i = a_{ii}/b_i$ and $m_i = c_i/b_i$.

In order to study the convexity of $f_i(b_i x + c_i, \mathbf{b}_{-i}x + \mathbf{c}_{-i})$ we consider Proposition 5.7 that was also presented in [101].

Proposition 5.7. *Consider two functions $h : \mathbb{R} \to \mathbb{R}$ and $g : \mathbb{R}^n \to \mathbb{R}$. Without loss of generality we can restrict to the case $n = 1$. We assume that h and g are twice differentiable. The convexity of the composition function $f = h \circ g : \mathbb{R}^n \to \mathbb{R}$, defined by $f(x) = h(g(x))$ reduces to $f'' \leq 0$. Where the second derivate of the composition function $f = h \circ g$ is given by*

$$f'' = h''(g(x))g'(x)^2 + h'(g(x))g''(x)\ . \tag{5.48}$$

To apply Proposition 5.7, we identify terms in (5.47) such that $h(x) = -\sqrt{g(x)}$ and $g(x) = \sum_i \frac{d_i}{x+m_i}$. Therefore, the second derivate of $f_i(b_i x + c_i, \mathbf{b}_{-i}x + \mathbf{c}_{-i})$ is given by

$$f_i''(b_i x + c_i, \mathbf{b}_{-i}x + \mathbf{c}_{-i}) = h''(g(x))g'(x)^2 + h'(g(x))g''(x) \tag{5.49}$$

with

$$h'(g(x)) = -\frac{g(x)^{-1/2}}{2} \; ; \; h''(g(x)) = \frac{g(x)^{-3/2}}{4} \; ;$$
$$g'(x) = -\sum_{i\in\Omega} \frac{d_i}{x+m_i} \; ; \; g''(x) = 2\sum_{i\in\Omega} \frac{d_i}{(x+m_i)^3} \; .$$

Now we need to show that $f_i'' \leq 0$, i.e.

$$f_i''(b_i x + c_i, \mathbf{b}_{-i} x + \mathbf{c}_{-i}) =$$
$$\frac{1}{4}\left(\sum_{i\in\Omega} \frac{d_i}{x+m_i}\right)^{-3/2} \left(\sum_{i\in\Omega} \frac{d_i}{(x+m_i)^2}\right)^2 -$$
$$\left(\sum_{i\in\Omega} \frac{d_i}{x+m_i}\right)^{-1/2} \sum_{i\in\Omega} \frac{d_i}{(x+m_i)^3} \leq 0 \; . \tag{5.50}$$

Rearranging terms we obtain

$$\sum_{i\in\Omega} \frac{d_i}{(x+m_i)^3} \left(\sum_{i\in\Omega} \frac{d_i}{x+m_i}\right)^{-1/2} \geq$$
$$\frac{1}{4}\left(\sum_{i\in\Omega} \frac{d_i}{x+m_i}\right)^{-3/2} \left(\sum_{i\in\Omega} \frac{d_i}{(x+m_i)^2}\right)^2 \; , \tag{5.51}$$

and dividing by $\left(\sum_{i\in\Omega} \frac{d_i}{x+m_i}\right)^{-3/2}$ we obtain

$$\sum_{i\in\Omega} \frac{d_i}{(x+m_i)^3} \sum_{i\in\Omega} \frac{d_i}{x+m_i} \geq \frac{1}{4}\left(\sum_{i\in\Omega} \frac{d_i}{(x+m_i)^2}\right)^2 \; . \tag{5.52}$$

Defining $s_i \doteq \frac{\sqrt{d_i}}{(x+m_i)^{3/2}}$, $t_i \doteq \frac{\sqrt{d_i}}{(x+m_i)^{1/2}}$, and the vectors $\mathbf{s} \doteq [s_1, \ldots, s_N]$ and $\mathbf{t} \doteq [t_1, \ldots, t_N]$, we obtain the Cauchy-Schwartz inequality

$$\|\mathbf{s}\|^2 \|\mathbf{t}\|^2 \geq |\mathbf{st}|^2 \; , \tag{5.53}$$

which confirms that $f_i'' \leq 0$. Since this proves that (5.46) is convex, $u_i(p_i, \mathbf{p}_{-i})$ is also convex because the component $-\beta p_i$ is affine. Finally, we can demonstrate that (5.16) is convex because the addition of convex functions such as $u_i(p_i, \mathbf{p}_{-i})$ is also a convex function.

In order to extend this proof for the case of multiple target nodes, we need to prove that (5.16) is convex. We recall that the utility function u_i (5.18) takes the form

$$u_i(p_i, \mathbf{p}_{-i}) = (\beta - 1) \cdot \sqrt{\frac{\sum_{j=1}^{M} g_j(\mathbf{p})}{M}} - \beta p_i = \\ -\frac{(1-\beta)}{\sqrt{M}} \cdot \left(-\sqrt{\sum_{j=1}^{M} g_j(\mathbf{p})} \right) - \beta p_i \ . \tag{5.54}$$

We have seen that the function (5.46) is a convex function for 1 target node. In this case with $M \geq 1$ target nodes, function (5.46) takes the form

$$f_i(p_i, \mathbf{p}_{-i}) = -\sqrt{\sum_{j=1}^{M} g_j(\mathbf{p})} = -\sqrt{\sum_{j=1}^{M} \sum_{i \in \Omega} a_{iij} \frac{1}{p_i}}. \tag{5.55}$$

To study the convexity of $f_i(p_i, \mathbf{p}_{-i})$ we also consider Proposition 5.7 being $g(x) = \sum_{j=1}^{M} \sum_{i \in \Omega} \frac{d_i}{x + m_i}$ in this case. Following the same steps as before and applying Cauchy-Schwartz inequality, it follows that $f_i'' \leq 0$ and therefore (5.16) for multiple targets is also convex.

6

WSN Topologies for Positioning

LOW energy consumption is one of the main priorities of WSNs, as sensors are typically battery-operated, and battery replacement may be costly or not even possible. As it was commented in the introduction (Chapter 2.1.1), this issue have to be addressed from the different levels of the protocol stack. In previous Chapters 4 and 5, power allocation and energy efficiency aspects for positioning in WSN were treated from a physical layer perspective, while this Chapter 6 is devoted to MAC and upper layers perspective.

6.1 Introduction

As it is crucial to employ energy-efficient protocols in WSN, the 802.15.4 [20] standard, was introduced for this goal, specifying both PHY and MAC layers. An alternative PHY, the IEEE 802.15.4a [29], based on ultra-wideband, has also been standardized for positioning purposes. Moreover, ZigBee [102] is an industrial standard that defines the network and application layers for sensor networks based on IEEE 802.15.4 PHY and MAC layers. IEEE 802.15.4 and Zigbee were introduced in Chapter 2.1.2, while IEEE 802.15.4a in Chapter 2.2.3. One of the features that

these standards characterize is the topology of the WSN. Besides a star topology, the 802.15.4/Zigbee standard supports mesh and cluster-tree topologies.

In the positioning based on range like trilateration, a subset of sensors, called anchor nodes, that know its own position helps other nodes determine theirs. Such techniques benefit from a high degree of connectivity, since range measurements from at least four anchor nodes are necessary (three-dimensional scenario). On the other hand, WSN topologies, most notably the cluster-tree topology, tend to limit connectivity between nodes to save energy. This results in very poor performance of the network in terms of positioning based on range.

In the literature, most of algorithms for positioning based on range and anchor nodes that have been proposed are based on mesh WSN. In Chapter 2.2.5 they were introduced under a classification of the algorithms. For positioning algorithms based on range, the success of the location discovery depends on the network connectivity [103]. In [48, 103] a multilateration algorithm for localization is presented as well as multi-hop ranging solutions for nodes with low connectivity to anchor nodes. However, previous studies do not take into account the limitations that MAC layer and network topologies supported by the standards can introduce in range-based positioning algorithms. While the connectivity between nodes in a mesh network is high, it is considerably reduced in a cluster-tree topology. This presents advantages, such as energy saving, but it severely degrades the performance of range-based positioning. The literature focuses, on one hand, in providing positioning algorithms that take advantages of the connectivity and cooperativity nature of mesh WSN, and, on the other hand, clustering algorithms with high energy efficiency [19, 104], such as, for example, the LEACH algorithm.

6.1.1 Contribution

The main contribution of this chapter is to provide a solution to improve positioning in cluster-tree topologies defined in the standards for WSN. In this direction, a solution to increment the connectivity between the sensor nodes and hence improve the range based positioning is presented. Moreover, we propose LACFA, a network formation algorithm that increases the probability of positioning of sensors in a cluster-tree topology. It does so by properly allocating anchor nodes to different clusters during the network formation phase, and by allowing peers in the same cluster to perform ranging with each other. This simple algorithm greatly improves the probability of positioning of sensor nodes for a moderate density of anchor nodes. As has been shown, it outperforms the well known LEACH algorithm without paying a penalty in terms of energy consumption. Moreover, results show that LACFA

increases one-hop connectivity from target to anchor nodes improving the one-hop range-based positioning.

The remainder of this chapter is organized as follows: In Section 6.2, peer-to-peer topologies in the IEEE 802.15.4/Zigbee and 802.15.4a standards are described. In Section 6.3, we explain the considered range-based positioning algorithm based on trilateration. In Section 6.4, we describe range-based positioning for the mesh and cluster-tree WSNs. Based on this analysis, the schemes for positioning in a cluster-tree topology are proposed. These solutions are used with our algorithm for localization aware cluster formation (LACFA) presented in Section 6.5. Numerical results are provided in Section 6.7, and conclusions are drawn at the end of the chapter.

6.2 Peer-to-Peer Networks under Standards: an Overview

The standard IEEE 802.15.4 defines two types of devices, RFD and FFD, where only a FFD may be the coordinator of a personal area network (PAN) or cluster. In the following, we will assume where necessary that sensors are FFDs. The 802.15.4/Zigbee standard supports star and peer-to-peer topologies. Within peer-to-peer topologies, we distinguish between mesh and cluster-tree networks [102], both shown in Figure 6.1.

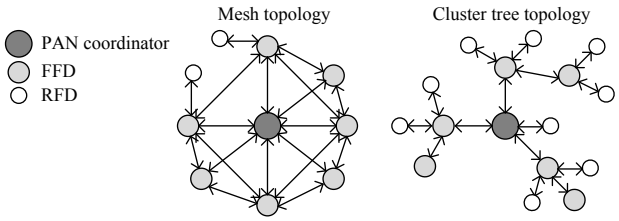

Figure 6.1: Mesh and cluster-tree topology examples.

In a mesh network, any sensor may communicate with any other sensor within its range, and route messages from other sensors, enabling the formation of complex self-organizing topologies. The mesh topology places no restrictions on the connectivity between nodes, maximizing network coverage. On the other hand, nodes need to listen to the medium continuously, causing this topology to be highly energy consuming. In a cluster-tree network as defined by Zigbee, a FFD, acting as PAN coordinator, initiates the network and becomes root. Sensors are then grouped in clusters where a coordinator is the cluster head, and several other devices are leaf or

child nodes. The cluster head sends periodic beacon frames that are used by sensors within its range to attach to the cluster as child nodes. These nodes may, in turn, send new beacons and form a new cluster, resulting in a cluster-tree. This structure is energy efficient since sensors synchronize with their parent node. Moreover, the resulting tree topology greatly simplifies routing. The 802.15.4a standard supports both star and mesh topologies, while the cluster-tree topology falls outside the scope of the standard, since upper layers are not addressed.

The MAC layer defined by the 802.15.4 standard [20] specifies two modes of operation: beacon-enabled and non-beacon. In the non-beacon mode, CSMA-CA is used, which requires long listening periods which decrease the energy efficiency of the protocol. The beacon-enabled mode greatly improves energy efficiency by defining the so-called superframe, shown in Figure 6.2. The superframe, managed by the cluster head, contains the synchronization beacon, followed by a CAP, and an optional CFP. During the CAP, the channel is accessed using slotted CSMA-CA. In order to minimize interference, neighboring clusters in a cluster-tree may concatenate superframes as shown in Figure 6.2, where rectangles denote active parts of the superframe (beacon in black and CAP in white).

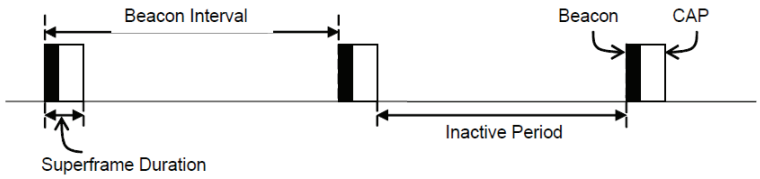

Figure 6.2: Superframe structure that consists of a beacon frame and a Contention Access Period (CAP). Also an inactive period is at the end of the superframe.

6.3 System Model

The problem under study involves the positioning of N target coordinators in a WSN that contains M reference coordinators emitting ranging signals to allow positioning of the latter. The following WSN topology configurations are considered: 802.15.4a mesh WSN; Zigbee mesh and Zigbee cluster-tree WSNs; and a WSN based on 802.15.4a PHY layer with cluster-tree topology similar to Zigbee. We assumed a uniform random deployment of the $N + M$ nodes in the scenario.

Different ranging models can be used depending on the technology. On the one hand, 802.15.4a allows TOA-based ranging which model is defined in 2.2.2. On the

other hand, RSS based ranging measures are commonly modeled using the log-normal path loss model defined in 2.2.1. We consider that RSS based positioning is used with 802.15.4/Zigbee technology.

Once range measurements are available, either resorting to TOA or RSS techniques, the target node computes its position based on a simple algorithm to solve the trilateration problem. A LS algorithm suffices for the purpose of this chapter, which is to propose and analyze network formations that improve the overall positioning performance. Thus, the well-known LS method is used here as a comparison tool among topology creation algorithms. Particularly, we consider one-hop ranging, meaning that ranging is performed considering only those reference nodes which are in view. The proposed steps for the network positioning algorithm are detailed as follows:

1. One-hop ranging to anchor nodes: anchor nodes start the ranging phase with coordinators within its range.

2. Positioning with multilateration: if target coordinator j has four or more anchor nodes within its range, its position is estimated with trilateration and LS algorithm. j becomes a located node (LN) that can be a reference for locating other target nodes within range. Otherwise, coordinator j continues trying to learn its position.

3. Cooperation: this process is repeated until the positions of all the nodes that eventually can have either four anchor or LN nodes are estimated.

4. Refinement: for LS, a larger value of anchor or LN nodes results in more accurate position estimation of a target node.

The next sections describe solutions and algorithms for topology formation to improve positioning in cluster-tree peer-to-peer networks. Indeed, this comes before the position solution described above, from a practical point of view. Current topology formation criteria are focused on purposes other than positioning; therefore, an effort is made in the sequel to the study existing methods and investigate clustering techniques aiming toward providing positioning quality of service to the WSN.

6.4 Network Positioning Constrained by Topology

6.4.1 Mesh and Cluster-tree Topologies

The success of range-based positioning depends on the connectivity between the nodes of the network [103]. For the case of range-based positioning with trilateration, it benefits from a high degree of connectivity, since range measurements from at least three anchor nodes are necessary in a two-dimensional scenario. Mesh topology allows a high connectivity between nodes because it places no restrictions on that. In fact in a Zigbee or 802.15.4a mesh WSN, any coordinator may communicate with any other coordinator within range. Therefore, the connectivity allowed by mesh topology is an advantage for range-based positioning.

However, in a cluster-tree topology, there are restrictions on the connectivity between the nodes. For Zigbee (and in our 802.15.4a WSN with cluster-tree topology), nodes are grouped in clusters where any coordinator may communicate only with its parent and its children of its cluster. This excludes communication with other coordinators that may be in range. As a result, less nodes are available for ranging and positioning. Therefore for one-hop ranging between nodes, one coordinator j could be located under the following conditions: (1) it has at least four range estimations with reference coordinators, and (2) these reference coordinators have parent or children relationship with the j coordinator.

The probability of positioning of a node in a mesh network follows a three-dimensional Poisson distribution $f_P(k, \lambda)$, where λ is the density and k the number of deployed anchor nodes within range. Therefore the probability to locate a node is the probability with at least $k \geq 4$. It is given by

$$Pr(k \geq 4, \lambda) = 1 - f_P(k < 4) = \tag{6.1}$$

$$= 1 - (f_P(k = 0) + f_P(k = 1) + f_P(k = 2) + f_P(k = 3)) \tag{6.2}$$

However with cooperation, the new deployment of LN nodes does not follow a Poisson distribution because these deployments are not random.

In a 802.15.4/Zigbee or 802.15.4a network with Zigbee, RFD devices may communicate only with one coordinator within its range, therefore, in this chapter, we consider the range-based positioning of FFD nodes of the WSN.

6.4.2 Improved Positioning in a Cluster-Tree Topology

In this section, a solution for the constraints of the range-based positioning in a cluster-tree network is presented. The goal of this solution is to improve the positioning, and thus to reach a trade-off between the connectivity of mesh topology and energy saving of cluster-tree topology.

For 802.15.4/Zigbee cluster-tree topology, ranging among parent and children can be done with RSS measurements using the data interchange of data frames. The Received Signal Strength Indicator (RSSI) defined in the standard [20] gives an estimation of the RSS measurement. Also for 802.15.4a, ranging among parent and children can be done using the message sequence for ranging explained in the standard [29] that also uses data frames interchanging. We propose the following solution to increase the ranging between coordinators overcoming this parent-children-based connectivity:

- Ranging is controlled by MAC layer: The ranging application is done in a MAC level, as in the IEEE 802.15.4 standard. The application layer (that controls the positioning algorithm) calls the corresponding MAC primitives directly for doing ranging between two nodes.

In order to follow this solution, the MAC level frames for ranging should work with the MAC superframe structures without collisions. For this propose, a scheme is proposed:

- Ranging during the CAP of the superframe (RCAPS): A coordinator j can do ranging with its parent coordinator and with its child coordinators using the ranging interchange of frames defined in the standards. The improvement achieved is that this coordinator j also uses the CAP of its parent cluster superframe for ranging with its brother coordinators (coordinators with same parent that follow the same superframe) within range. Figure 6.3 shows the RCAPS solution with the superframes structures of the corresponding parent and children of three interconnected clusters. In Fig. 6.4, the interchange of frames between two brothers of a cluster with RCAPS solution is presented. Figure 6.5 shows an example where cluster-tree and cluster-tree with RCAPS are compared.

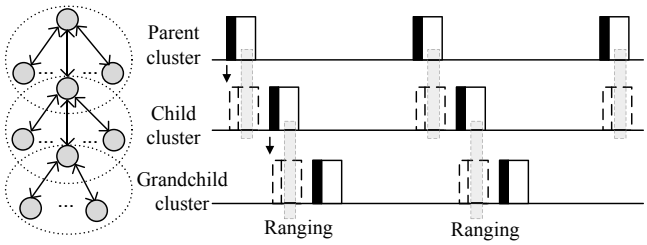

Figure 6.3: RCAPS solution with the superframes structures of the corresponding parent and children of three interconnected clusters.

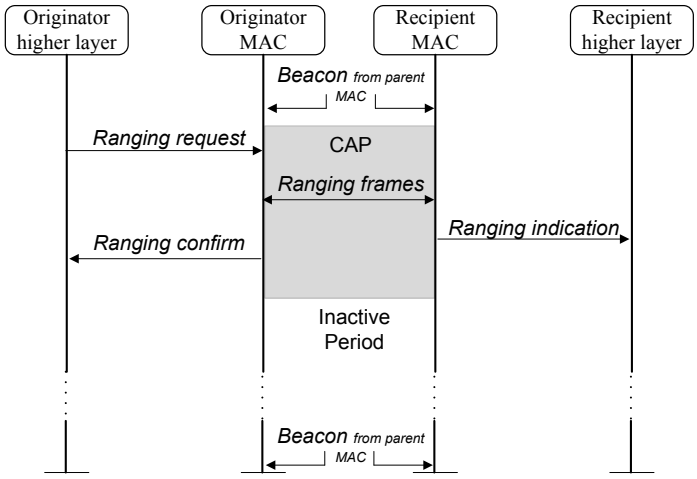

Figure 6.4: The figure shows the protocol between two coordinators (that share the parent coordinator) of a cluster which do ranging. The exchange of frames for ranging is done during the CAP of the superframe (RCAPS solution).

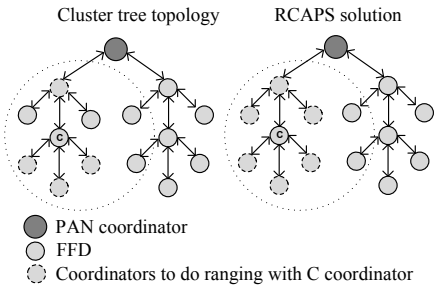

Figure 6.5: In the example the coordinators within range of C to do ranging are shown. In the unmodified cluster-tree case only parent–child ranging is allowed. In RCAPS ranging with coordinators sharing the same parent is also possible.

6.5 LACFA: Localization Aware Cluster Formation Algorithm

This section presents the design of a cluster-tree formation algorithm with the objective of improving of the average number of positioned target nodes. As the necessary signals for positioning of target nodes are emitted by anchor nodes, the design of a clustering algorithm that maximizes the connectivity of the anchor nodes in the cluster-tree topology is proposed. For that aim, Graph Theory [105] is resorted. We demonstrate that in a cluster-tree topology, the best connectivity of anchor nodes is held by those nodes being cluster heads. Also, we propose that our algorithm controls the maximum number of anchor nodes in the clusters.

Graph theory describes the communication flow among the nodes of a network by an undirected graph $\mathscr{G} = (\mathscr{V}, \mathscr{E})$ where $\mathscr{V} = \{1, \ldots, N\}$ is the set of vertices (the set of $N = N_n + N_r$ nodes in our case), and $\mathscr{E}$ is the set of edges (i.e., their links). The edge e_{ij} represents a bidirectional communication link between a pair of distinct nodes i and j. The set of neighbors of a node i was defined previously as $\mathcal{N}_i = \{j \in \mathscr{V} : e_{ij} \in \mathscr{E}\}$ for all $i, j = \{1, \ldots, N\}$, which represents the set of indexes of the nodes sending information to node i.

The connectivity matrix of a graph is a $N \times N$ matrix with entries

$$[\mathbf{A}]_{ij} = \begin{cases} 1 & \text{if } i \text{ and } j \text{ are connected} \\ 0 & \text{otherwise} \end{cases}, \tag{6.3}$$

with the degree of a vertex being the number of edges at i. The degree is equal to the number of neighbors $d_i = |\mathcal{N}_i|$, or equivalently

$$d_i = \sum_{j \in \mathcal{N}_i} [\mathbf{A}]_{ij}. \tag{6.4}$$

Let us define the following sets:

- $\mathscr{V}_\ell$ as the set of nodes in the ℓth cluster;
- $\mathscr{V}_{\ell,p}$ as the set of parent nodes in the ℓth cluster including the cluster-head, i.e., those generating a cluster;
- $\mathscr{V}_r$ as the set of anchor nodes in the graph, $N_r = |\mathscr{V}_r|$.
- $\mathscr{V}_n$ as the set of target nodes in the graph, $N_n = |\mathscr{V}_n|$.

The necessary signals for positioning of target nodes are emitted by anchor nodes. Therefore, for our purposes, it is necessary to design a clustering algorithm that maximizes the connectivity of the anchor nodes in the cluster-tree topology. We base on Proposition 6.1 to state that such algorithm should ensure that cluster heads are the anchor nodes of the network.

Proposition 6.1. *Let the undirected graph $\mathscr{G} = (\mathscr{V}, \mathscr{E})$ define a cluster-tree topology. Then, for the ℓth cluster we have that*

$$d_{\ell,\mathrm{CH}} \geq d_{\ell,j} \quad , \quad \forall j \in \mathscr{V}_\ell \backslash \mathscr{V}_{\ell,p} \ , \tag{6.5}$$

with $d_{\ell,\mathrm{CH}}$ being the degree of the ℓth cluster head.

Proof. The proof follows easily if one realizes that $d_{\ell,\mathrm{CH}} = |\mathscr{V}_\ell|$, as the cluster-head is connected to all the nodes in its cluster. For the rest of the non-parent nodes, we have two schemes. On the one hand, in the conventional cluster-tree topology, we know that $|\mathscr{V}_\ell \backslash \mathscr{V}_{\ell,p}| = |\mathscr{V}_\ell| - |\mathscr{V}_{\ell,p}| < |\mathscr{V}_\ell|$ since a cluster-child can only do ranging with its parent node. On the other hand, in the RCAPS scheme, since a cluster-child can do ranging with its parent node and other cluster-child (within range) that share the same parent, we have that $|\mathscr{V}_\ell \backslash \mathscr{V}_{\ell,p}| \leq |\mathscr{V}_\ell|$ with equality only if all child are in range with each other. □

Therefore, it arises that, in a cluster-tree topology, the best connectivity is held by anchor nodes being cluster-heads. Since, the objective of this chapter is to provide enhanced connectivity of target nodes to anchor nodes in cluster-trees, we conclude that a suitable algorithm should enforce that $\mathscr{V}_{\ell,p} \subseteq \mathscr{V}_r$, with anchor nodes being cluster-heads.

Another preferable feature of the proposed positioning-aware topology formation algorithm is to design the maximum number of anchor nodes in the clusters $R_{\max}$. The algorithm proceeds as follows. Initially, $\ell = 1$, and $\mathscr{V}_{\ell,p} = \mathrm{CH}_{\ell=1}$ is the cluster-head (anchor node) of the first cluster. For each cluster ℓ, the cluster-head sends beacon frames to find cluster-children and join them to the cluster. This set of nodes $\mathcal{N}_\ell$ is composed of target and anchor nodes within range, that is $\mathcal{N}_\ell = \mathcal{N}_\ell^n \cup \mathcal{N}_\ell^r$. They are selected randomly and for the anchor nodes $|\mathcal{N}_\ell^r| \leq R_{\max}$. Notice that LACFA controls $|\mathcal{N}_\ell^r| \leq R_{\max}$, but the maximum value of $\mathcal{N}_\ell$ is configured by the standard. Then, the anchor members $\mathcal{N}_\ell^r$ of $\mathcal{N}_\ell$ start to send beacons to form its own clusters setting $\mathscr{V}_{\ell,p} \subseteq \mathscr{V}_r$. The process is performed sequentially until $\bigcup_{\ell'=1}^{\ell} \mathcal{N}_{\ell'}^r = \mathscr{V}_r$, that is, when all reference nodes have been included in one of the clusters. Notice that this is a completely distributed algorithm.

For a better understanding of LACFA's operation, Fig. 6.6 shows the state machine running in each anchor coordinator in the network. Initially, state S0 represents

the situation in which a node is listening to the environment, waiting for a beacon signal of a cluster-head. Once the node receives it, a request to join that particular cluster is emitted in S1. If joining fails, for instance, because cluster-head does not admit another child, then the node returns to S0; otherwise it moves to S2. In such situation, the node is correctly incorporated into a cluster, and its aim becomes to associate coordinators to its own cluster. To do so, it emits periodically beacons. If a beacon response from an anchor coordinator is received, then the node processes it in S3. If the responding anchor coordinator requests cluster joining, the node might reject or accept it following the rules explained earlier. In the latter, $\mathcal{N}_\ell^r$ should be updated to $\mathcal{N}_\ell^r + 1$. Another situation accounted in S3 is that of an anchor node leaving the cluster, and thus $\mathcal{N}_\ell^r = \mathcal{N}_\ell^r - 1$. Analogously, S4 deals with messages received from target coordinators.

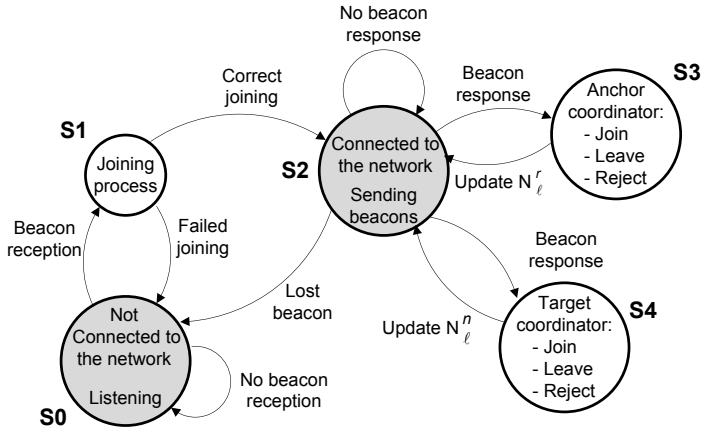

Figure 6.6: State machine of LACFA's algorithm.

Considering the cooperation between nodes, that is, if a target node is located it might act as a reference for other coordinators target nodes, LACFA can be straightforwardly applied. In our case, the cluster-children coordinators (coordinators that share the same parent coordinator) that are positioned with the initial anchor coordinators can work as references to the positioning of other cluster-children coordinators (within range) of the same cluster using RCAPS solution.

6.6 LACFA Protocol in Mobile Sensor Networks

So far, the scenario addressed consist of a WSN where cluster formation takes place during the network startup phase. In mobile scenarios, the network topology will inevitably suffer changes as nodes move. IEEE 802.15.4/ZigBee supports a fault-

tolerance mechanism for orphaned coordinator's realignment [102]. This process can start when the communication is lost between the child coordinator and its parent or when the child loses synchronization with its parent. This process is based on two different behaviors depending on the change: the orphaned realignment procedure with the same parent coordinator when it is possible, or otherwise, reset the MAC parameters leading to a new association procedure to the network.

Following this fault-tolerance mechanism, for our case depending on which node is moving, the impact on the topology will be small or considerable. Notice that in mobile scenarios, the anchor parents of a cluster have to count the set $\mathcal{N}_\ell^r$ to be $|\mathcal{N}_\ell^r| \leq R_{\max}$. For this purpose, when a node joins or leaves the cluster, it is notified with the corresponding primitives of the standard. However, also periodically, the anchor parents should send a request frame using the periodic beacons to the cluster-children to cover the situation when a cluster-child leaves the cluster without notification.

In the following, we classify the events associated with the mobility of a particular node.

Target node mobility:

- Event 1: Target node gains or loses coverage of 3 or more anchor nodes. It will impact its own positioning capability.
- Event 2: Target node leaves cluster coverage area. It will cause the target node to reconnect, if possible, at a different cluster. It may impact its own positioning capability.

Non-cluster-head anchor node mobility:

- Event 3: Target nodes within area of influence of anchor node gain or lose coverage. It may impact their positioning capability.
- Event 4: Anchor node leaves cluster coverage area. The old cluster loses one anchor node, reducing its positioning capability. The anchor node might join a new cluster following LACFA's algorithm, see Fig. 6.6.

Cluster-head mobility:

- Event 5: Child nodes may leave coverage area as cluster head moves. This is accounted for in previously defined mobility events $(1:4)$.

- Event 6: Cluster head leaves parent cluster coverage area. It follows the procedure defined by LACFA to reconnect to a new parent cluster, as in Fig. 6.6.

Notice that all these mobility events have implications in the network connectivity, such as the necessary updates on the routing tables. However, in this article, we focus on implications on positioning only.

6.7 Simulations and Results

In this section, the simulations of the range-based positioning algorithm explained in Section 6.3 are presented. The following WSN topologies are considered: mesh topology defined by Zigbee and 802.15.4a standards, cluster-tree topology defined by Zigbee, and a cluster-tree topology with 802.15.4a PHY layer. Also, we present the results of our solution RCAPS for the cluster-tree topologies with our clustering algorithm for positioning LACFA, and we compare it with the well-known clustering algorithm LEACH. All the considered WSNs consist of $N_n + N_r$ coordinators with $N_n = 100$ target coordinators and N_r reference coordinators. Nodes are randomly deployed in a cell of dimensions 50×50 m^2. The range of the nodes equals 20 m, the standard deviation for TOA $\sigma_t = 0.3$, m and the standard deviation for RSSI $\sigma_t = 0.6$ dBm.

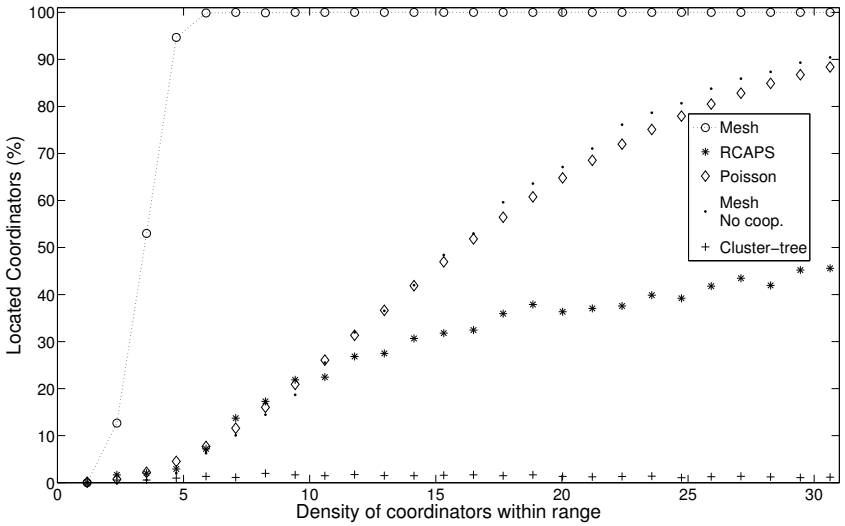

Figure 6.7: Located coordinators (%) vs density of coordinators within range ($nR = nN/3$).

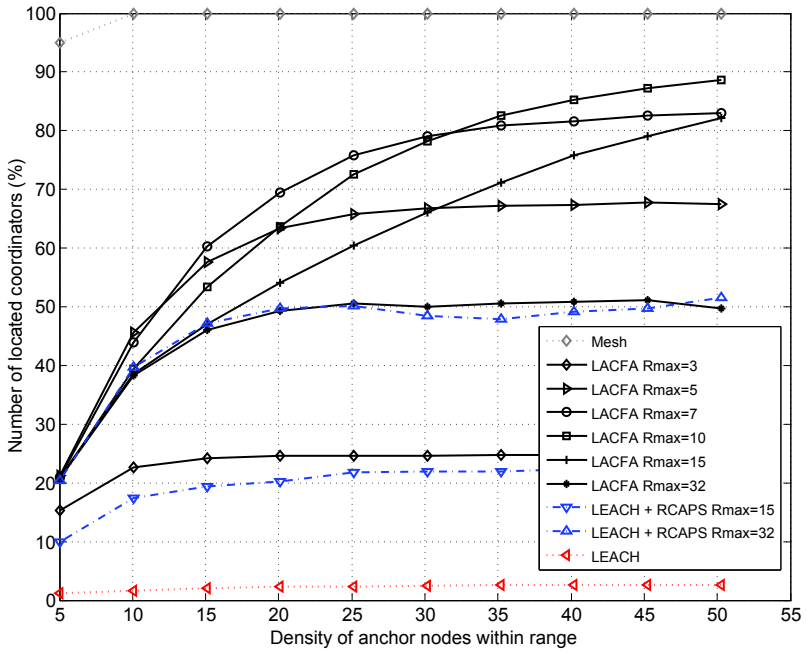

Figure 6.8: Located coordinators (%) versus density of coordinators within range.

Taking into account the described scenario, Figure 6.7 show the number of located coordinators (%) versus the density of coordinators N_n within range for the RCAPS solution, the mesh and the cluster-tree WSN. The anchor coordinators number increases as $N_r = N_n/6$. When there is no cooperation for positioning, with mesh topology the number of located nodes is small and also follows a Poisson distribution. While when there is cooperation for positioning, once a node is located it becomes a reference for other nodes. This process depends on the connectivity between nodes. In this case, for cluster-tree topology, the number of located nodes is very small. However in a WSN with mesh topology, the positioning of all nodes (100%) is performed for density of $N_n = 6$ coordinators within range (and $N_r = 3$ coordinators). For cluster-tree topology with RCAPS solution, the total number of located coordinators increases with respect to cluster-tree topology. In a cluster-tree topology, coordinators can do ranging with its parent, children, while with RCAPS solution coordinators can do ranging with its parent, children and also between cluster-children within range.

Figure 6.8 shows the number of located coordinators (%) versus the density of anchor coordinators N_r within range for LACFA algorithm. With cluster-tree topology and the LEACH algorithm, the number of located nodes is very low because ranging only can be done between parent and children. Results improve with LEACH algorithm and RCAPS solution because ranging can be done between par-

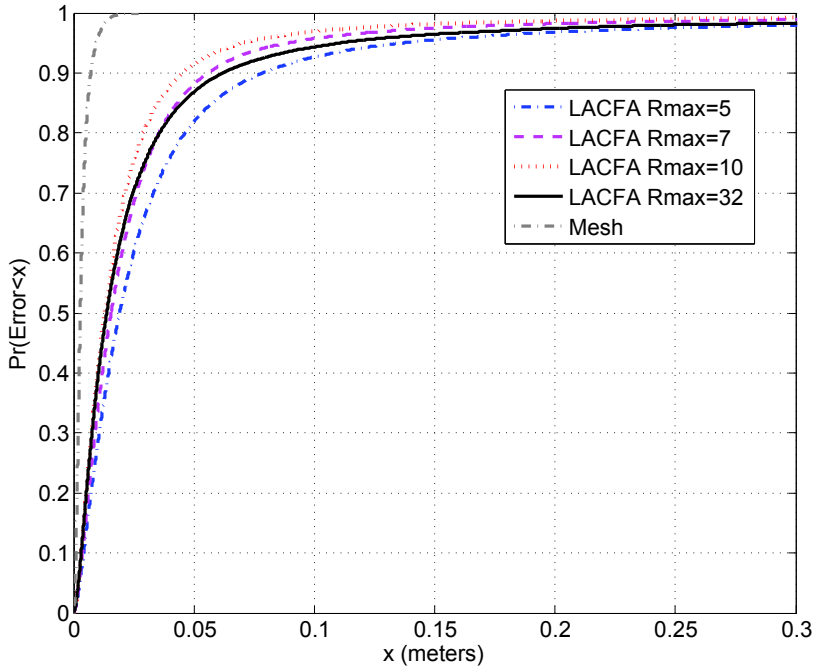

Figure 6.9: CDF of the position error with TOA-based ranging technique.

ent and children and also between cluster-children within the range of the same cluster. However, our clustering algorithm LACFA with RCAPS solution obtains better results than LEACH, because our algorithm increases the connectivity of the anchors coordinators. Also controlling the maximum number of anchor coordinators in a cluster ($R_{\max}$) improves results. Best results are obtained with values of $R_{\max}$ between 7 and 10. For $R_{\max} = 7$ and density of anchor nodes within range equal to 12, the number of located nodes is 50%; for density of anchor nodes within range equal to 30, the number of located nodes is 80%. Mesh topology is the upper limit because there are not limitations in the connectivity between nodes due to topology. In this case, the positioning of all nodes (100%) is performed for density of anchor coordinators within the range equal to 10.

Figure 6.9 shows the Cumulative Distribution Function (CDF) of the position error for TOA based ranging technique. For all the cases with our clustering algorithm LACFA, between 90 and 100% of the nodes have a position error less than 0.15 m. For mesh topology, the 100% of the nodes have an error less than 0.04 m.

The CDF of the position error for RSS based ranging technique is showed in Fig. 6.10. The error increases for all the cases with respect to TOA CDF. With our clustering algorithm LACFA, between 90 and 100% of the nodes have a position

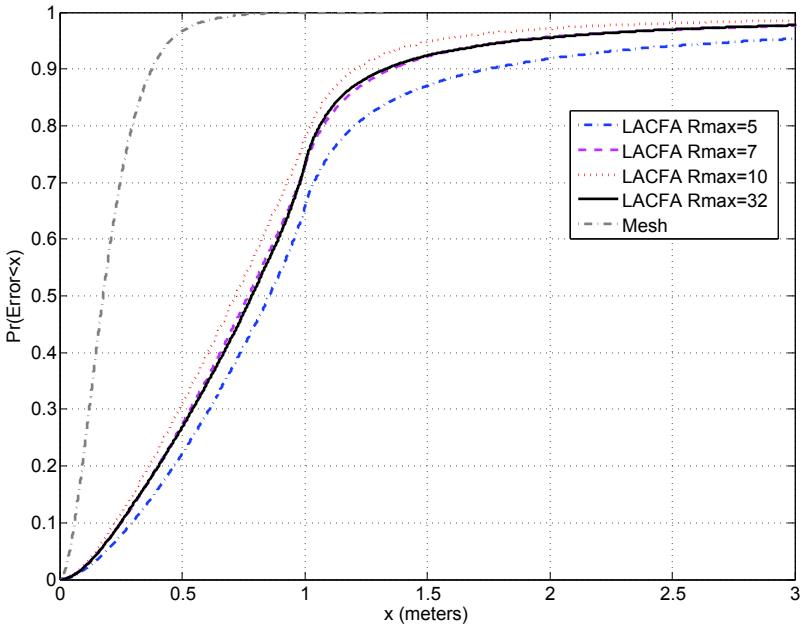

Figure 6.10: CDF of the position error with RSS based ranging technique.

error less than 1.8 m. For mesh topology, the 100% of the nodes have an error less than 0.8 m.

The histogram of the frequency that target nodes have anchor nodes within the range is represented in Fig. 6.11. For LACFA with $R_{\max} = 7$, the majority of target nodes are located with five anchor nodes within range and the maximum is 7. For LACFA with $R_{\max} = 10$, the target nodes are located with higher number of anchor nodes until 10. However, for $R_{\max} = 32$, the frequency is lower, and it is distributed for all the numbers of anchor nodes until 30. Therefore, the information of this figure explains that in Figs. 6.9 and 6.10, for CDF of the cases with LACFA, the best results are obtained for $R_{\max} = 10$.

Once a coordinator knows its position, it becomes a reference for positioning of other cluster-children coordinators (coordinators that share the same parent coordinator) within range of the same cluster. We consider this kind of cooperation between coordinators in Fig. 6.12 where we compare it with the case of absence of cooperation shown in Fig. 6.8. This cooperation improves results for low R_{max}, and for all the cases, the cooperation improves for low densities. Also, as cooperation increases the number of references for positioning in the clusters, the CDF decreases as shown in Fig. 6.13 for TOA-based ranging technique.

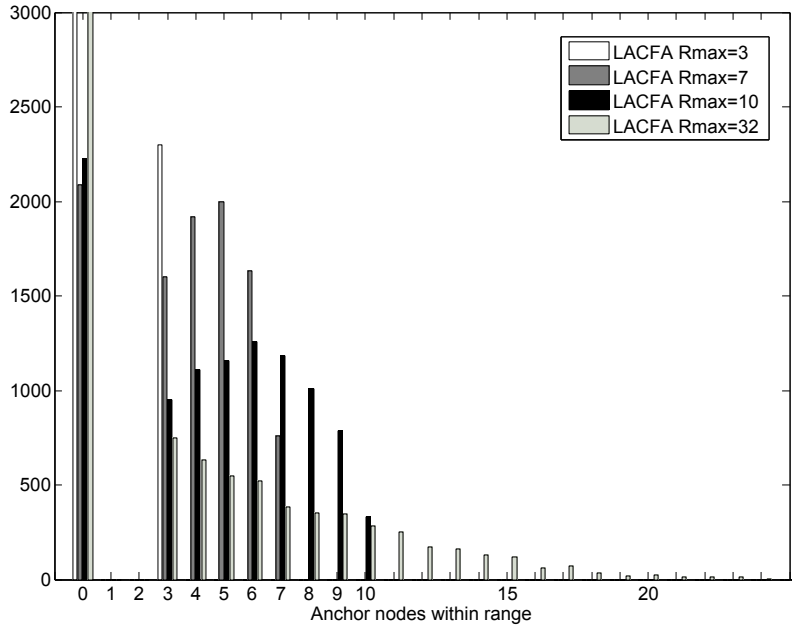

Figure 6.11: Histogram of the frequency that target nodes have anchor nodes within range.

In mobile scenarios, LACFA can recompose the occurred events because of movement in the cluster-tree. It is done in a distributed way as explained in Section 6.6. An example is shown in Fig. 6.14 with a density of 30 anchor nodes within the range and $R_{\max} = 7$. Anchor and target coordinators change its position following a random walk in each step. The number of located coordinators is maintained between 75 and 80%.

In this study, one-hop range-based positioning has been considered. However, LACFA could also improve the performance of multi-hop ranging in a cluster-tree topology as follows: first, as one-hop connectivity to anchor nodes increases with LACFA, it can be expected that second-hop connectivity will improve as well. Second, since LACFA provides a higher degree of one-hop connectivity, it is expected to reduce positioning error in multi-hop algorithms as well, since more one-hop distance measurements will be available. If an algorithm like the weighted least squares is used, then one-hop links can be given higher weight thus reducing the error.

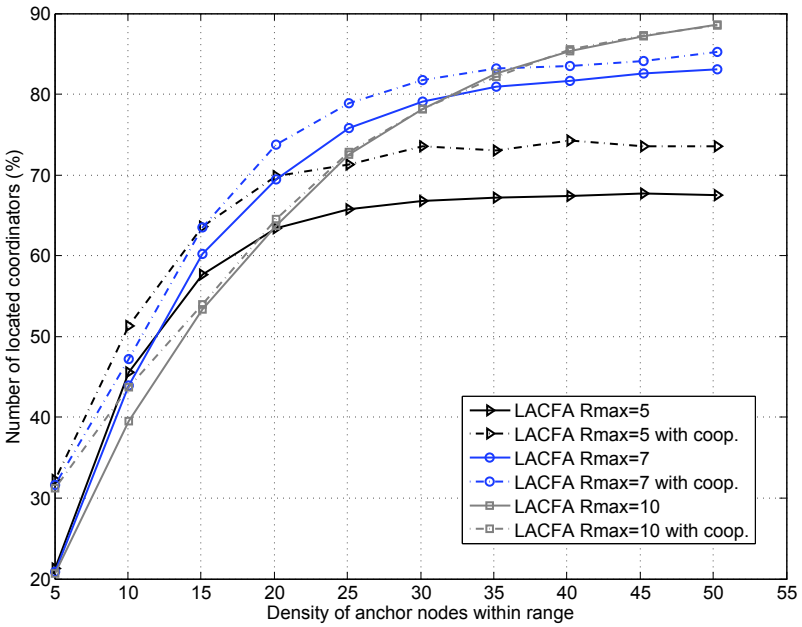

Figure 6.12: Located coordinators (%) versus density of coordinators within range with cooperation among coordinators that share the same parent of the each cluster.

6.8 Chapter Summary and Conclusions

This chapter has been focused on increasing the probability of positioning of sensors in a cluster-tree WSN. The scenario of interest consists of a set of sensors, anchor or reference nodes, that is aware of its own position and helps target nodes determine theirs through range-based positioning algorithms. Since at least four range measurements with anchor nodes are necessary for positioning of target nodes (three-dimensional scenario), range-based algorithms benefit from a high degree of connectivity. However, cluster-tree topology tends to limit connectivity between nodes in order to save energy. This results in very poor performance of the network in terms of positioning. In order to improve range-based positioning in a cluster-tree topology, a solution called RCAPS has been proposed which allows increase connectivity between sensor nodes of a cluster-tree. In this chapter, we have considered one-hop range-based positioning to show the results. However, RCAPS can be used with multi-hop range-based algorithms like [48] in which ranging can be done with reference nodes not within range. Multi-hop range-based algorithms allow positioning of nodes with low connectivity. RCAPS solution can increase the one-hop ranging number between nodes in a multi-hop ranging case. With one-hop ranging the error positioning is more accurate than with multi-hop ranging, therefore RCAPS solution may allow to improve the distance estimation accuracy.

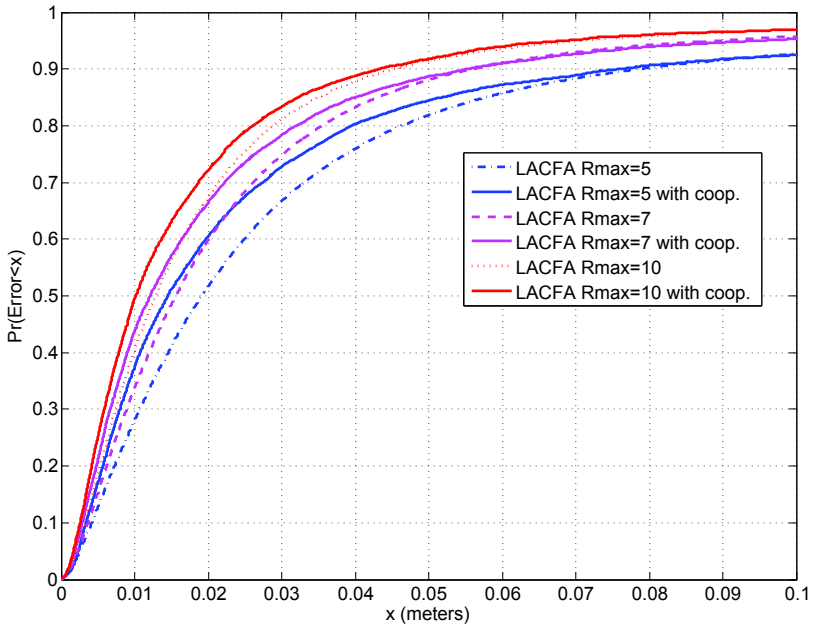

Figure 6.13: CDF of the position error with TOA based ranging technique and cooperation among coordinators that share the same parent of the each cluster.

Moreover, in this chapter we have proposed LACFA: a Localization-Aware Cluster Formation Algorithm in WSN. It does so by properly allocating anchor nodes to different clusters during the network formation phase, and by allowing peers in the same cluster to communicate with each other (RCAPS solution). Results showed this simple distributed cluster-formation algorithm greatly improves the probability of positioning of sensor nodes for a moderate density of anchor nodes. Results showed that LACFA increases one-hop connectivity from target to anchor nodes improving the one-hop range-based positioning. Also, LACFA outperforms LEACH without paying a penalty in terms of energy consumption.

The research of low power sensors yields to standardize new MAC layers. In recent years the IEEE 802.15.4e standard has gained position for industrial market. Thus, the study of this chapter can be extended to other more recent low power MAC layer specifications, for example IEEE 802.15.4e standard. The most important difference that may affect this study may be that the MAC of IEEE 802.15.4e standard is based on TDMA.

The results presented in this chapter were partially published in:

- Journal:
  [106] Moragrega, Ana, Pau Closas, and Christian Ibars. "LACFA: an algorithm

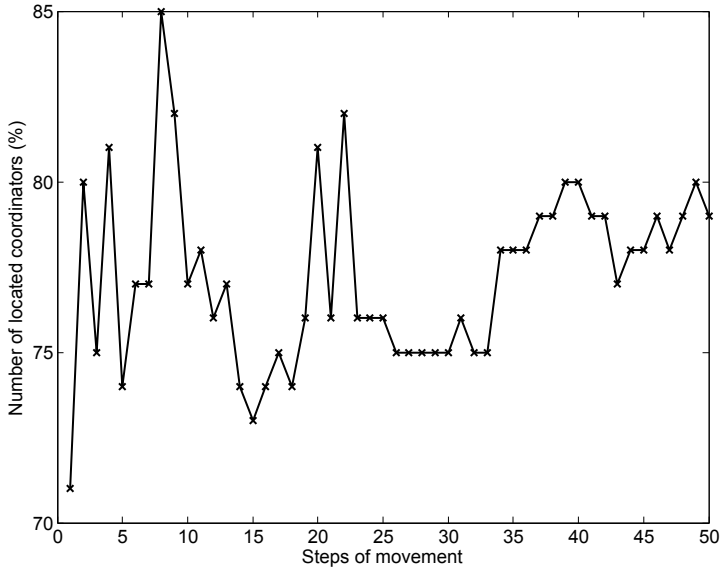

Figure 6.14: Located coordinators (%) versus steps of movement.

for localization aware cluster formation in wireless sensor networks.", special issue on Localization in Mobile Wireless and Sensor Networks, EURASIP Journal on Wireless Communications and Networking 2011.1 (2011): 1-14.

- Conference:
  [107] Moragrega, A.; Ibars, C., "Performance analysis of cooperative and range based localization algorithms for Zigbee and 802.15.4a Wireless Sensor Networks," Personal Indoor and Mobile Radio Communications (PIMRC), 2010 IEEE 21st International Symposium on , vol., no., pp.1996,2001, 26-30 Sept. 2010.

7

Conclusions and Future Work

THIS PhD dissertation addressed power optimization in wireless sensor networks with positioning capabilities. Besides the requirement of accuracy for positioning, energy efficiency is an important aspect to maximize the battery life. The study of both requirements focused on different protocol layers. In this chapter we summarize the main contributions and point out topics for further work.

Chapter 4

From a Physical layer perspective, we addressed the optimization of resource allocation in terms of transmit power and active node selection in WSN with RSS-based positioning capabilities. The proposed algorithm performed power control and minimized the number of anchor nodes for positioning, thus saving energy. The algorithm was based on a non-cooperative game that felt into the category of Exact Potential Games. The proposed solution provided a distributed approach to select the power levels of anchor nodes such that a predefined positioning quality was ensured, as quantified by the GDOP metric. GDOP for RSS depends on geometry and distance between target and anchor nodes and it is a discontinuous function. It led us to design piecewise utility function and a threshold for the average GDOP of the network. However the amount of information exchange required to estimate the global GDOP does not scale well, therefore two distributed metrics were proposed to estimate the average GDOP using merely the local information available

at each anchor node. First, an average metric with neighbors information, second, a local metric based on worst case GDOP. Next, we presented a possible solution to implement the distributed algorithm, including its computational complexity analysis. The quartic relation of the computational complexity with the number of anchor nodes might be an issue in large-scale networks. A possible workaround is to limit the total number of anchor nodes used for positioning at the target nodes and employing the aforementioned local GDOP metrics. Performance was assessed by means of computer simulations in two scenarios, a static setup and a mobile one. For the static scenario, results showed the evolution towards the NE for one game, revealing that the distributed algorithm obtained results which are comparable to a global approach, as well as requiring much less computational resources. The complexity is on the order of $\mathcal{O}(n_p^N)$ and $\mathcal{O}(n_p)$ for the global and proposed solutions, respectively, with n_p being the number of available power levels at the anchors nodes. For the mobile scenario, results showed the evolution towards the NE for several games with different anchor nodes as players. The activity of the anchor nodes revealed that node selection strategy was performed. Anchor nodes that did not contribute to positioning were turned off saving energy. We learned that the density of target nodes affects the performance of the distributed error metrics. For low density, the approximation of the worst case metric as the global metric was the best option. However, the approximation of the local GDOP average as the global metric is valid for increasing density of target nodes, while the worst case metric becomes more conservative. Finally, while the analysis of our positioning algorithm was made in the context of WSN, we note that it may well be applicable to other communications systems using RSS for positioning.

There are some open research lines related to this topic which might be worth studying in the future:

- In this chapter, we assume a dynamic game in which the players update their strategy sequentially (Gauss-Seidel algorithm) with Best Response until NE of the game is reached. This process might be performed with Jacobi algorithm, thus all the players optimize their own strategies in a parallel fashion. In [64], authors claim the convergence of Jacobi algorithm with Gradient projection response. Related to that, in static games the players make their moves simultaneously without knowing what the other players do. Sequential or simultaneous moves have different performance that could be worth studying.

- In our game, anchor and target nodes need to know information that is passed with ranging frames RRi and CFi. Each player knows some information regarding the utilities and strategies of other players, which is use to estimate global GDOP averaging. Moreover, players have knowledge of previous moves in the game. Therefore, the potential game is currently designed with complete information. The ad-

vantage of a game with incomplete information is that players do not need to know information of the game such as utility of others players. To address a game with incomplete information, instead of the potential game, the problem might be solved with other type of games. For example, in Bayesian games players may have certain beliefs about the payoffs of other players. However, a game with incomplete information based on beliefs may reach equilibrium with less accurate results in terms of positioning.

Chapter 5

From a Physical layer perspective, we addressed the optimization of resource allocation in terms of transmit power in WSN with TOA-based positioning capabilities. To that aim, we proposed a distributed algorithm for power allocation using the framework provided by supermodular games. The proposed solution provides a distributed approach to select the power levels of anchor nodes, according to a trade-off between transmitted power and positioning accuracy, quantified by the GDOP. The proposed utility function of the game shows that the trade-off may be tuned by a parameter. It was proved that the resulting power selection problem is a supermodular game with a unique equilibrium point. PoA results showed the game suffers a small loss with respect to the centrally computed solution. We presented a possible solution for the algorithm implementation. The computational analysis reveals that the costs might be an issue in large-scale sensor networks. A possible workaround is to limit the number of anchor nodes used for positioning at the target nodes. The effects of this limitation were assessed by means of computer simulations showing that the game reached the NE equilibrium. Moreover, the RMSE decreased as the number of iterations increased due to an averaging of the distance in each iteration of the game (refinement phase). The proposed algorithm was applied to WSN, but it could also be applied to other technologies with TOA-based positioning. Moreover, the proposed algorithm can be employed in hybrid positioning with TOA-based ranging and other ranging techniques.

There are some research lines which might be worth studying in the future:

- In this chapter, we showed the dependence between CRB and SNR for TOA based ranging. In turn, SNR may be affected by transmit power, but also by other parameters such as modulation or signal waveform. Therefore, the study could be extended to other parameters that affect the CRB of TOA.

- The number of iterations of the algorithm might be controlled to save power and energy consumption. Once the players reach the equilibrium, and a certain error value is reached, the algorithm should stop.

- Similarly as in Chapter 5, the use of incomplete information by means of Bayessian games could be explored.

Chapter 6

From a MAC layer perspective, the main objective was the study of positioning performance with standard protocols and topologies of WSN. In this chapter, we addressed the study of anchor and range based positioning with the topologies and MAC layers of the WSN standards. Whereas cluster-tree topologies limit connectivity to parent and children in a cluster to save energy, mesh topologies allow larger connectivity. In a cluster-tree parent and children coordinators use CAP of parent superframe to communicate. We found that connectivity limitation causes poor performances in positioning. Therefore, we proposed RCAPS solution to increment connectivity between nodes. The improvement achieved is that a coordinator node uses the CAP of its parent cluster superframe for ranging with coordinators sharing the same parent. We also proposed a network formation algorithm, LACFA, to maximize the connectivity of the anchor nodes in the cluster-tree topology. Graph theory was used to prove that in a cluster-tree topology the best connectivity for anchor nodes was attained if they were cluster heads. Computer simulations showed that positioning in a cluster-tree topology improved with the RCAPS solution. LACFA was compared with a state-of-the-art network formation algorithm LEACH, improving its performance. Moreover, the limitation of the maximum number of anchor nodes per cluster, and also cooperation (a target node that estimate its position became a reference for other nodes), improved results with LACFA algorithm.

There are some research lines which might be worth studying in the future:

Due to the nature of WSN, range and anchor based positioning is a suitable solution. However, there are some challenges when this type of positioning comes to work with different MAC protocols and topologies. In this chapter, the study of range and anchor based positioning was performed with IEEE 802.15.4 MAC layer and mesh and cluster-tree topologies. This study might be extended to other types of MAC layers from new standards, for example IEEE 802.15.4e.

8

Publications

DURING the elaboration of the dissertation a number of contributions were published. At the end of each chapter, the contributions were listed. However, there are more publications performed during the PhD degree. A list of all publications are provided.

Book chapters

- C. Ibars, M. Navarro, C. Fernández-Prades, X. Artiga, A. Moragrega, C. George-Gavrincea, A. Mollfulleda, M. Nájar, "Filter bank transceiver design for ultra wideband", *chapter in "Ultra Wideband", edited by B. Lembrikov. IN-TECH Online 2010, ISBN 978-953-307-139-8. Available online at http://www.intechopen.com/* .

Journals

- A. Moragrega, P. Closas and C. Ibars, "Potential Game for Energy-Efficient RSS based Positioning in Wireless Sensor Networks", IEEE Journal on Selected Areas in Communications, 2015, Vol. 33, Issue 7, pp. 1394-1406.
- A. Moragrega, P. Closas, C. Ibars, "Supermodular Game for Power Control in TOA-Based Positioning", IEEE Transactions on Signal Processing, Vol. 61, No. 12, pp. 3246-3259, June 2013.

- A. Moragrega, C. Ibars and P. Closas, "LACFA: An Algorithm for Localization Aware Cluster Formation in Wireless Sensor Networks", Eurasip Journal on Wireless Communication and Networking, special issue on Localization in Mobile Wireless and Sensor Networks, Vol. 2011.

Conferences

- J. M. Castro-Arvizu, A. Moragrega, P. Closas, J. A. Fernandez-Rubio, "Assessment of RSS Model Calibration with Real WLAN Devices", 2015 IEEE Twelfth International Symposium on Wireless Communication Systems (IEEE ISWCS), 2528 August 2015, Brussels (Belgium).

- A. Moragrega, P. Closas and C. Ibars, "Supermodular game for energy efficient TOA-based positioning", 2012 IEEE 13th International Workshop on Signal Processing Advances in Wireless Communications (IEEE SPAWC), pp.35-39, 17-20 June 2012.

- A. Moragrega, P. Closas, C. Ibars, "Energy-Efficient Positioning in Sensor Networks by a Game Theoretic Approach", in Proceedings of 19th European Signal Processing Conference (EUSIPCO 2011), 29-2 September 2011, Barcelona (Spain).

- A. Moragrega, C. Ibars, "Performance Analysis of Cooperative and Range Based Localization Algorithms for Zigbee and 802.15.4a Wireless Sensor Networks", *in Proceedings of IEEE International Symposium on Personal, Indoor and Mobile Radio Communications (IEEE PIMRC 2010)*, 26-29 Sept. 2010, Istanbul (Turkey).

- A. Moragrega, X. Artiga, C. George-Gavrincea, C. Ibars, M. Navarro, M. Nájar, P. Miŝkovský, Jr., F. Mira, M. Di Renzo, "Ultra-Wideband Testbed for 6.0-8.5 GHz Ranging and Low Data Rate Communication", *in Proceedings of IEEE 6th European Radar Conference (EuRAD 2009), of the European Microwave Week 2009 (EuMW 2009)*, 30-2 October 2009, Rome (Italy).

- C. George-Gavrincea, X. Artiga, A. Moragrega, C. Ibars, M. Di Renzo, "Flexible FPGA-DSP Solution for an IR-UWB Testbed", *in Proceedings of IEEE International Conference on Ultra-Wideband (ICUWB 2009)*, 9-11 September 2009, Vancouver (Canada).

- A. Moragrega, C. Ibars, Y. Geng, "Energy efficiency of a cooperative Wireless Sensor Network", *in Proceedings of Second International Workshop on Cross Layer Design, (IWCLD 2009)*, 11-12 June 2009, Palma de Mallorca (Spain).

- A. Moragrega, C. Ibars, X. Artiga, "Digital transmitter based on spread spectrum codes for Ultra-Wideband", *in Proceedings of XXIV Simposium Nacional de la Unión Científica Internacional de Radio (URSI'09)*, 16-18 September 2009, Santander (Spain).

- M. López, A. Osorio, J. M. Gómez, A. Moragrega, A. Herms, "Energy saving strategies for 802.15.4 based wireless communications", *in Proceedings of XXI Conference on Design of Circuits and Integrated Systems (DCIS'06)*, Barcelona (Spain), November 2006.

- A. Moragrega, M. López, J. M. Gómez, A. Osorio-Marti, J. Sieiro and J. M. López-Villegas, "Hardware and software co-design for IEEE 802.15.4 based sensor nodes", *in Proceedings of XXI Conference on Design of Circuits and Integrated Systems (DCIS'06)*, Barcelona (Spain), November 2006.

- M. López, J. M. Gómez, A. Moragrega, A. Osorio-Marti, J. Sieiro, J. M. López-Villegas and A. Fernández, "Analysis of power consumption on wireless sensor networks", *in Proceedings of XIX Eurosensors*, Barcelona (Spain), September 2005.

Bibliography

[1] I. Akyildiz, W. Su, Y. Sankarasubramaniam, and E. Cayirci, "A survey on sensor networks," *IEEE Commun. Mag.*, vol. 40, pp. 102–114, 2002.

[2] V. Srivastava, J. Neel, A. Mackenzie, R. Menon, L. Dasilva, J. Hicks, J. Reed, and R. Gilles, "Using game theory to analyze wireless ad-hoc networks," *IEEE Communications Surveys and Tutorials*, vol. 7, no. 4, pp. 46–56, 2005.

[3] *CC2420, 2.4GHz IEEE 802.15.4/Zigbee-ready RF Transceiver*, Chipcon.

[4] M. Johnson, M. Healy, P. van de Ven, M. Hayes, J. Nelson, T. Newe, and E. Lewis, "A comparative review of wireless sensor network mote technologies," in *Sensors, 2009 IEEE*, Oct 2009, pp. 1439–1442.

[5] A. Moragrega, M. Lopez, J. Gomez, A. Osorio-Marti, J. Sieiro, and J. Lopez-Villegas, "Hardware and software co-design for IEEE 802.15.4 based sensor nodes," in *Proceedings of XXI Conference on Design of Circuits and Integrated Systems (DCIS'06)*, November 2006.

[6] S. Gajjar, N. Choksi, M. Sarkar, and K. Dasgupta, "Comparative analysis of wireless sensor network motes," in *Signal Processing and Integrated Networks (SPIN), 2014 International Conference on*, Feb 2014.

[7] V. Raghunathan, C. Schurgers, S. Park, and M. Srivastava, "Energy aware wireless microsensor networks," *IEEE Signal Process. Mag.*, vol. 19, no. 2, p. 4050, May 2002.

[8] S. Sudevalayam and P. Kulkarni, "Energy harvesting sensor nodes: Survey and implications," *Communications Surveys Tutorials, IEEE*, no. 99, pp. 1 –19, 2010.

[9] *MSP430x12x Mixed Signal Microcontroller*, Texas Instruments (TI).

[10] W. Wang, M. Hempstead, and W. Yang, "A realistic power consumption model for wireless sensor network devices," in *Proc. IEEE Sensor and Ad Hoc Communications and Networks SECON'06*, 2006.

[11] A. Moragrega, C. Ibars, and Y. Geng, "Energy efficiency of a cooperative wireless sensor network," in *Cross Layer Design, 2009. IWCLD '09. Second International Workshop on*, June 2009, pp. 1 –5.

[12] S. Cui, A. Goldsmith, and A. Bahai, "Energy-efficiency of mimo and cooperative mimo techniques in sensor networks," *IEEE J. Select. Areas Commun*, vol. 22, pp. 1089–1098, 2004.

[13] J. Boyer, D. Falconer, and H. Yanikomeroglu, "Mulithop diversity in wireless relaying channels," *IEEE Trans on Communications*, vol. 52, pp. 1820–1830, 2004.

[14] J. Haapola, Z. Shelby, C. Pomalaza-Raez, and P. Mahonen, "Multihop medium access control for WSNs: an energy analysis model," *IEEE EURASIP Journal on Wireless Communication and Networking*, vol. 4, pp. 523–540, 2005.

[15] R.Min, M. Bharwaj, N. Ickes, A. Wang, and A. Chandrakasan, "The hardware and the network: total-system strategies for power aware wireless microsensors," in *CAS Workshop on Wireless Communication and Networking. Invited paper.*, 2002.

[16] H. Yu Shwe, J. Xiao-hong, and S. Horiguchi, "Energy saving in wireless sensor networks," *Journal of Communication and Computer*, vol. 6, no. 5, May 2009.

[17] A. Bachir, M. Dohler, T. Watteyne, and K. Leung, "MAC essentials for wireless sensor networks," *Communications Surveys Tutorials, IEEE*, vol. 12, no. 2, pp. 222–248, 2010.

[18] G. Anastasi, M. Conti, M. Di Francesco, and A. Passarella, "Energy conservation in wireless sensor networks: A survey," *Elsevier Ad Hoc Networks journal*, vol. 7, pp. 537–568, 2009.

[19] A. A. Abbasi and M. Younis, "A survey of clustering algorithms for wireless sensor networks," *Elsevier Computer Communications*, vol. 2007, pp. 2826–2841, 2007.

[20] *Wireless LAN Medium Access Control (MAC) and Physical Layer (PHY) Specification for Low-Rate Wireless Personal Area Networks (WPANs)*, IEEE Std. 802.15.4, 2006.

[21] N. Patwari, J. Ash, S. Kyperountas, A. HeroIII, R. Moses, and N. Correal, "Locating the nodes: cooperative localization in wireless sensor networks," *IEEE Signal Processing Magazine*, vol. 22, no. 4, pp. 54–69, July 2005.

[22] D. Dardari, P. Closas, and P. Djuric, "Indoor tracking: Theory, methods, and technologies," *Vehicular Technology, IEEE Transactions on*, vol. 64, no. 4, pp. 1263–1278, April 2015.

[23] A. Bardella, N. Bui, A. Zanella, and M. Zorzi, "An experimental study on IEEE 802.15. 4 multichannel transmission to improve RSSI-based service performance," in *Real-World Wireless Sensor Networks*. Springer, 2010, pp. 154–161.

[24] A. Goldsmith, *Wireless communications*. Cambridge university press, 2005.

[25] J. Castro-Arvizu, A. Moragrega, P. Closas, and J. Fernandez-Rubio, "Assessment of RSS model calibration with real WLAN devices," in *Twelfth International Symposium on Wireless Communication Systems (ISWCS'15)*, Aug 2015.

[26] S. Gezici, Z. Tian, G. Giannakis, H. Kobayashi, A. Molisch, H. Poor, and Z. Sahinoglu, "Localization via Ultra-wideband radios: a look at positioning aspects for future sensor networks," *Signal Processing Magazine, IEEE*, vol. 22, no. 4, pp. 70–84, July 2005.

[27] P.-C. Chen, "A non-line-of-sight error mitigation algorithm in location estimation," in *Wireless Communications and Networking Conference, 1999. WCNC. 1999 IEEE*, 1999, pp. 316–320 vol.1.

[28] E. Serpedin and Q. M. Chaudhari, *Synchronization in Wireless Sensor Networks: Parameter Estimation, Performance Benchmarks, and Protocols*. Cambridge University Press, 2009.

[29] *Amendment to IEEE Std 802.15.4-2006 adding alternate Physical Layer*, IEEE Std. 802.15.4a, 2007.

[30] M. Navarro and M. Najar, "Frequency domain joint toa and doa estimation in IR-UWB," *Wireless Communications, IEEE Transactions on*, vol. 10, no. 10, pp. 1–11, October 2011.

[31] N. Patwari, A. Hero, M. Perkins, N. Correal, and R. O'Dea, "Relative location estimation in wireless sensor networks," *Signal Processing, IEEE Transactions on*, vol. 51, no. 8, pp. 2137–2148, 2003.

[32] C. Ibars, X. Artiga, M. Navarro, M. Najar, A. Mollfulleda, A. Moragrega, C. Gavrincea, and C. Fernandez, *Filter Bank-based Transceiver Design for Ultrawideband (book title: Ultra Wideband).* Boris Lembrikov (Ed.), Sciyo, 2010.

[33] A. Moragrega, X. Artiga, C. Gavrincea, C. Ibars, M. Navarro, M. Najar, P. Miskovsky, F. Mira, and M. di Renzo, "Ultra-wideband testbed for 6.0-8.5 ghz ranging and low data rate communication," in *Radar Conference, 2009. EuRAD 2009. European*, October 2009, pp. 358 –361.

[34] A. Moragrega, C. Ibars, and X. Artiga, "Transmisor digital basado en códigos de espectro ensanchado para ultra-wideband," September 2009.

[35] J. Romme and L. Piazzo, "On the power spectral density of time-hopping impulse radio," in *IEEE Conf. on Ultra-Wideband Systems and Technologies*, May 2002.

[36] S. Gezici, Z. Sahinoglu, H. Kobayashi, and H. Poor, *Ultra Wideband geolocation*, Z. C. H. Arslan and M. D. Benedetto, Eds. Berlin (Germany): Ultra Wideband Wireless Communications (Wiley-Interscience), 2006.

[37] J. Zhang, P. Orlik, Z. Sahinoglu, A. Molisch, and P. Kinney, "UWB systems for wireless sensor networks," *Proceedings of the IEEE*, vol. 97, no. 2, pp. 313–331, 2009.

[38] H. Liu, H. Darabi, P. Banerjee, and J. Liu, "Survey of wireless indoor positioning techniques and systems," *Systems, Man, and Cybernetics, Part C: Applications and Reviews, IEEE Transactions on*, vol. 37, no. 6, pp. 1067–1080, 2007.

[39] N. Bulusu, J. Heidemann, and D. Estrin, "GPS-less low-cost outdoor localization for very small devices," *Personal Communications, IEEE*, vol. 7, no. 5, pp. 28–34, 2000.

[40] D. Niculescu and B. Nath, "DV based positioning in ad hoc networks," *Telecommunication Systems*, vol. 22, no. 1-4, pp. 267–280, 2003.

[41] J. Larranaga, L. Muguira, J.-M. Lopez-Garde, and J.-I. Vazquez, "An environment adaptive Zigbee-based indoor positioning algorithm," in *Indoor Positioning and Indoor Navigation (IPIN), 2010 International Conference on*, September 2010, pp. 1–8.

[42] G. Sun, J. Chen, W. Guo, and K. Liu, "Signal processing techniques in network-aided positioning: a survey of state-of-the-art positioning designs," *Signal Processing Magazine, IEEE*, vol. 22, no. 4, pp. 12 – 23, July 2005.

[43] C.-D. Wann and H.-C. Chin, "Hybrid TOA/RSSI wireless location with unconstrained nonlinear optimization for indoor UWB channels," in *Wireless Communications and Networking Conference, 2007.WCNC 2007. IEEE*, March 2007, pp. 3940 –3945.

[44] G. Mao and B. Fidan, *Localization Algorithms and Strategies for Wireless Sensor Networks*. Information Science Reference, 2009.

[45] T. Watteyne, I. Augé-Blum, M. Dohler, S. Ubéda, and D. Barthel, "Centroid virtual coordinates - a novel near-shortest path routing paradigm," *Comput. Netw.*, vol. 53, pp. 1697–1711, July 2009.

[46] J. A. Costa, N. Patwari, and A. O. Hero III, "Distributed weighted-multidimensional scaling for node localization in sensor networks," *ACM Transactions on Sensor Networks (TOSN)*, vol. 2, no. 1, pp. 39–64, 2006.

[47] P. Biswas, T. chen Liang, T. chung Wang, and Y. Ye, "Semidefinite programming based algorithms for sensor network localization," *ACM Transactions on Sensor Networks*, vol. 2, p. 2006, 2006.

[48] K. Langendoen and N. Reijers, "Distributed localization in wireless sensor networks: a quantitative comparison," *Elsevier Computer Networks*, vol. 43, no. 4, pp. 499–518, November 2003.

[49] A. Savvides, H. Park, and M. B. Srivastava, "The bits and flops of the n-hop multilateration primitive for node localization problems," in *Proceedings of the 1st ACM international workshop on Wireless sensor networks and applications (WSNA '02)*. New York, NY, USA: ACM, 2002, pp. 112–121.

[50] H. Wymeersch, J. Lien, and M. Win, "Cooperative localization in wireless networks," *Proceedings of the IEEE*, vol. 97, no. 2, pp. 427 –450, February 2009.

[51] S. M. Kay, *Fundamentals of Statistical Signal Processing. Estimation Theory*. Prentice Hall, 1993.

[52] V. Savic, A. Población, S. Zazo, and M. García, "Indoor positioning using non-parametric belief propagation based on spanning trees," *EURASIP J. Wirel. Commun. Netw.*, vol. 2010, pp. 9:1–9:13, January 2010.

[53] M. R. Gholami, "Wireless sensor network positioning techniques," Ph.D. dissertation, Chalmers University of Technology, 2013.

[54] S. Gezici, I. Guvenc, and Z. Sahinoglu, "On the performance of linear least-squares estimation in wireless positioning systems," in *Communications, 2008. ICC'08. IEEE International Conference on.* IEEE, 2008, pp. 4203–4208.

[55] R. Yarlagadda, I. Ali, N. Al-Dhahir, and J. Hershey, "GPS GDOP metric," *Radar, Sonar and Navigation, IEE Proceedings*, vol. 147, no. 5, pp. 259–264, oct. 2000.

[56] X. Li, "RSS-based location estimation with unknown pathloss model," *Wireless Communications, IEEE Transactions on*, vol. 5, no. 12, pp. 3626–3633, 2006.

[57] R. Vaghefi, M. Gholami, R. Buehrer, and E. Strom, "Cooperative received signal strength-based sensor localization with unknown transmit powers," *Signal Processing, IEEE Transactions on*, vol. 61, no. 6, pp. 1389–1403, 2013.

[58] H. Lee, "A Novel Procedure for Assessing the Accuracy of Hyperbolic Multilateration Systems," *IEEE Trans. Aerosp. Electron. Syst.*, vol. AES-11, no. 1, pp. 2 –15, Jan. 1975.

[59] N. Levanon, "Lowest GDOP in 2-D scenarios," *Radar, Sonar and Navigation, IEE Proceedings* -, vol. 147, no. 3, pp. 149–155, jun. 2000.

[60] D. Fudenberg and J. Tirole, *Game Theory.* Cambridge: The MIT press, 1991.

[61] E. Altman, T. Boulogne, R. El-Azouzi, T. Jiménez, and L. Wynter, "A survey on networking games in telecommunications," *Comput. Oper. Res.*, vol. 33, pp. 286–311, Feb. 2006.

[62] R. S. Komali and A. B. MacKenzie, "Effect of Selfish node behaviour on Efficient Topology Design," *IEEE Trans. on Mobile Computing*, vol. 7, no. 6, June 2008.

[63] M. Felegyhazi and J.-P. Hubaux, "Game theory in wireless networks: A tutorial," École polytechnique fédérale de Lausanne (EPFL), Tech. Rep. LCA-REPORT-2006-002, 2006.

[64] G. Scutari, S. Barbarossa, and D. Palomar, "Potential games: A framework for vector power control problems with coupled constraints," in *Acoustics, Speech and Signal Processing, 2006. ICASSP 2006 Proceedings. 2006 IEEE International Conference on*, vol. 4, May 2006.

[65] G. Scutari, D. P. Palomar, F. Facchinei, and J.-S. Pang, "Convex optimization, game theory, and variational inequality theory," *Signal Processing Magazine, IEEE*, vol. 27, no. 3, pp. 35–49, 2010.

[66] J. B. Rosen, "Existence and uniqueness of equilibrium points for concave n-person games," *Econometrica*, vol. 33, no. 3, pp. 520–534, 1965.

[67] D. Monderer and L. S. Shapley, "Potential games," *Games and Economics Behaviour*, vol. 14, no. 14, pp. 124–143, 1996.

[68] D. M. Topkis, "Equilibrium points in nonzero-sum n-person submodular games," *SIAM J. Control Optim.*, vol. 17, pp. 773–778, 1979.

[69] E. Altman and Z. Altman, "S-modular games and power control in wireless networks," *Transactions on Automatic Control, IEEE*, vol. 48, no. 5, pp. 839–842, May 2003.

[70] R. D. Yates, "A framework for uplink power control in cellular radio systems," *Journal on selected areas in communications, IEEE*, vol. 13, no. 7, pp. 1341–1347, Sept. 1995.

[71] E. Altman, T. Boulogne, R. El-Azouzi, T. Jiménez, and L. Wynter, "A survey on networking games in telecommunications," *Computers & Operations Research*, vol. 33, no. 2, pp. 286–311, 2006.

[72] C. Saraydar, N. Mandayam, and D. Goodman, "Efficient power control via pricing in wireless data networks," *Communications, IEEE Transactions on*, vol. 50, no. 2, pp. 291–303, Feb. 2002.

[73] Z. Han, *Game theory in wireless and communication networks: theory, models, and applications*. Cambridge University Press, 2012.

[74] B. Wang, Y. Wu, and K. R. Liu, "Game theory for cognitive radio networks: An overview," *Comput. Netw.*, vol. 54, no. 14, pp. 2537–2561, Oct. 2010.

[75] F. Meshkati, A. Goldsmith, H. Poor, and S. Schwartz, "A game-theoretic approach to energy-efficient modulation in cdma networks with delay constraints," in *Radio and Wireless Symposium, 2007 IEEE*, Jan 2007, pp. 11–14.

[76] V. Krishnamurthy, M. Maskery, and G. Yin, "Decentralized adaptive filtering algorithms for sensor activation in an unattended ground sensor network," *Signal Processing, IEEE Transactions on*, vol. 56, no. 12, pp. 6086 –6101, Dec. 2008.

[77] J. Yuan and W. Yu, "Distributed cross-layer optimization of wireless sensor networks: A game theoretic approach," in *Global Telecommunications Conference, 2006. GLOBECOM'06. IEEE.* IEEE, 2006, pp. 1–5.

[78] H. Ren, M.-H. Meng, and L. Xu, "Conflict and coalition models in inhomogeneous power allocation for wireless sensor networks," in *Robotics and Biomimetics, 2008. ROBIO 2008. IEEE International Conference on*, Feb 2009, pp. 2056–2060.

[79] N. Chenglianq, L. Donqxin, Z. Tingxian, and L. Lihonq, "Distributed power control algorithm based on game theory for wireless sensor networks," *Systems Engineering and Electronics, Journal of*, vol. 18, no. 3, pp. 622–627, Sept 2007.

[80] R. Kannan, S. Wei, V. Chakravarthy, and G. Seetharaman, "Using misbehavior to analyze strategic versus aggregate energy minimization in wireless sensor networks," *International Journal of Distributed Sensor Networks*, vol. 2, no. 3, pp. 225–249, 2006.

[81] Z. Ji and K. Liu, "Cognitive radios for dynamic spectrum access - dynamic spectrum sharing: A game theoretical overview," *Communications Magazine, IEEE*, vol. 45, no. 5, pp. 88–94, May 2007.

[82] H.-Y. Shi, W.-L. Wang, N.-M. Kwok, and S.-Y. Chen, "Game theory for wireless sensor networks: A survey," *Sensors*, 2012.

[83] B. Béjar, P. Belanovic, and S. Zazo, "Cooperative localisation in wireless sensor networks using coalitional game theory," in *European Signal Processing Conference (Eusipco)*, Aalborg(Denmark), August 2010, pp. 1459–1463.

[84] D. Gu, "A game theory approach to target tracking in sensor networks," *Systems, Man, and Cybernetics, Part B: Cybernetics, IEEE Transactions on*, vol. 41, no. 1, pp. 2–13, Feb 2011.

[85] D. Yan, J. Wang, L. Liu, and J. Gao, "Target tracking based on cluster and game theory in wireless sensor network," 2008.

[86] O. N. Gharehshiran and V. Krishnamurthy, "Coalition formation for bearings only localization in sensor networks - a cooperative game approach," *Signal Processing, IEEE Transactions on*, vol. 58, no. 8, pp. 4322 –4338, August 2010.

[87] Y. Qi and H. Kobayashi, "On relation among time delay and signal strength based geolocation methods," in *Global Telecommunications Conference, 2003. GLOBECOM '03. IEEE*, vol. 7, 2003, pp. 4079–4083.

[88] P. Tarrio, A. Bernardos, and J. Casar, "A transmission rate and energy design for power aware localization in ad hoc and sensor networks," in *Personal, Indoor and Mobile Radio Communications, 2007. PIMRC 2007. IEEE 18th International Symposium on*, Sept 2007, pp. 1–5.

[89] D. Lieckfeldt, J. You, and D. Timmermann, "Distributed selection of references for localization in wireless sensor networks," in *Positioning, Navigation and Communication, 2008. WPNC 2008. 5th Workshop on*, March 2008, pp. 31–36.

[90] M. Zoghi and M. Kahaei, "Adaptive sensor selection in wireless sensor networks for target tracking," *Signal Processing, IET*, vol. 4, no. 5, pp. 530–536, Oct 2010.

[91] F. Gustafsson, F. Gunnarsson, N. Bergman, U. Forssell, J. Jansson, R. Karlsson, and P.-J. Nordlund, "Particle filters for positioning, navigation, and tracking," *Signal Processing, IEEE Transactions on*, vol. 50, no. 2, pp. 425–437, 2002.

[92] A. Moragrega, P. Closas, and C. Ibars, "Potential game for energy-efficient RSS-based positioning in wireless sensor networks," *Selected Areas in Communications, IEEE Journal on*, vol. 33, no. 7, pp. 1394–1406, July 2015.

[93] ——, "Energy-efficient positioning in sensor networks by a game theoretic approach," in *in Proceedings of 19th European Signal Processing Conference (EUSIPCO 2011)*, Barcelona(Spain), Sep. 2011, pp. 619 –624.

[94] M. R. Gholami, E. Ström, and M. Rydström, "Indoor sensor node positioning using UWB range measurements," in *in Proceedings of European Signal Processing Conference (EUSIPCO 2009)*, Glasgow, Scotland, Aug. 2009.

[95] J. Chaffee and J. Abel, "GDOP and the Cramér-Rao Bound," in *Position Location and Navigation Symposium, 1994., IEEE*, apr. 1994, pp. 663–668.

[96] E. Koutsoupias and C. Papadimitriou, "Worst-case equilibria," in *16th Annual Symposium on Theoretical Aspects of Computer Science*, 1999, pp. 404–413.

[97] A. Bel, J. L. Vicario, and G. Seco-Granados, "Localization algorithm with on-line path loss estimation and node selection," in *Sensors 2011*, 2011, pp. 6905–6925.

[98] A. Moragrega, P. Closas, and C. Ibars, "Supermodular game for power control in TOA-based positioning," *Signal Processing, IEEE Transactions on*, vol. 61, no. 12, pp. 3246 –3259, 2013.

[99] ——, "Supermodular game for energy efficient toa-based positioning," in *Signal Processing Advances in Wireless Communications (SPAWC), 2012 IEEE 13th International Workshop on*, June 2012, pp. 35–39.

[100] J. E. Gentle, *Matrix Algebra: Theory, Computations, and Applications in Statistics*. Springer, 2007, no. v1.

[101] S. P. Boyd and L. Vandenberghe, *Convex Optimization*. Cambridge University Press, 2004.

[102] *Zigbee Specification*, Zigbee Alliance, Dec 2005.

[103] A. Savvides, C.-C. Han, and M. B. Strivastava, "Dynamic fine-grained localization in Ad-hoc networks of sensors," in *Proceedings of the 7th annual international conference on Mobile computing and networking, MobiCom '01*, 2001, pp. 166–179.

[104] O. Boyinbode, H. Le, A. Mbogho, M. Takizawa, and R. Poliah, "A survey on clustering algorithms for wireless sensor networks," in *Network-Based Information Systems (NBiS), 2010 13th International Conference on*, September 2010, pp. 358 –364.

[105] C. Godsil and G. Royle, *Algebraic graph theory*. Graduate Texts in Mathematics. Berlin, Germany: Springer-Verlag, 2001, vol. 207.

[106] A. Moragrega, P. Closas, and C. Ibars, "LACFA: An algorithm for localization aware cluster formation in wireless sensor networks," *EURASIP Journal on Wireless Communication and Networking, special issue on Localization in Mobile Wireless and Sensor Networks*, vol. 2011, 2011.

[107] A. Moragrega and C. Ibars, "Performance analysis of cooperative and range based localization algorithms for zigbee and 802.15.4a wireless sensor networks," in *Personal Indoor and Mobile Radio Communications (PIMRC), 2010 IEEE 21st International Symposium on*, September 2010, pp. 1996 – 2001.